School of Doctoral Studies in Biological Sciences

University of South Bohemia in České Budějovice

Faculty of Science

Stable isotope characterization of fungal water and inorganic carbon assimilation signals and ecosystem fluxes

Ph.D. Thesis

MSc. Stanislav Jabinski

Supervisor: Travis B. Meador, Ph.D.
Institute of Soil Biology and Biogeochemistry

České Budějovice 2024

This thesis should be cited as:
Jabinski, S., 2024: **Stable isotope characterization of fungal water and inorganic carbon assimilation signals and ecosystem fluxes**. University of South Bohemia, Faculty of Science, School of Doctoral Studies in Biological Sciences, České Budějovice, Czech Republic, 106.

Annotation

Fungi are a group of major decomposers in soils and therefore play a key role in the biogeochemical cycles in environmental systems. To get a better understanding of their metabolic role, we extended a dual stable isotope probing assay which applies labeled bicarbonate as inorganic C and heavy water (^2H_2O). The advantages of this approach are that both are overly abundant in the environment and therefore do not disturb or add nutrients into natural systems. Only little information could be found in the literature regarding the potential of inorganic carbon assimilation by fungi and no information could be found for the hydrogen water assimilation. Therefore, this PhD was aimed to investigate the isotopic signatures of a diverse phylogenetic range of saprotrophic fungi to explore the variations in the fungi when grown under different substrate classes before applying the obtained knowledge to incubations of natural systems. To fully apply this assay potential, we investigated under laboratory conditions the potential of assimilation of inorganic C and the hydrogen water assimilation into the membrane lipid biomarkers of fungi to distinguish differences in metabolic modes specifically targeting the difference in growth on labile vs more complex C sources.

Declaration

I hereby declare that I am the author of this dissertation and that I have used only those sources and literature detailed in the list of references.

Stanislav Jabinski
České Budějovice
October 2024

This thesis originated from a partnership of Faculty of Science, University of South Bohemia, and Institute of Soil Biology and Biogeochemistry, Academy of Sciences of the Czech Republic, supporting doctoral studies in the Ecosystem Biology study program.

Přírodovědecká fakulta Faculty of Science

KATEDRA BIOLOGIE EKOSYSTÉMŮ

BIOLOGY CENTRE CAS

Financial support

The research was supported by the Czech Science Foundation GACR nr. 20-223805 (FUNSIF) and supported by MEYS CZ grant LM2015075 Projects of Large Infrastructure for Research, Development and Innovations as well as the European Regional Development Fund-Project: research of key soil-water ecosystem interactions at the SoWa Research Infrastructure (No. CZ.02.1.01/0.0/0.0/16_013/0001782). Erasmus+ Student mobility for traineeship of the University of South Bohemia (Erasmus ID code: CZ CESKE01) supported travel expenses for this international collaboration.

Acknowledgements

This PhD thesis was accomplished in the IRMS Lab/group at the Institute of biology and biogeochemistry under the supervision of Dr. Travis B. Meador. I would like to thank Travis for the opportunity to be part of this wonderful group for the past 5 years and surviving of being my supervisor, which must have been not an easy task. Thank you for everything you have done for me and hopefully we will stay in contact.

I cannot find the right words to express my gratitude towards my lab colleagues how have left along the way, Ana and Sofia, and who stayed, Karelys, Astolfo and Nana, and survived with me through the past 5 years of continuous support and help with all kinds of productive or stupid conversations we had. Thank you everyone so much.

I want also to give special thanks to Ljuba who endured me in the office and the lab and was always supportive and helpful, also outside of work. Thank you so much for the good times we spent in this lab together.

I Also want to thank the program of Ecosystem Biology and my committee for evaluating my PhD thesis.

And Last but not least I want to thank my family who were supporting me independent of what I was doing and sending me Stani care-packages all the time and also Niro and all the other friend who did not forgot about me after moving away and to all the new friends I encountered on this journey.

List of papers and author's contribution

The thesis is based on the following papers (listed chronologically):

I. **Jabinski, S.,** d. M. Rangel, W., Kopáček, M., Jílková, V., Jansa, J., & Meador, T. B. (2024). Constraining activity and growth substrate of fungal decomposers via assimilation patterns of inorganic carbon and water into lipid biomarkers. Applied and Environmental Microbiology, 90(4), e02065-23. (IF = 3.9)

Jabinski S. contributed The Conceptualization, Data curation, Formal analysis, Investigation, Methodology, Software, Validation, Visualization, Writing the original draft, reviewing and editing the original manuscript.

II. **Jabinski, S.,** Kucera, V., Kopáček, M., Jansa, J., & Meador, T. B. (2024). Fungi incorporate distinguishable isotope signals when grown on glycolytic versus TCA cycle intermediates (manuscript).

Jabinski S. contributed The Conceptualization, Data curation, Formal analysis, Investigation, Methodology, Software, Validation, Visualization, Writing the original draft, reviewing and editing the original manuscript.

III. **Jabinski, S.,** Jílková, V., Kopáček, M., & Meador, T. B. (2024). Seasonal accounts of microbial production and turnover forest soil horizons. (manuscript).

Jabinski S. contributed The Conceptualization, Data curation, Formal analysis, Investigation, Methodology, Software, Validation, Visualization, Writing the original draft

IV. **Jabinski, S.,** Pilecky, M., Wassenaar L.I., Kainz, M.J., & Meador, T. B. (2024). Production and dark carbon assimilation of aquatic macroplankton and microbial heterotrophs. (manuscript).

Jabinski S. contributed The Conceptualization, Data curation, Formal analysis, Investigation, Methodology, Software, Validation, Visualization, Writing the original draft

Co-author agreement

Dr. Travis B. Meador, supervisor of this Ph.D. thesis and co-author of paper I and manuscripts II, III and IV fully acknowledges the stated contribution of Stanislav Jabinski to these manuscripts.

……

Travis B. Meador, Ph.D.

Travis B. Meador

Digitally signed by Travis B. Meador
Date: 2024.10.22 16:30:12 +02'00'

Table of contents

1. **Introduction** ..... **- 1 -**
1.1 ***Soil organic carbon (SOC)*** ..... ***- 1 -***
1.2 ***Microbial metabolism*** ..... ***- 2 -***
1.2.1 *Recalcitrant lignin decomposition pathways in soils* ..... *- 4 -*
1.2.2 *Anaplerotic reactions (inorganic carbon fixation)* ..... *- 4 -*
1.3 ***Fungal metabolism and role as decomposers*** ..... ***- 5 -***
1.4 ***Assessing microbial abundance and activity*** ..... ***- 6 -***
1.4.1 *The Biomarker approach* ..... *- 7 -*
1.4.2 *Molecular structure* ..... *- 7 -*
1.4.3 *Fatty Acid nomenclature* ..... *- 8 -*
1.4.4 *Sterols* ..... *- 9 -*
1.4.5 *Taxonomic resolution* ..... *- 9 -*
1.5 ***Stable isotopes as powerful tools to study metabolic activity*** ..... ***- 11 -***
1.5.1 *Isotopes fractionation.* ..... *- 11 -*
1.5.2 *C metabolism* ..... *- 13 -*
1.5.3 *H metabolism* ..... *- 14 -*
1.5.4 *Dual SIP* ..... *- 16 -*
1.6 ***Thesis goals and outline*** ..... ***- 17 -***
2. **Results** ..... **- 18 -**
2.1 ***Summary results of paper I*** ..... ***- 18 -***
2.2 ***Summary results of manuscript II*** ..... ***- 18 -***
2.3 ***Summary results of manuscript III*** ..... ***- 18 -***
2.4 ***Summary results of manuscript IV*** ..... ***- 19 -***
Paper I. ..... - 20 -
Manuscript II ..... - 38 -
Manuscript III ..... - 58 -
Manuscript IV ..... - 75 -
3. **Conclusion and future prospects** ..... **- 92 -**
4. **References** ..... **- 92 -**
5. **Curriculum vitae** ..... **- 104 -**

1. Introduction

Carbon (C) is the fourth most abundant element in the universe. On Earth, C is the building block of all forms of life, including structural molecules such as proteins, carbohydrates, lipids and nucleic acids and other complex compounds. Thus, the well-being and function of our planet depends on biogeochemical cycles of C, and its interactions with Earth's systems. Earth's habitats can be regarded as a mixture of complex redox processes, which are maintained by a constant influx of energy from the sun and the constant heat from the depths of Earth's core. This balance has driven Earth's climate as long as the planet has existed (Madsen et al., 2011), which greatly influences our daily lives. But in turn, anthropogenic disturbances of the balance through rapid release of stored organic carbon from small inactive carbon pools, like fossil fuels, or small active carbon pools, like deforestation, into the small actively cycled pool of the atmosphere over the last 200 years (Francey et al., 2013), have taken a direct influence into Earth's climate. Climate change/global warming has already induced measurable consequences, such as ocean acidification, permafrost warming, and the reduction of ice coverage, which challenge our daily and future lives. Therefore, it is of the uttermost importance to investigate the mechanisms of biogeochemical reactions that occur in water, sediments, and soils to get a better process that have sustained a stable climate and how they will respond to environmental change and future climate developments.

1.1 Soil organic carbon (SOC)

Each year roughly one-sixth of atmospheric carbon (~ 115 Pg C) is cycled through terrestrial vegetation, channeled into the soils below, and respired back to CO_2 (IPCC 2007). In addition to this key flux, soils contain more C than atmosphere and terrestrial vegetation combined, thereby functioning as important environmental reactors in the global C cycle as they represent a major nutrient source for plants and microbial communities (Falkowski et al., 2000; Janzen 2006). Reservoirs of soil organic carbon represent the net balance between C inputs in the form of leaf, stem and root litter accumulating at the surface, with its ultimate source resulting from CO_2 fixation by plants (Trumbore, 1997), and C outputs, including the decomposition of organic C by soil microbes (Tian et al., 2015). SOC stocks typically decrease with depth, having estimations of 2400 Gt C to 2 m soil depth (Beillouin et al., 2022) leaving only a little organic C below the plant root zone (Paul, 2015). SOC storage is controlled by the regional climate, parental material, vegetation, topography, and time, with production and turnover being limited in arid or semi-arid environments were water availability limits net primary production. In contrast, water availability is sufficient in temperate environments where net primary production is limited by nutrient release from microbial activity (Wiesmeier et al., 2019). Small changes in the processing of SOC induces feedback forcing to atmospheric carbon dioxide (CO_2) and methane (CH_4) concentrations and effects soil physical properties, such as soil structure and aggregation, thermal conductivity, soil moisture conditions, soil nutrient availability, and soil biota (Lal, 2004).

Soils are very complex systems which provide a tremendous range of habitats and food sources to support an enormous biomass which is estimated to harbor $5*10^{30}$ prokaryotic cells alone, and harbor much of Earth's genetic diversity (Fuhrman 2009; Sokol et al., 2022). Soil fauna microorganisms (bacteria, archaea, viruses, protists and fungi) are important for the function of the ecosystems due to their cumulative mass and activity, where bacteria and fungi manly dominate the soil microbial biomass by several orders of magnitude over other microbial groups

(Sokol et al., 2022). The complexity of microbial population and its community structure are well acknowledged, and over 99% of the potentially viable microbial species remain unknown due to major challenges in cultivation (Locey and Lennon, 2016; Pedrós-Alió and Manrubia, 2016). An important way to improve our understanding of ecosystem functions is to know the different kinds of organisms and their abundance and variations in time and space (Fuhrman 2009). Soil microorganisms metabolize substrates and/or transform/decompose them into soil organic matter (SOM), which can be more resistant organic compounds, or release them as CO_2 back into the atmosphere (Fuhrman 2009; Trumbore, 1997). SOC turnover thus is an important parameter for biogeochemical model systems to forecast or estimate climate systems and global C cycle developments in the future (Dungait et al., 2012). In practice, components of SOC fall along a continuum of characteristic turnover times from days to centuries (Schmidt et al., 2011; Lehmann & Kleber 2015) within a given ecosystem. But the relationship between SOC reactivity and prolonged forcings, such as climate change and nitrogen pollution, which can affect SOC decomposition and change microbial activity and community structures (Curiel et al., 2007), lead to high uncertainties (Scharlemann et al., 2014). In addition, questions remain regarding whether the turnover of different C stocks behave fundamentally similar. Due to the different microbial communities among leaves, roots and soils, and different chemical composition of such pools, rates of C turnover have the potential to vary widely across generalized classes of C stocks. While several studies reported positive relationships between temperature and SOC turnover (Chen et al., 2013; Trumbore et al., 1996; Bird et al., 1996; Carvalhais et al., 2014), others have called the generality of such relationships into question (Giardina and Ryan 2000). For example, climate is considered to be a "master regulator" of leaf litter (Zhang et al., 2018), root (Gill and Jackson, 2000; Silver and Miya, 2001) and soil organic C pools (Davidson and Janssens, 2006). However, recent findings have pointed out that soil microbial community composition may play a more important role in litter decomposition rates than climate or litter quality (Bradford et al., 2016; Keiser and Bradford, 2017). Therefore, SOC is a key component for estimating the global C budget in the terrestrial biosphere, as well as the interactions among climate, ecosystems, and humans (Tian et al., 2015). However, to reduce the uncertainties in the role of soils in mitigating climate change, new datasets and methods have emerged and still must be developed to refine the estimation of the effects of various drivers on SOC distribution and reactivity (Beillouin et al., 2022).

1.2 Microbial metabolism

To understand the impact of microorganisms on global biogeochemical cycles, including SOM remineralization, one must acknowledge the large diversity of metabolisms that have evolved to gain energy and build up biomass (Pace, 1997). Metabolic diversity can be conceptualized by three criteria: the energy source, the electron donor, and the carbon source (Table 1; Jørgensen, 2006). Most of the substrates taken up by microbial cells are processed through central C metabolic pathways: glycolysis, Krebs (TCA) cycle, and pentose phosphate pathway (PPP). Thus, approximately 60 reactions of heterotrophic central carbon metabolism provide the building blocks and energy at appropriate rates and stoichiometries to fuel about 300 anabolic reactions (Fuhrer & Sauer, 2009). In the context of the reactivity of SOM, OM ultimately derives from plant photosynthesis (light energy), and this energy is transferred to soils by plant litter, root litter and root exudate. Soils provide habit for heterotrophic microbes to mineralize/decompose this OM to CO_2 (catabolism) and build biomass (anabolism). Catabolic reactions supply the organisms with energy, in the form of adenosine triphosphate (ATP), by the breakdown of

compounds (e.g., glucose) into subunits. ATP functions as the universal energy currency for all life on earth. Anabolic reactions, on the other hand, require ATP to assemble macromolecular structures out of subunits or molecular building blocks. Often in soils, the energy source and the carbon source are the same organic molecules (e.g., glucose) owing to the prevalence of heterotrophic metabolism. Heterotrophic microbes also produce new compounds (e.g., as waste) that may contribute to the stabilization of SOM. When microbial substrate use is high (i.e., high-quality litter), the ratio of microbial anabolism to catabolism is high, which results in relatively less CO_2 and more microbial residue production per amount of plant litter metabolized. When substrate use is low (i.e., low-quality litter), microbial biomass is relatively low and fewer microbial residues are produced per amount of plant litter metabolized, resulting in relatively small accumulation of stable SOM (Castellano et al., 2015).

Most of the ATP and biosynthetic precursors that are needed for cell growth and maintenance are produced in these central metabolic pathways (Dijkstra et al., 2011). The C flux through these various pathways varies with the demand for ATP, NADH, NADPH and biosynthetic precursors, substrate availability, and environmental conditions. For example, when soil oxygen concentration is low, C flux through the Krebs cycle is reduced relative to glycolysis (Dijkstra et al., 2011). Temperature decreases often cause a shift in activity from glycolysis and NADH production to pentose phosphate pathway, and NADPH production in cultured microorganisms (Wittmann et al., 2007) and plants (Malone et al., 2006). This shift is thought to be in response to an increased NADPH demand needed to protect the cell against radical oxygen species (Ralser et al., 2007), increased pentose and NADPH demand for biosynthesis (Fuhrer & Sauer, 2009), or a way to maintain high Krebs cycle activity while circumventing temperature-inhibited steps in glycolysis (Dijkstra et al., 2011). The main role of the redox cofactor NADH is to generate ATP via oxidative phosphorylation (Fig. 4). The chemically alike NADPH, in contrast, drives anabolic reductions. To fulfill these functions, the two redox couples are generally not in thermodynamical equilibrium and the NADPH-to-NADP ratio is in a more reduced state than the NADH-to-NAD ratio (Fuhrer & Sauer, 2009). The rate of formation of NADPH depends on the actual C fluxes through these catabolic pathways, which vary significantly with environmental conditions. The anabolic demand for NADPH, in contrast, is coupled to the rate of biomass formation (Fuhrer & Sauer, 2009). Although most biosynthetic reactions use NADPH as a reductant, some NADH coupled reductions occur in the conversion of central metabolites (pyruvate, oxaloacetate, acetyl CoA) to cellular monomers, for example in amino acid biosynthesis (Bakker et al., 2001).

Table 1: Overview of metabolic classification and criteria with representative pathways and organisms (Table taken from Jørgensen, 2006).

Metabolism		Energy source	Carbon source	Electron donor	Organisms
Photoautotroph		Light	CO_2	H_2O	Green plants, algae, cyanobacteria
				H_2S, S^0, Fe^{2+}	Purple and green sulfur bact. (*Chromatium, Chlorobium*), Cyanobacteria
Photoheterotroph			Org. C ± CO_2		Purple and green non-sulfur bact. *(Rhodospirillum, Chloroflexus)*
Chemo-lithotroph	Chemolitho-autotroph	Oxidation of inorganic compounds	CO_2		Aerobic:
				H_2S, S^0, $S_2O_3^{2-}$, FeS_2	Colorless sulfur bact. (*Thiobacillus, Beggiatoa*)
				NH_4^+, NO_2^-	Nitrifying bact. (*Thiobacillus, Nitrobacter*)
				H_2	Hydrogen bact. (*Hydrogenomonas*)
				Fe^{2+}, Mn^{2+}	Iron bact. (*Ferrobacillus, Shewanella*)
					Anaerobic:
				$H_2 + SO_4^{2-}$	Some sulfate reducing bact. (*Desulfovibrio spp.*)
				$H_2S/S^0/S_2O_3^{2-} + NO_3^-$	Denitrifying sulfur bact. (*Thiobac. denitrificans*)
					Nitrate reducing sulfur bacteria *(Thiomargarita)*
				$H_2 + CO_2 \rightarrow CH_4$	Methanogenic archaea
				$H_2 + CO_2 \rightarrow$ acetate	Acetogenic bact.
	Mixotroph		CO_2 or Org. C	H_2S, S^0, $S_2O_3^{2-}$	Colorless sulfur bact. (some *Thiobacillus*)
	Chemolitho-heterotroph		Org. C	H_2S, S^0, $S_2O_3^{2-}$	Colorless sulfur bact. (some *Thiobacillus, Beggiatoa*)
				H_2	Some sulfate reducing bact.
Heterotroph (=chemoorganotroph)		Oxidation of organic compounds	Org. C (max. 30% CO_2)	Org. C	Aerobic: Animals, fungi, many bacteria
					Anaerobic:
					Denitrifying bacteria
					Mn- or Fe-reducing bacteria
					Sulfate reducing bacteria
					Fermenting bacteria
			Org. C_1 (30-90% CO2)	$CH_4 + O_2$	Methane oxidizing bacteria
				$CH_4 + SO_4^{2-}$	Methane oxidizing archaea

1.2.1 Recalcitrant lignin decomposition pathways in soils

Almost 20% of the total C fixed by photosynthesis in land ecosystems is incorporated into lignin, making it the second main constituent of plant biomass after cellulose (Ruiz-Duenas & Martinez, 2009). Lignin consists of 3 major subunits termed hydroxyphenyl (H), guaiacyl (G), and syringyl (S) (Ragauskas et al., 2014); and its decomposition supports detrital food webs and drives macronutrient cycles (Sinsabaugh & Shah, 2011). During the early stages of plant litter decomposition, once the cell wall breaks, the cellulose part becomes easily degradable to glucose and joins the labile C pool. In contrast, the lignin part becomes more stable due to the radical polymerization of substituted phenyl propylene units (Ragauskas et al., 2014) and strong C-C bonds, and therefore, it joins the recalcitrant C pool (Sinsabaugh & Shah, 2011).

1.2.2 Anaplerotic reactions (inorganic carbon fixation)

The main pathway of inorganic carbon fixation during heterotrophic growth is termed anaplerosis or anaplerotic reactions (Kronberg 1965). This process serves as a replenishment flux for intermediates in the TCA cycle, which

have been used up for the synthesis of cellular building blocks (e.g. amino acids and fatty acids) and would otherwise be lacking for the well-functioning of the cell (Erb 2011; Kornberg 1965; Owen et al., 2002). Therefore, heterotrophic CO_2 fixation can account for amount of 2 – 8% of the cell's carbon biomass (Romanenko 1964; Roslev et al., 2004;). Although heterotrophic inorganic carbon uptake has been known for a long time and found in several verities of organisms (Braun et al., 2021 and references within), with the main enzymes pyruvate carboxylase, phosphoenolpyruvate (PEP) carboxylase, PEP carboxykinase, and malic enzyme being responsible for these processes (Owen et al. 2002), they are scarily quantified and represent an underrated but significant role in the global C cycle (Šantrůčková et al., 2018).

1.3 Fungal metabolism and role as decomposers

Fungi (eukaryotes, eumycota) are among the few organisms on the planet that can feed on chemically stable forms of organic C, such as cellulose (Šnajdr et al., 2011) and lignin (Kirk & Farrell, 1987; Fioretto et al., 2005; Baldrian et al., 2011). They are also known to directly access recently produced plant photosynthate (Högberg et al., 2001; Smith & Read, 2008) and even to degrade polyvinyl chloride (PVC) and aromatic hydrocarbons associated with petroleum products and agricultural pesticides (Pepper & Gentry, 2015; Sánchez, 2009). As major decomposers in soil ecosystems, fungi are thought to have been vital for the colonization of land by the ancestors of terrestrial plants, and to have contributed C deposition into geological reserves (Heckman et al., 2001; Simon et al., 1993; Taylor & Sinsabaugh, 2015; Taylor & Osborn, 1996). Their invention of polyphenolic-degrading enzymes (Floudas et al., 2012), and the development of new pathways to degrade recalcitrant structural compounds that are unique to vascular plants (De Boer et al., 2005), paired with their filamentous lifestyle in soil habitats gives them the ability to redistribute C, minerals and water through a vast soil environment (Taylor & Sinsabaugh, 2015). There are two major ecotypes of fungi, mycorrhizal and saprophytic fungi. Mycorrhizal fungi are living in symbiosis in the roots of plants, who provide them with the organic substrates (e.g., sugars) in return for nutrients and water (Jansa et al., 1999). In contrast, saprophytic fungi get their organic substrates by degrading dead material and more recalcitrant OM (Jonas et al., 2007). Their growth and production of cell-wall material, including chitin (as a nitrogenous compound), is crucial to stabilization of soil aggregates, as the fungal hyphae of both mycorrhizal and saprophytic fungi along with fibrous roots, can physically trap soil particles and microaggregates into larger aggregated units (Pepper & Gentry, 2015). Without mycorrhizal fungi, which have established a symbiosis with almost all higher plants to act as their extension of the root system, plant growth would not exist as we know it (Pepper & Gentry, 2015). With the monopolization of two important niches in terrestrial ecosystems, namely mycorrhiza formation and decomposition of lignocellulose, fungi have obtained a pivotal role in the functioning of terrestrial ecosystems (De Boer et al., 2005). Despite their importance, fungal community diversity and functioning remains poorly understood, compared to that of bacterial communities (Anderson & Cairney, 2004).

Fungi can live and survive in almost all prominent soils, thereby serving as a prominent reference point for the "everything is everywhere" hypothesis (Taylor & Sinsabaugh, 2015), with Aspergillus and Penicillium as the most common fungi involved in nutrient cycling in the soil environment (Oliveira et al., 2013; Taylor & Sinsabaugh, 2015; Anderson & Cairney, 2004). They can also be found in deep sea sediments and hydrothermal vents, subglacial sediments, ancient permafrost, sea ice, hot and cold deserts, and soils of Antarctica (Cantrell et

al., 2011). There are roughly 10^6 described taxa (Kirk et al., 2008) and an estimated 5.1 million fungal species (Blackwell, 2011). Fungi generally dominate microbial biomass and activity in soil organic horizons, particularly in forests (Joergensen & Wichern, 2008). Bacterial-to-fungal ratios tend to be lower in acidic, low-nutrient soils with recalcitrant litter and high C-to-N ratios (10-20 for fungi and 5-10 for bacteria) (Fierer et al., 2009); whereas bacteria are increasingly prominent in high N+P, saline, alkaline, and anaerobic (waterlogged) soils (Joergensen & Wichern, 2008). Estimates of fungal biomass turnover in soils are on the order of months (i.e., 130-150 days; Rousk & Baath, 2011), which is comparable to studies of fungal growth rates on submerged litter (Gulis et al., 2008). Saprophytic fungi can be found ubiquitous in soils and are the primary components of fungal food webs. They may decompose more plant residues and soil organic matter than bacteria and therefore help to balance nutrient and OM turnover in soils (Coleman et al., 1983; Jonas et al., 2007). Arbuscular mycorrhizal fungi (AMF) are in symbiosis with plant roots and are responsible for giving plants access to elusive phosphorus and nitrogen reservoirs in exchange for plant derived C (Smith & Read, 2010). Nitrogen is accessed through protein degradation of peptides (Hofmockel et al., 2010) as well as chitin. Some studies have used chitinase activity as an indicator for fungal biomass and metabolism (Taylor & Sinsabaugh, 2015). While most symbioses have positive effects on the productivity of AMFs, some plant species can have a negative effect, which results in very varied and complex effects on plant community and performance (Jonas et al., 2007). Metabolically, fungi are chemoheterotrophs, with most of them being aerobic, but yeasts and zoosporic fungi are anaerobic. These anaerobic fungi generally ferment sugars and produce a variety of useful by-products, such as ethanol, acetic acid and lactic acid, making them important for the production of many staple foods (e.g., yogurt, cheese, bread) and alcoholic products such as beer and wine. Fungi can also produce active secondary metabolites, such as the antimicrobial penicillin produced by Penicillium notatum (Pepper & Gentry, 2015).

1.4 Assessing microbial abundance and activity

Microorganisms are too small to be seen with the naked eye (typically 0.5-10 µm). Therefore, classical environmental microbiological investigations began with counting cells under the microscope (Kallmeyer et al., 2012; Parkes et al., 2014), which normally includes staining of nucleic acid-binding dyes (e.g., 4′ 6-diamidino-2-phenylindole (DAPI); Hamada & Fujita, 1983). While cell counting provides a general overview of the abundance of microorganisms, it cannot decipher microbial community composition or determine their activity. Nowadays, the most frequently used method to analyze microbial communities, abundance, and activity, is by targeting the genetic material and information encoded in DNA and RNA. In particular, the genes encoding for 16S rRNA or 18S rRNA are commonly sequenced, due to their hyper conservative and hyper variable regions (Pepper & Gentry, 2015), to determine prokaryotic and eukaryotic phylogenetic diversity (Killham & Posser, 2015; Tringe & Hugenholtz, 2008). This technique informs many characteristics of the microorganism, including its phylogenetic lineage and metabolisms it may perform (e.g., methanogenesis, sulfate reduction). Amplicon sequencing of rRNA has projected, as for example, only around 0.001 - 1% of the entire microbial community is estimated to be accessible to cultivation (Amman et al., 1995; Rappe & Giovannoni, 2003; Joint et al., 2010). However, the presence of gene sequences in natural samples does not necessarily indicate the activity of the corresponding microorganisms nor the magnitude of their metabolic fluxes. DNA and RNA are labile compounds

that degrade quickly after cell death (Schippers et al., 2005). While they are presumably representative of active microbial populations, newer studies show that DNA can also persist in the environment after cell death and can therefore represent information of past microbial communities (Tori et al., 2015).

1.4.1 The Biomarker approach

Biomarker molecules are natural products with distinctive structural and/or isotopic attributes that encode the origins of the molecule. They are readily measured in environmental samples because their recalcitrant nature allows them to be tracked through chemical changes that ensue after death (diageneses). For environmental studies, there are only a limited number of effective biomarkers assigned to well-defined sources, but they can be proxies for different biogeochemical processes taking place in modern environments as well as chemical fossils that afford a palaeobiological record of the past activities of living communities (Summons & Lincoln, 2012). For a biomarker to serve as an indicator of activity, it is essential that it be removed from the system upon cell death. This underpins the use of intact polar lipids (IPL), which are major components of the cell membranes of living organisms and stay intact in living cells, but hydrolyze quickly after cell death (Harvey et al., 1986). Therefore, they have the capacity to reflect changes in microbial populations (Watzinger, 2015; Evershed et al., 2006). It worth to note that the most studied molecular biomarkers in the environment are lipids because other biomolecules, such as carbohydrates, proteins, and nucleic acids cycle more rapidly, are accessible food sources for bacteria and fungi (Summons & Lincoln, 2012), and generally do not accumulate to the quantities of discernable individual lipids after the death of a cell.

1.4.2 Molecular structure

Lipids are the main building blocks of microbial cell membranes (Fig. 1), which separate the cytoplasm from the extracellular environment. This physical barrier also contains coordinated protein systems that control the fluxes of ions, nutrients, and metabolic products to be taken into the cell or released from the cell. Membrane lipids are composed of a hydrophilic polar head group, a backbone (often glycerol-based), and a hydrophobic tail, altogether forming an intact polar lipid (IPL).

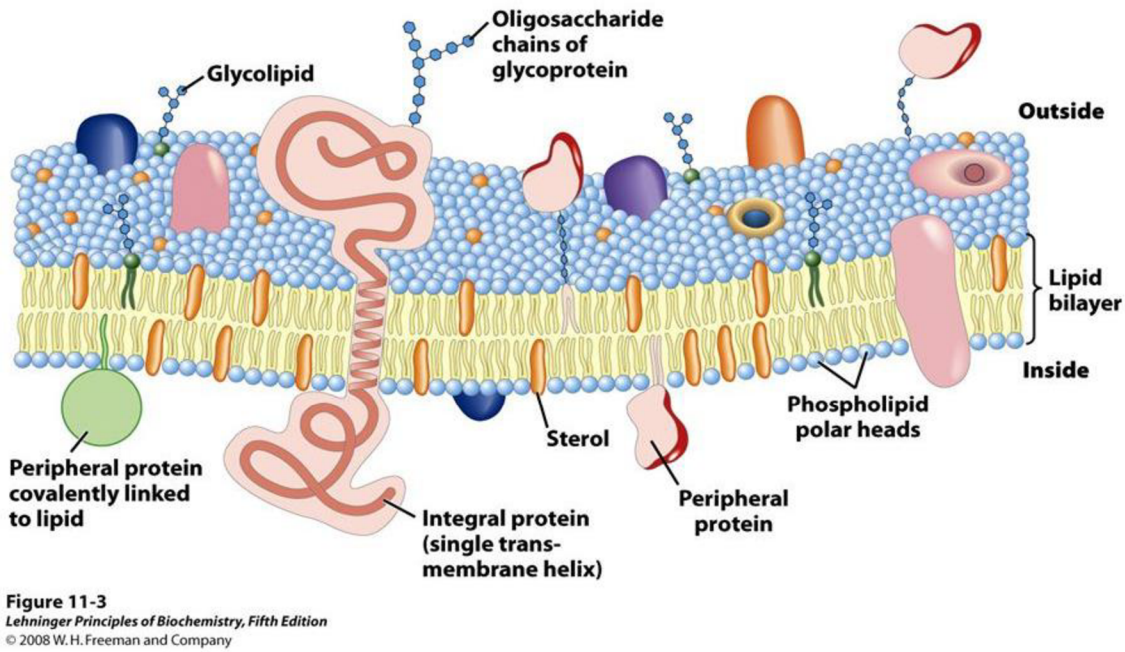

Figure 1: Microbial membrane consists of a lipid bilayer which includes the fatty acids (core) bound to a polar head group. Also, in the membrane are proteins and carrier systems as well as sterols. Figure taken from Nelson & Cox, 2008.

Examples of polar head groups are glycosidic, phosphatidyl (i.e., PLFA), amino- or sulfate based. After cell death, the bonds to hydrophilic head groups are hydrolyzed quickly, leaving only the backbone with its hydrophobic tail, which is referred to as a core lipid (CL; (Harvey et al., 1986). The fluidity of the microbial membrane to allow either solutes transfer, or retention is thought to depend on the composition and structure of the hydrophobic tail, which in turn, depends on environmental conditions, such as temperature, salinity, and nutrient availability (Beney and Gervais, 2001). CLs are relatively resistant to degradation and last as molecular fossils in the geological record (Kuypers et al. 2011). They can be used as proxies of past environmental conditions (e.g., Brassell et al., 1986; Schouten et al., 2002). Thus, chemical signatures of these molecules may reveal both the dominant metabolic pathways and activity of microbial populations, because organisms may adapt their membrane lipid structures to environmental changes. This approach has led to the development of organic geochemical proxies to explore both present and past environments.

1.4.3 Fatty Acid nomenclature

Based on guidelines of the International Union of Pure and Applied Chemists (IUPAC) and the International Union of Biochemistry and Molecular Biology (IUBMB), the nomenclature of lipids falls into two main categories: systematic names and common names (Fahy et al., 2009). Fatty acids nomenclature starts usually by the indication of the chain length of carbon atoms (C) and is separated by a colon for the degree of unsaturation (D) (e.g., for octadecanoic acid or stearic acid C:D is C18:0). The location of the double bond (i.e., unsaturation) is followed by a Δ (nearest to the carboxyl end) or ω (nearest to the aliphatic end) and a number which indicates the position of the unsaturation (C18:1ω6 or C18:1Δ12). The prefixes a, i, cy, and d refer to anteiso, iso, cyclopropyl branching and dicarboxylic fatty acids, respectively. ME indicates the position of a methyl group. The prefixes α and β indicate that the OH groups of a hydroxy fatty acid are located at positions 2 and 3, respectively, while numbers preceded by v indicate the position of OH groups from the aliphatic end of the fatty

acids (Zelles, 1999).

1.4.4 Sterols

Sterols are essential components of the membrane as their concentration and functions include the control of membrane fluidity and permeability (Bossche, 1990; Volkman, 2003). They are synthesized from the basic unit of the five-carbon branched isoprene groups, isopentyl pyrophosphate (IPP) and dimethylallyl pyrophosphate (DMAPP). In plants and animals, these precursors are used to synthesize a variety of lipids that include cholesterol, vitamin D, coenzyme Q, and steroid hormones (Watts & Ristow, 2017). Sterol abundances in organisms are almost constant and account for ca. 0.1% wet weight (Nes, 1974), with the predominant fungal sterol, ergosterol, comprising up to 10% of the cell dry weight (Rodriguez et al., 1985).

1.4.5 Taxonomic resolution

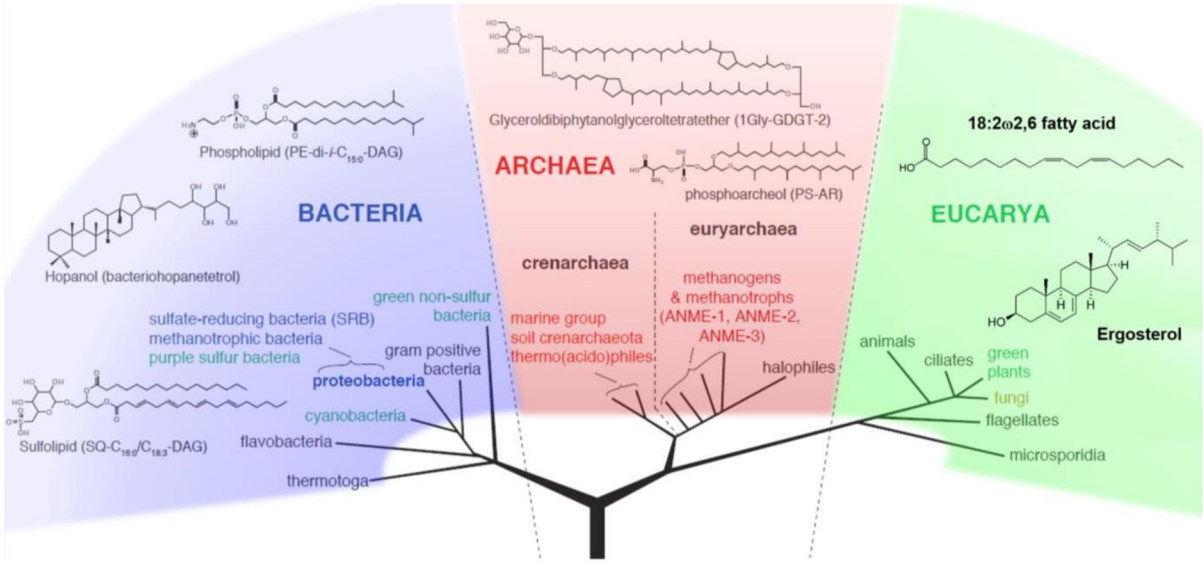

Figure 2: Biomarker Tree of Life. Modified after Schubotz 2009.

Although lipid biomarkers provide relatively low taxonomic resolution (≈ phyla; Fig. 2; Table 2), this approach remains useful for constraining fungal abundance distributions in the environment. Indeed, fungi were shown to correlate with the concentration of the fatty acid 18:2ω6,9 in soils (Frostergard & Baath 1996; Olsson & Wallander 1998), although this lipid is missing in arbuscular mycorrhizal fungi (Butler et al., 2003; Olsson et al., 1995). But, phospholipid fatty acid (PLFA) content varies significantly between fungal species (Klamer & Baath 2004), thereby introducing uncertainty in PLFA-based estimates of fungal biomass. In addition to fatty acids, fungal cell membranes also contain ergosterol, which has served as a useful target for estimating of fungal production (Gulis & Bärlocher, 2017; Lau et al., 2006). However, ergosterol cell quota is also known to vary between species, cultivation media, and with culture age (e.g., Klamer & Baath 2004). Despite these caveats, lipid biomarkers have offered key insights into the metabolic potential of fungi to access C substrates (e.g., Treonis et al., 2004), the environmental factors that may control fungal production (e.g., Rousk et al., 2009), and the relative rates of fungal versus bacterial turnover in soils (e.g., Rousk & Frey, 2015). Each of these studies were able to track fungal controls on soil C flow via the stable C isotope labeling of fungal lipid biomarkers.

Table 2: Fatty Acid biomarker and their taxonomic potential from different studies (Table modified after Vestal & White, 1989; Zelles, 1999; and references within).

Indicator	Indicator	Interpretation	reference
PLFA	Phospholipids Fatty Acid	Microbial biomass	Zelles et al., 1994, 1995, 1999
FA	Fatty acids		
EL-SATFA	Ester-linked saturated FA	Prokaryotes, eukaryotes	Balkwill et al., 1988
Straight	straight chain FA	eukaryotes; widsread	
15:0, 17:0		Eubacteria Common markers	Vestal & White 1989
16:0,		Fungi	Zelles 1997
Straight >20C	saturated straight chains longer then 20C	eukaryotes; mosses, vascular plants	
Cy	Cyclopropyl rings in FA	gram negative bacteria (Rhodospirillum, Cromatium/legionella); gram positive bacteria (Clostridium, Bifidobacterium	
cy17:0, cy19:0		Anaerobes	Federle 1986
cy15:1		Clostridia	Bobbie & White 1980
iso/anteiso		gram negative bacteria (Cytophaga, Acetobacter, Flavobacterium), gram positive bacteria,	Brennan 1988; Haack et al., 1994
i15:0, a15:0, i17:0, a17:0, a19:0, i19:0		Eubacteria Common markers	Vestal & White 1989
Br	unknowing methyl branching position	gram positive bacteria (Actinomycetes)	Lechevalier and Lechevalier 1988
10ME	Methyl branching on 10C atom	Actinomycetes Same as eubacteria plus 10Me18:0	Kroppenstedt 1992; O'Leary & Wilkinson 1988
10Me16:0		Sulfate-reducing bacteria	
EL-MUFA	Ester-linked monounsaturated FA		
16:1ω3t		Plants and green algae Diatoms	Gillian & Hogg 1984
16:1ω5, 18:1ω5		Eubacteria Common markers	Vestal & White 1989
17:1ω6		Sulfate-reducing bacteria	
ω7	Vaccenic type (anaerobic desaturase pathway)	gram negative aerobes, strictly anaerobes	
16:1ω7, 16:1ω7t, 18:1ω7		Aerobes	Guckert et al., 1986
i17:1ω7		Sulfate-reducing bacteria	
18:1ω7t		Eubacteria Common markers	Vestal & White 1989
ω8		Methane-oxidizing bacteria	Bowman et al., 1993
ω9	Oleic type (C18)	Gram positive bacteria, widespread	
16:1ω9		Eubacteria Common markers	Vestal & White 1989
18:1ω9		Fungi, Green algae, Higher plants	Zelles 1997, Galbraith & Wilkinson 1991
18:1ω11		Higher plants	Galbraith & Wilkinson 1991
16:1ωl3t,		Green algae	
C16		Type I methanotrophs	Bowman et al., 1993
EL-PUFA	Ester-linked polyunsaturated FA	Eukaryotes; cyanobacteria	Lösel 1988
C18:2ω6, 18:3ω6, 18:3ω3		Fungi	Zelles 1997
20:5, 22:6		Barophilic, psychrophilic bacteria	DeLong & Yayanos 1986
20:3ω6, 20:4ω6		Protozoa	
20:5ω5, 20:5ω3		Plants and green algae Diatoms	Gillian & Hogg 1984, Galbraith & Wilkinson

			1991
18:3ω3		Green algae, higher plants	Galbraith & Wilkinson 1991
16:3ω6		Microalgae	
EL-HYFA	Ester-linked hydroxy FA		
Alpha (α)	Hydroxy substitution at 2 positions nearest to carboxyl end	Pseudomas, Gram negative bacteria, actinomycetes	Galbraith & Wilkinson 1991,
Beta (β)	Hydroxy substitution at 3 positions nearest to carboxyl end	Mycobacterium	
Omega (ω)	Hydroxy substitution at 2 positions nearest to aliphatic end	Fungi	
Mid-chain	unknown position of hydroxy group		

1.5 Stable isotopes as powerful tools to study metabolic activity

DNA and RNA sequencing has evolved in recent years and provides considerable insight into microbial metabolism (Blattner et al., 1997; Rowland et al., 2018), but these techniques alone cannot quantitatively constrain metabolic activity or carbon substrate utilization. In contrast, isotope studies extend our understanding of global geochemical cycles and reach down to the metabolism of a single cell (Johnston & Fischer, 2012). Thus, stable isotopes emerged as tools for biogeochemists to investigate natural and experimental systems aiming to shed light on unexplored interrogatives from microbial metabolism in modern and ancient environments. Therefore, experiments studying the isotopic composition of biomass in comparison to the available substrates (either using natural abundance or isotope labeling experiments; Fig. 9) are performed to assess microbial substrate utilization, based on the "you are what you eat" hypothesis (e.g., Hinrichs et al., 1999, Lin, 2009). Such studies provide insights about their metabolic strategies by identifying the flow of carbon through an ecosystem (e.g., $\delta^{13}C$ of carbon sources; Hinrichs et al., 1999; Fig. 9). As microbial growth rates and turnover time can differ drastically among organisms (Lin, 2009), stable isotope probing (SIP) techniques have been developed to target specific autotrophic and heterotrophic metabolic pathways. SIP introduces an isotopically labelled substrate to a microorganism or a community by increasing the natural abundance of certain isotopes in growth media or the local environment. The fate of this isotope spike is subsequently tracked via analysis of biomolecules indicative of cell growth or metabolism, thereby increasing our understanding of how the original substance is processed throughout the cell and the biochemical (or physiological) processes involved (Staddon, 2004).

1.5.1 Isotopes fractionation

Many of the biologically essential elements have more than one stable isotope (e.g., hydrogen (^{1}H, ^{2}H), carbon (^{12}C, ^{13}C), nitrogen (^{14}N, ^{15}N), oxygen (^{16}O, ^{17}O, ^{18}O), sulfur (^{32}S, ^{33}S, ^{34}S, and ^{36}S), and iron (^{54}Fe, ^{56}Fe, ^{57}Fe, and ^{58}Fe)). The chemical properties of a given element are controlled by the number of protons (H^{+}) that element contains and its configuration of electrons (e^{-}). In addition to protons, the nucleus (core) of an atom also contains neutrons (n) that have a similar mass but have no charge. Isotopes are defined by the sum of protons and neutrons. Because isotopes of an element contain the same number of protons and only differ in the number of neutrons, all isotopes of the same element undergo similar chemical reactions. (Johnston & Fischer, 2012). For example, the atomic mass of carbon isotopes ^{12}C to ^{13}C differ by ca. 8% in mass, and although they have the same chemical properties, the strength of the bonds they form and the rates at which they react are related to the mass of the

isotope. Differences in bond energies caused by isotopic substitution (i.e. ^{13}C taking the place of ^{12}C), can be expressed with the concept of zero-point energies (ZPE) (Johnston & Fischer, 2012). As heavier isotopes are exchanged into a molecule, the energy required for breaking this bond increases, and as a result, the bonds are more difficult to dissociate; this leads to a preferential breaking of bonds with the lighter isotopes. The influence of mass on bond energy is the principal driver of isotope effects. Knowledge of the variations in the relative abundance of the isotopes of an element allows us to evaluate the various geochemical and biochemical cycles through which the element passes (Craig, 1957).

Equilibrium isotope exchange reactions involve the redistribution of isotopes of an element among various species or compounds (in a strict sense, this only occurs in a closed, well-mixed system at chemical equilibrium). At isotopic equilibrium, the forward and backward reaction rates of any isotope are identical (Kendall & Caldwell, 1998). This does not mean that the isotopic compositions of two compounds at equilibrium are identical, but only that the ratios of the different isotopes in each compound are constant for a certain temperature. During equilibrium reactions, the heavier isotope generally preferentially accumulates in the species or compound with the higher oxidation state, for example, $\delta^{13}C$ and $\delta^{18}O$ values increase in the order: $CO_2 < HCO_3^- < CaCO_3$. During phase changes, the ratio of heavy to light isotopes in the molecules in the two phases changes. For example, as water vapor condenses in rain clouds (a process typically viewed as an equilibrium process), the heavier water isotopes (^{18}O and ^{2}H) become enriched in the liquid phase, while the lighter isotopes (^{16}O and ^{1}H) remain in the vapor phase. In general, the higher the temperature, the less the difference between the equilibrium isotopic compositions of any two species (because the differences in ZPE between the species become smaller) (Kendall & Caldwell, 1998).

The fractionation associated with the equilibrium exchange reaction between two substances *A* and *B* (i.e., the fractionation of *A* relative to *B*) can be expressed using the isotope fractionation factor α (alpha; eq. 1).

$$\alpha_{A-B} = \frac{R_A}{R_B}$$

Equation 1: The fractionation factor α is calculated by the isotope ratio (R= heavier to lighter isotope) of compound A and B

The value of α depends mainly on temperature, but chemical composition, crystal structure and pressure may also play a role. For simple molecules, α values are calculated based on spectral data and differ only by small percent from the equal-energy value of 1.00 (Kendall & Caldwell, 1998). Because the fractionation factors are close to 1, they are also expressed as ε (epsilon, isotope enrichment factor; eq. 2; Hoefs, 2018).

$$\varepsilon_{A-B} = (\alpha_{A-B} - 1) * 1000$$

Equation 2: The isotope enrichment factor is calculated based on the fractionation factor and is reported in ‰ values.

In environmental sciences, the report of isotopic compositions of compounds are commonly referred to as δ-values (delta; eq. 3; Hoefs, 2018) or are reported in terms of fractional abundance (Neubauer et al., 2018; eq. 4).

$$\delta_A = \left(\frac{R_A}{R_{std}} - 1\right) * 1000\ (‰)$$

Equation 3: The δ-notation with R_A as the ratio of compound A and R_{STD} as the ratio of the known standard. Δ-values are reported in ‰

$$F^A = \frac{R_A}{(1 + R_A)}$$

Equation 4: The Fractional abundance is based on the Ratio of one compound and is reported in %.

Kinetic fractionation effects occur when the rate of a chemical reactions is sensitive to atomic mass at a particular position in one of the reacting compounds (Hoefs, 2018). Most of the fractionations associated with biological processes are of kinetic fractionation (Johnston & Fischer, 2012). Because reaction rates are isotope specific, and lighter isotopes react more quickly, the products of a reaction preferentially accumulate the light isotopes (Hoefs, 2018; Johnston & Fischer, 2012). Kinetic isotope effects associated with enzymatic processes are often difficult to define, because local (intracellular) conditions influence both substrate concentrations and the activity of the enzyme, and subsequently alter the fractionation. Most biological processes involve numerous enzymatic steps, meaning that the net fractionation for a given process is the sum of a series of intermediate steps (Hayes, 2001).

1.5.2 C metabolism

C isotopes in natural systems vary in a broad range (Fig. 3). The ratio of ^{12}C to ^{13}C in environmental samples is expressed in the δ (‰) notation, determined relative to a reference standard Vienna Pee Dee belemnite (VPDB) (eq.5).

$$\delta^{13}C\ (sample) = \left(\frac{\frac{13C}{12C}(sample)}{\frac{13C}{12C}(VPDB)} - 1 \right) * 1000$$

Equation 5: the VPDB $^{13}C/^{12}C$ ratio is accepted to be 0.0112372 and has per definition a $\delta^{13}C$ value of 0‰

The enzymes involved in the metabolism of carbon substrates react more rapidly with the lighter isotope (e.g., ^{12}C) than the heavier isotope (e.g., ^{13}C) due to the higher bond strength of the latter, leading to a kinetic fractionation effect. The lighter isotope is therefore preferentially metabolized in biosynthetic products, enriching the reactant substrate in the heavier isotope (Hayes, 2001). One example for C fractionation can be found in plants. Photosynthetic pathways of C3 and C4 differ significantly in their isotopic composition. C3 plants utilize the Calvin pathway and incorporate atmospheric CO_2 by carboxylation of ribulose bis-phosphate (RuBP), producing first a C3 molecule, whereas C4 plants use the Hatch-Slack pathway and incorporate CO_2 by carboxylation of phosphoenolpyruvate (PEP), producing a C4 molecule. The different carboxylase enzymes discriminate differently toward ^{13}C, and as a result, the $\delta^{13}C$ values of C3 plants generally range from -32‰ to -22 ‰, in contrast those of C4 plants range from -23‰ to -9‰ (Rounick & Winterbourn, 1986). Another example for tracing metabolic pathways in environmental samples is the anaerobic oxidation of methane in anoxic marine sediments, which leads to extremely low $\delta^{13}C$ values of membranes lipids of archaea, because they consume methane that is depleted in ^{13}C due to the kinetic isotopic fractionation of enzymes involved in methanogenesis (Elvert et al., 1999; Hinrichs et al., 1999). Boschker et al. (1998) reported SIP as a technique to link specific biogeochemical processes to microbial metabolic pathways in environmental samples by tracing the incorporation of ^{13}C-labeled substrates into biomass. SIP has been broadly applied for labeling DNA, RNA (Manefield et al., 2002; Friedrich, 2006; Uhlik et al., 2009), proteins (von Bergen et al., 2013) and lipids (Whitby et al., 2005; Kreuzer-Martin, 2007).

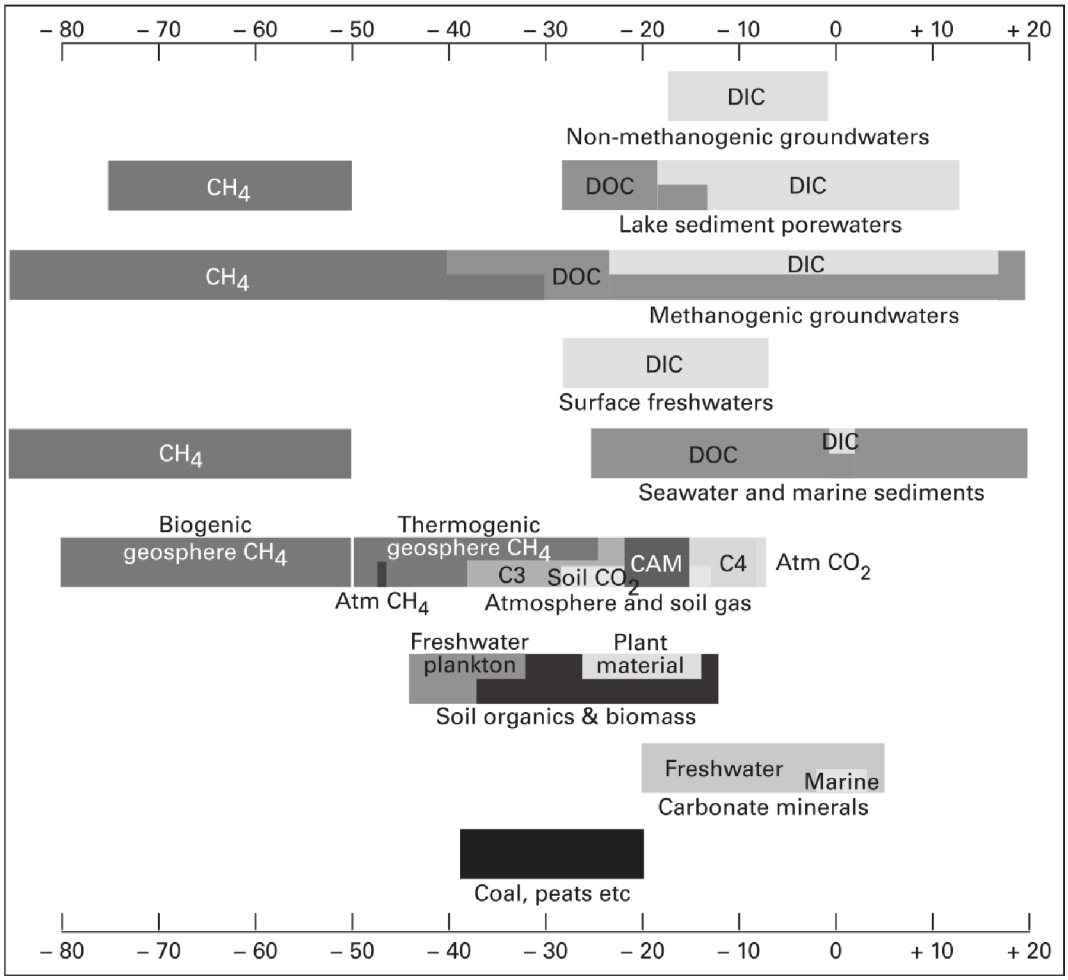

Figure 3: Carbon $\delta^{13}C$ ranges of different species and sources (axis in permil to VPDB). Figure from Darling et al., (2006).

1.5.3 H metabolism

Similarly to carbon, stable isotope ratios of hydrogen, i.e., protium ^{1}H and deuterium ^{2}H or D ($^{2}H/^{1}H$ or D/H ratio), are recurrently reported using the δ notation (eq. 6), relative to the internal standard Vienna Standard Mean Ocean Water (VSMOW). The low relative natural abundance of D (^{D}F = 0.015 %) enables the use of very small amounts of label to achieve high sensitivity of the isotopic tracer (Kopf et al., 2015).

$$\delta D(sample) = \left(\frac{\left(\frac{D}{H}\right) sample}{\left(\frac{D}{H}\right) VSMOW} - 1 \right) * 1000$$

Equation 6: the VSMOW D/H ratio is accepted to be $155.76*10^{-6}$ and has per definition a δD value of 0‰

Additional calculations are required for water isotope fractionation factors (eq. 7). The relationship between water and lipid hydrogen isotopes of newly synthesized fatty acids comprehends the combination of the mole fraction of water-derived hydrogen and associated net hydrogen isotope fraction with substrate-derived hydrogen, which includes metabolic water with average substrate isotopic composition and associated net isotope fractionation (Kopf et al., 2015).

$$F^{D}{}_{Lipid} = X_w * \alpha_{Lipid/water} F^{D}{}_{water} + (1 - X_w)\, \alpha_{Lipid/substrate} F^{D}{}_{substrate}$$

Equation 7: $F^{D}{}_{Lipid}$, $F^{D}{}_{water}$ and $F^{D}{}_{substrate}$ are the measured deuterium fractional abundance of lipids, water, and substrates, respectively. X_w $\alpha_{Lipid/water}$ (a_w) is defined as the water hydrogen assimilation factor, which is a physiological factor and indicates the ultimate water hydrogen contribution to lipids without considering the net isotope fractionation factor (Kopf et al., 2015).

Strong relationships between microbial lipids and water have also shown to be a useful tracer of microbial activity of a total community in a diverse range of environments (Caro et al., 2023; Huguet et al., 2017; Kellermann et al., 2012; Kopf et al., 2015), as water is required by all microbes. Water is the ultimate source of H in all-natural organic compounds (Hoefs, 2018; Kopf et al., 2015). Hydrogen isotopes have the strongest kinetic isotope effect due to the large difference in atomic mass between protium and deuterium. In chemical and biochemical reactions, deuterium reacts slower than protium, due to the lower ZPE of D-C bonds relative to H-C bonds (Kselíková, 2019). δD-variations in individual compounds within a single cell or organism can be related to differences in biosynthesis, as large H-isotope fractionations, with δD-values between −400‰ and +200‰, have been observed during biosynthetic hydrogen conversion of water to organic matter (Sachse et al., 2012; Zhang et al., 2009). Accurate isotope fractionation factors among organic molecules and water are difficult to determine, although tremendous progress to elucidate the δD of individual biochemical compounds has been achieved through the introduction of the compound-specific hydrogen isotope analysis (Sauer et al., 2001; Sessions & Hayes, 2005). For example, strong correlations between hydrogen isotopes of water medium and microbial lipid were shown to also correlate with the type of metabolism used during growth (e.g., heterotrophs *vs* chemoautotrophs, Fig. 4; Zhang et al., 2009)

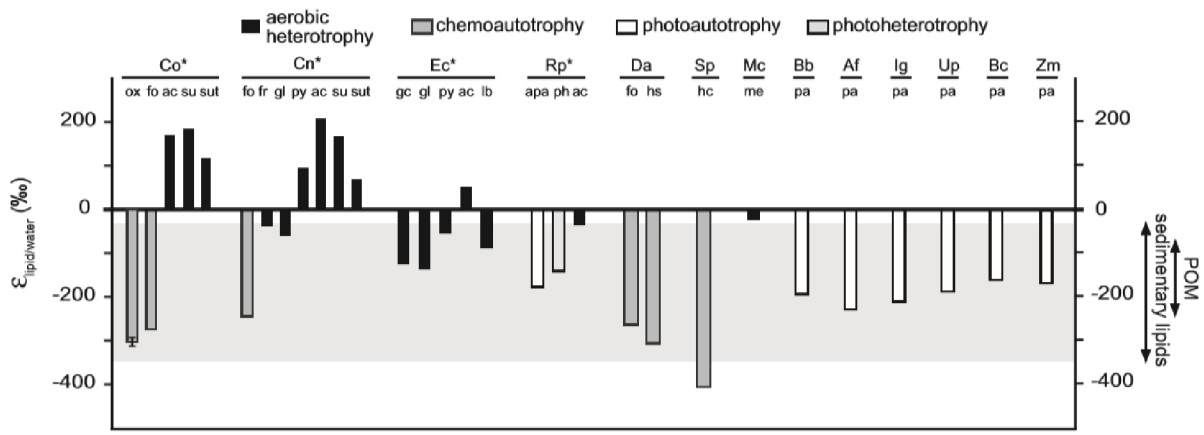

Figure 4: Incubation experiment results by Zhang et al., 2009. Summarized are the D/H fractionation values of the fatty acid (palmic acid) and medium water in the observed culture experiments for different bacteria fed with different substrates. (Figure taken from Zhang et al., 2009).

Variability in fatty acid hydrogen isotopes is suggested to be controlled by the involvement of the hydrogen transporters and electron acceptor NADPH and NADH, as they are the main portals for hydrogen transport (accounting for around 50%) in fatty acid biosynthesis pathways, 25% coming directly from the water and 25% coming from the acetyl-CoA (Wijker et al., 2019; Zhang et al., 2009). The isotopic composition of the H transferred from NADPH to biosynthetic substrates is one of the most important factors controlling the hydrogen isotopic composition of organic matter (Hayes, 2001). Specialized mechanisms exist for the oxidation of NADH and for the reduction of NADP+. If they are not activated and do not continuously regenerate NAD^+ or NADPH, the amount of oxidation or reduction that can occur within a cell is strictly limited (Hayes, 2001). It was confirmed

that dehydrogenases and transhydrogenases play a major role in lipid δD values, but the kinetic isotopic fractionation of these reactions are relatively constant across different organisms (Wijker et al., 2019).

1.5.4 Dual SIP

To fully exploit the potential of SIP experiments, a new lipid-based dual-SIP approach was developed to track total microbial production by adding heavy water (D_2O) together with labeled ^{13}C-DIC to enable estimates of total and autotrophic metabolism, respectively (Wegener et al., 2012; Fig. 5). Because bicarbonate is often present in relatively high abundances in natural systems, adding ^{13}C-bicarbonate and D_2O to incubation experiments does not change or alter biogeochemical conditions (Wegener et al., 2012). The ratio of D_2O incorporation and ^{13}C assimilation rates into lipid biomarkers can then distinguish microbial metabolism of autotrophs (ratio ~1) and heterotrophs (ratio < 0.3) (Fig. 5; Wegener et al., 2012) The latter cutoff owes to heterotrophic assimilation of inorganic carbon (e.g. CO_2) via anaplerotic reactions (section 1.2.2) that remove intermediates from the tricarboxylic acid cycle (Kornberg, 1965). Due to hydrogen incorporation into lipids from the available hydrogen of water, microbes may incorporate the spiked water hydrogen isotopes without discrimination. Total lipid production rates are based on D incorporation, and inorganic carbon assimilation indicates autotrophic production, which are calculated according to Wegener et al., 2012 (eq. 8).

$$prod_{Lipids} = conc_{lipids} \times \frac{\Delta F^{D}{}_{Lipid}}{F^{D}{}_{med} \times time}$$
$$assim_{IC} = conc_{Lipid} \times \frac{\Delta F^{13C}{}_{Lipid}}{F^{13C}{}_{med} \times time}$$

Equation 8: lipid concentration ($conc_{lipid}$), the fraction of isotopic label in the medium (F^{D}_{med}, F^{13C}_{med}), and enrichment of label in fungal lipid (ΔF^{D}_{lipid}, ΔF^{13C}_{lipid}), where F^{D} and F^{13C} in lipids and incubation medium are calculated from the isotope ratios $F^{D} = R^{D/H}/(R^{D/H} + 1)$; $F^{13C} = R^{13C/12C}/(R^{13C/12C} + 1)$ (Hayes, 2004).

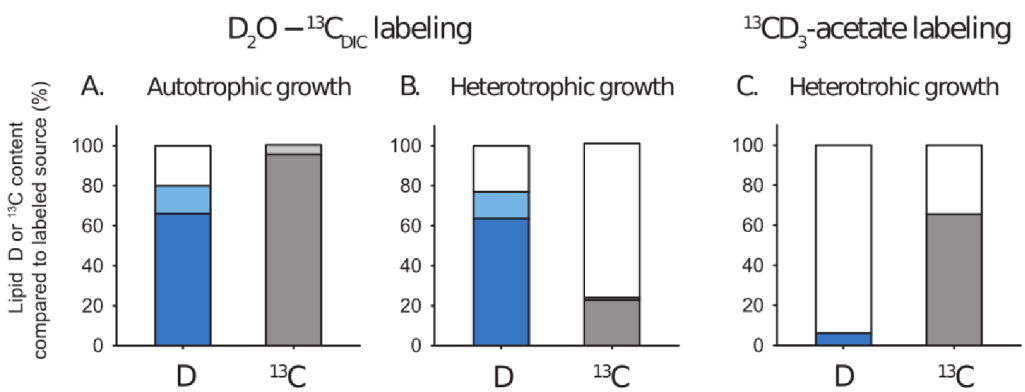

Figure 5: Dual-SIP experiment of Desulfosarcina variabilis grown on different substrates and labeled compounds. Panel A (hydrogen as energy source) and B (acetate as energy source) were labeled with ^{13}C-DIC and D_2O to distinguish autotrophic vs. heterotrophic growth (light bars include corrections for isotope fractionations). Figure from Wegener et al., (2012).

1.6 Thesis goals and outline

This doctoral thesis aimed (i) to assess the isotope signals of membrane lipids from fungi grown under different carbon substates (labile *vs* stable) and (ii) to use the insights gained to develop a dual stable isotope probing approach for evaluating fungi-related C turnover in subsurface environments. In order to address the research goals, (A) the isotopic signals of saprotrophic fungi grown on different substrates (labile vs. stable C) were determined for fungal membranes from pure cultures and (B) the dual stable isotope probing approach of adding labeled inorganic carbon and heavy water was employed as an assay to assess the substrate specific assimilation rates, and predominant mechanisms of C turnover in in soils and aquatic ecosystems based on the culture-determined isotopic signals. Isotopic signals from fungal membranes were addressed in one peer-reviewed publication, while assays improving the scope and showing the applicability of the dual stable isotope probing assays are found in three different manuscripts. All publications and manuscripts are indexed in the following section.

2. Results

2.1 Summary results of paper I

In the first paper we investigated the isotopic signatures of inorganic C assimilation and heavy water incorporation into different fungal species belonging to the Ascomycota, when grown in pure cultures with the relatively labile C substrates of glucose and glutamic acid. We tested if we could distinguish between the two metabolic pathways based on the fungal biomarker C18:2ω6 and Ergosterol. Also, we developed an assay to measure fungal biomarkers via Pyrolysis-GC-IRMS to directly combust the biomass and access the biomarkers without excessive wet chemistry works. Our results demonstrated that the application of Pyr-GC-IRMS is a good alternative to measure fungal biomarkers for their isotopic signatures of ^{13}C and ^{2}H but lacks in the analysis to quantify its lipid content. We could also demonstrate that the isotopic signatures of the different fungal species were distinguishable between the fungi grown on glucose vs glutamic acid when applying the Dual-SIP assay and calculating the ratio of inorganic ^{13}C assimilation vs the water assimilation factor. This works very well for the fatty acid biomarker, but for ergosterol there was no distinguishable signal, therefore we concluded that ergosterol might not be good marker for labile substrates but still needs to be tested for labile vs stable C substrates.

2.2 Summary results of manuscript II

In the second paper we continued the investigation of isotopic signatures of fungal biomarkers with a more diverse selection of fungal species of Ascomycota, Basidiomycota and Zygomycota grown on glucose, succinic acid as the labile substrates and β-cyclodextrin and tannic acid as more complex substrates. Here we applied the pyrolysis assay that we developed in paper I to analyze the lipid biomarkers without wet chemistry extractions. Not all fungal species were able to grow on all substrates. There was a significant difference in substrates that presumably triggered the glycolysis pathway verses TCA cycle, when comparing the assimilation of ^{13}C and ^{2}H incorporation into fungal biomarkers, but no distinction could be obtained between the labile and the more complex substrate utilization. Nevertheless, we could demonstrate a broader scope of water assimilation for fungal lipids and put forth that the average water assimilation for fungal lipids varies around 69%, and that fungal lipid C can have a contribution of less than 3% from inorganic C assimilation.

2.3 Summary results of manuscript III

In the third paper we applied the dual-SIP assay to different layers of soil from the nature reservation area Blanský les (Czech Republic). Our goal was to quantify the production and turnover rates of bacteria and fungi in different soil horizons during spring and autumn seasons, which should offer a diverse spectrum of C substrates. We could demonstrate that fungal biomass was dominating root and O horizon and had equal contributions in the A horizon in both seasons, but bacteria had higher production and turnover rates in spring which reversed in Autumn. Only in the root incubations did fungal biomass and production dominate in both seasons, and fungal turnover times were always faster in in autumn compared to spring. The SIP approach could discern the activity of highly abundant and minor populations of microorganisms (e.g., SRB), and we were able to identify which populations were most active in relation to carbon use efficiency estimates. These fluxes likely depended on the available C

substrate and growth strategies of bacteria and fungi, and our estimates have informed the C demand of the local heterotrophic microbial community.

2.4 Summary results of manuscript IV

In the fourth paper we tested the dual-SIP assay in an aquatic environment in the subalpine oligotrophic lake Lunz (Lunz am See/Austria). Our goal was to quantify the microbial and fungal activity in the lake in different seasons (spring and autumn) and different depts (Epilimnion and Hypolimnion) for inorganic C uptake and total biomass production without the influence of phytoplankton. Our results demonstrate that biomass C was equally distributed between the depths in both seasons, but the total C biomass was 80 times higher in spring than in autumn. By comparing turnover times among heterotrophic taxa, we could conclude that fungal turnover times and likely their roles in the hypolimnion ecosystem modulated between spring and autumn, even though fungal contribution was only in the minor component of a quite active community. Fatty acids that acquired inorganic C were identified based on the rates of inorganic C assimilation vs production and were attributed to potential anaplerotic reactions used to recycle detrital lipids.

Paper I

Constraining activity and growth substrate of fungal decomposers via assimilation patterns of inorganic carbon and water into lipid biomarkers

Jabinski S., Rangel W.d.M., Kopacek, M., Jilkova V., Jansa J., Meador T.B., (2024)

ASM Journals
Applied and Environmental Microbiology
Vol. 90, No. 4
(IF = 3.9)

AMERICAN SOCIETY FOR MICROBIOLOGY | Applied and Environmental Microbiology

Environmental Microbiology | Full-Length Text

Constraining activity and growth substrate of fungal decomposers via assimilation patterns of inorganic carbon and water into lipid biomarkers

Stanislav Jabinski,[1,2] Wesley d. M. Rangel,[2] Marek Kopáček,[1,3] Veronika Jílková,[2] Jan Jansa,[4] Travis B. Meador[1,2,3]

AUTHOR AFFILIATIONS See affiliation list on p. 15.

ABSTRACT Fungi are among the few organisms on the planet that can metabolize recalcitrant carbon (C) but are also known to access recently produced plant photosynthate. Therefore, improved quantification of growth and substrate utilization by different fungal ecotypes will help to define the rates and controls of fungal production, the cycling of soil organic matter, and thus the C storage and CO_2 buffering capacity in soil ecosystems. This pure-culture study of fungal isolates combined a dual stable isotope probing (SIP) approach, together with rapid analysis by tandem pyrolysis-gas chromatography-isotope ratio mass spectrometry to determine the patterns of water-derived hydrogen (H) and inorganic C assimilated into lipid biomarkers of heterotrophic fungi as a function of C substrate. The water H assimilation factor (a_W) and the inorganic C assimilation into $C_{18:2}$ fatty acid isolated from five fungal species growing on glucose was lower (0.62% ± 0.01% and 4.7% ± 1.6%, respectively) than for species grown on glutamic acid (0.90% ± 0.02% and 7.4% ± 3.7%, respectively). Furthermore, the assimilation ratio ($R_{IC/aW}$) for growth on glucose and glutamic acid can distinguish between these two metabolic modes. This dual-SIP assay thus delivers estimates of fungal activity and may help to delineate the predominant substrates that are respired among a matrix of compounds found in natural environments.

IMPORTANCE Fungal decomposers play important roles in food webs and nutrient cycling because they can feed on both labile and more recalcitrant forms of carbon. This study developed and applied a dual stable isotope assay (^{13}C-dissolved inorganic carbon/^{2}H) to improve the investigation of fungal activity in the environment. By determining the incorporation patterns of hydrogen and carbon into fungal lipids, this assay delivers estimates of fungal activity and the different metabolic pathways that they employ in ecological and environmental systems.

KEYWORDS dual stable isotope probing, fungal membrane lipids, heterotrophic CO_2 assimilation, water hydrogen assimilation factor, pyrolysis-gas-chromatography, dissolved inorganic carbon (DIC)

The relatively large fluxes between atmospheric and terrestrial carbon (C) reservoirs determine climate-soil feedbacks, especially because soils are highly sensitive to global and local climate variability (1). As such, small changes in soil C reservoirs may have big impacts on atmospheric CO_2 concentration (2–4) and are one of the largest unknowns in the global C budget (5). Uncertainty in future climate models can be improved with increased understanding of the activity of organisms that decompose the wide variety of substrates that constitute soil organic matter (SOM) (6–8). While most studies of SOM dynamics have focused on bacteria, fungi are known to be one of the major decomposers in soils and may play a unique but underappreciated role

Editor John R. Spear, Colorado School of Mines, Golden, Colorado, USA

Address correspondence to Travis B. Meador, travis.meador@bc.cas.cz.

The authors declare no conflict of interest.

See the funding table on p. 15.

Received 17 November 2023
Accepted 22 February 2024
Published 25 March 2024

Copyright © 2024 American Society for Microbiology. All Rights Reserved.

(9). Fungi are known to feed on chemically stable forms of organic C, such as cellulose (10) and lignin (11–13), and are also known to directly access recently produced plant photosynthates (14, 15).

Heterotrophic microorganisms who mainly feed on organic substrates also fix a variable amount of inorganic C. This flux acts to replenish intermediates in the tricarboxylic acid (TCA) cycle that have been released for biosynthesis (16). It has been suggested that 2%–8% of heterotrophic biomass originates from CO_2 incorporated via carboxylation reactions (17–19), largely depending on the redox state of the organic substrate. Although these processes were described decades ago (16, 20), the relevance and the (metabolic) controls on how much inorganic C is fixed by heterotrophic microorganisms are poorly understood due to the lack of reliable estimates for most organisms and habitats (19). Despite their prevalence as decomposers, estimates of inorganic C fixation by heterotrophic fungi are scarce (20).

In recent years, hydrogen (H) isotope incorporation from water has been shown to be a useful tracer of microbial community activity in a diverse range of environments (21–24), as water is required by all microbes and there exists a strong relationship between the stable H isotopic composition of microbial lipids and water, which is the ultimate source of H in all-natural organic compounds (22, 25). Strong correlations between H isotopes of water medium and microbial lipids were shown to correlate with the type of growth metabolism (26), with slightly higher δ^2H values for aerobic heterotrophs, to lower δ^2H values for phototrophs, to lowest δ^2H values for chemoautotrophs (26, 27).

To fully exploit the potential of stable isotope probing (SIP) experiments, a new lipid-based dual-SIP approach was developed to track total microbial production by adding heavy water (D_2O), together with labeled ^{13}C-dissolved inorganic carbon (DIC), to enable estimates of total and autotrophic metabolisms, respectively (28, 29). Because bicarbonate is often present in relatively high concentrations in natural systems, adding ^{13}C-bicarbonate and D_2O to incubation experiments does not alter ambient biogeochemical conditions (28). The ratio of D_2O incorporation and ^{13}C-DIC assimilation into lipid biomarkers can then distinguish the microbial metabolism of autotrophs (ratio ~1) and heterotrophs (ratio <0.3) (28).

The purpose of this work was to apply the dual-stable isotope approach to determine heterotrophic inorganic C fixation and the water H assimilation factor (α_W) for fungal lipid biomarkers produced during growth of pure-culture fungal isolates on labile substrates (glucose and glutamic acid), with the hypothesis that growth substrate will activate alternative metabolic pathways with characteristic assimilation ratios of ^{13}C versus ^{2}H. We further tested the applicability of pyrolysis coupled with gas chromatography-mass spectrometry (GC-MS) and isotope ratio mass spectrometry (IRMS) as a rapid, direct analysis of isotope incorporation into fungal biomarkers.

RESULTS

All five microscopic fungal species *Aspergillus dimorphicus* (AD), *Cordyceps farinosa* (CF), *Penicillium janczewskii* (PJ), *Acremonium polychromum* (AP), and *Aspergillus brasiliensis* (AB), and the yeast species *Yarrowia lipolytica* (YL) were pure cultures and exhibited a capacity to grow in the modified minimum media Czapek-Dox broth (30), with either glucose or glutamic acid as a sole carbon source and having various enrichment levels of ^{13}C-DIC and D_2O. These fungal species were extracted for their membrane lipid fatty acids and analyzed by GC-IRMS for their isotopic composition. The results reported and evaluated in this study include stable isotopic compositions of DIC, CO_2, water, and the fungal biomarkers $C_{18:2}$ and ergosterol.

Fungal growth

CO_2 concentrations in the fungal incubations increased linearly, and the biomass was harvested when the CO_2 headspace concentration reached 4%–6% vol/vol (Fig. 1), which required incubations times ranging between 2 and 4 weeks for glucose and between 4 and 8 weeks for glutamic acid. Incubations with CF grown on glucose were performed

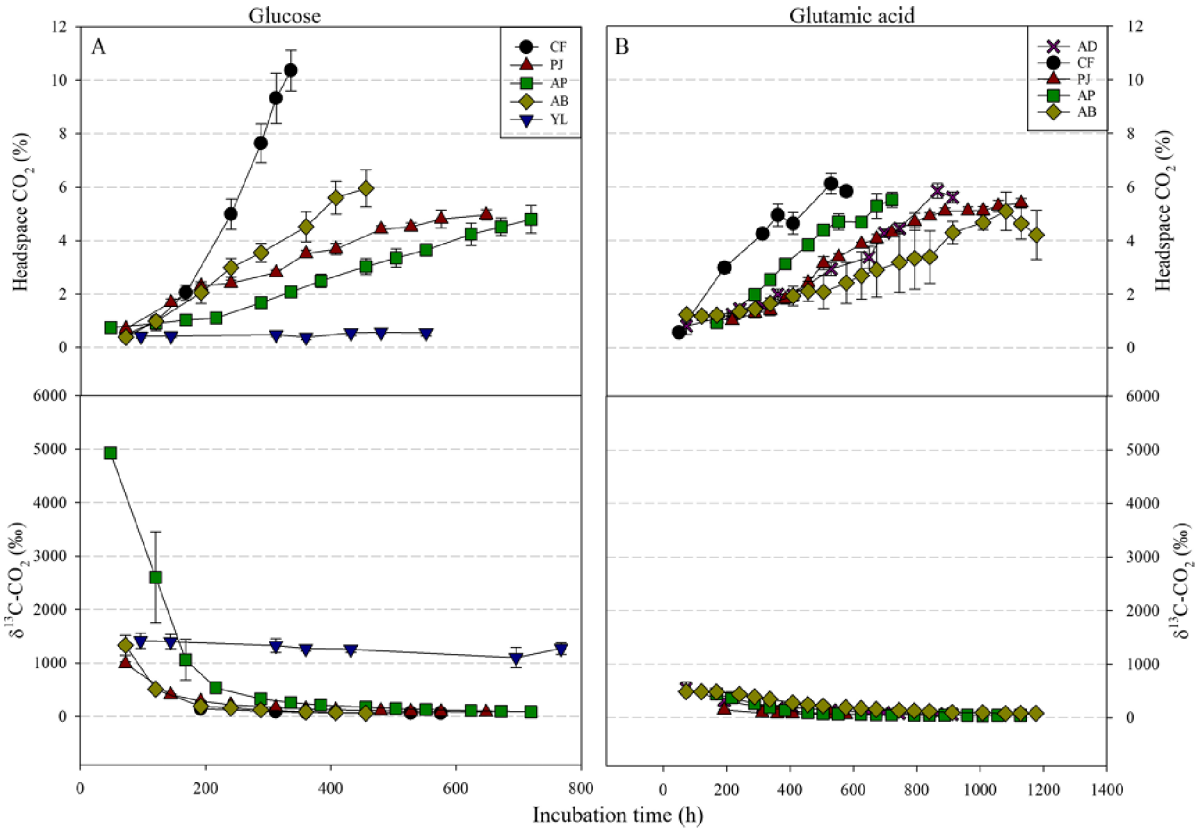

FIG 1 Headspace CO_2 concentrations for the fungal incubation grown on glucose (A) and glutamic acid (B) over time with their respective $\delta^{13}C$-CO_2 values in the lower panels. Incubation was stopped when CO_2 concentrations in the headspace reached 4 - 6% (v/v), which is indicative that roughly half of the carbon substrate was respired, and based on a mol-to-mol comparison, ensures the incubation was still under aerobic conditions. AB, *Aspergillus brasiliensis*; AD, *Aspergillus dimorphicus*; AP, *Acremonium polychromum*; CF, *Cordyceps farinosa*; PJ, *Penicillium janczewskii*; YL, *Yarrowia lipolytica*.

in 1-L bottles and reached higher CO_2 concentrations of ~10%. YL grown on glucose did not show any increase in CO_2 concentration in the headspace during the incubation period of 6 weeks. $\delta^{13}C$ of headspace CO_2 decreased from a maximum value of +5,000‰, measured 3 days after inoculation, to a minimum of approximately +40‰ at the end of the incubation, as CO_2 released during the respiration of unlabeled glucose or glutamic acid slowly diluted the ^{13}C-label. Biomass harvested from each incubation bottle amounted to 50- to 100-mg dry weight.

Analysis of extracted fungal lipids by GC-FID/MS/IRMS

Fatty acid distributions

The fatty acid composition of all strains were similar, except for YL, which contained only four different fatty acids (Fig. 2). The fatty acids $C_{16:0}$, $C_{18:0}$, $C_{18:1}$, and $C_{18:2}$ accounted for about 80%–100% of the total lipid content when grown on glucose. The fatty acids $C_{16:0}$ and $C_{18:2}$ accounted for 80%–94% of the total lipid content when grown on glutamic acid. Higher fatty acid diversity was found for fungi grown on glucose versus those grown on glutamic acid.

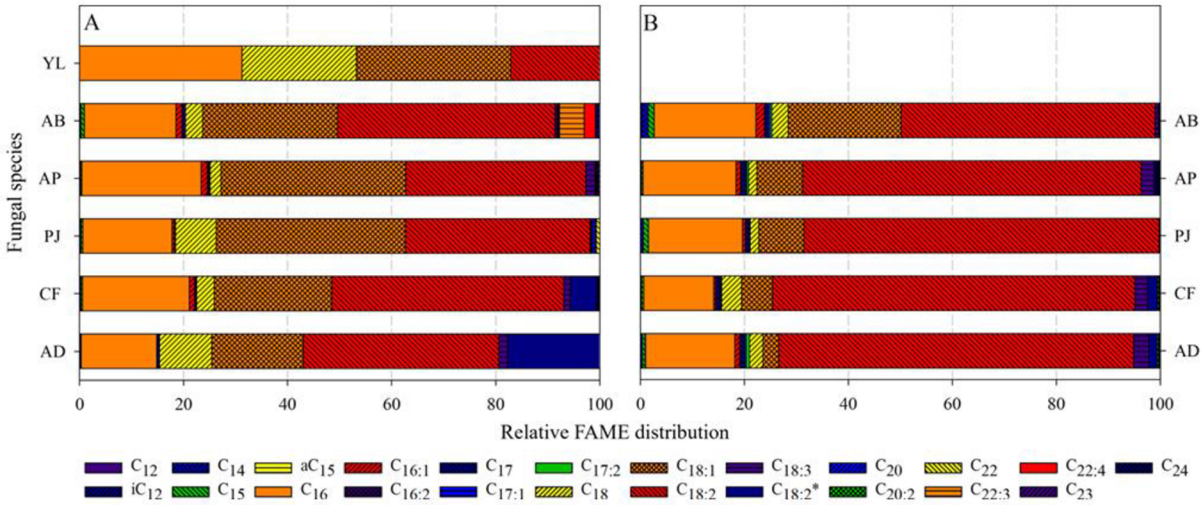

FIG 2 The fatty acid composition for all strains grown on glucose (A) and glutamic acid (B), and determined by conventional GC-flame ionization detector. A slightly higher diversity of fatty acids was found when grown on glucose with the dominant fatty acids $C_{16:0}$, $C_{18:0}$, $C_{18:1}$ and $C_{18:2}$ accounting for more than 80%. The dominant fatty acids when grown on glutamic acid were $C_{16:0}$ and $C_{18:2}$, accounting for more than 80% of total fatty acid content. $C_{18:2}$ represents a fatty acid with two unsaturations in the C_{18} chain at positions 9 and 12, whereas $C_{18:2}$* represents the sum of all other isomers with two unsaturations in the C_{18} chain. AB, *Aspergillus brasiliensis*; AD, *Aspergillus dimorphicus*; AP, *Acremonium polycromum*; CF, *Cordyceps farinosa*; PJ, *Penicillium janczewskii*; YL, *Yarrowia lipolytica*. FAME, fatty acid methyl ester.

Carbon isotopes

The $\delta^{13}C$ values of fungal biomarkers $C_{18:2}$ and ergosterol produced under natural cultivation conditions with glucose (i.e., non-labeled, $AT\%_{DIC}$ ~1%) ranged from −31.2‰ to −27.5‰ and from −28.6‰ to −24.8‰, respectively, across all strains. Fungal lipids were typically depleted in ^{13}C relative to glucose ($\delta^{13}C_{glucose}$ = −26.5‰), with an isotope effect {$\varepsilon_{lipids/glucose} = [(\delta_{lipid} + 1) / (\delta_{glucose} + 1) - 1)] \times 1{,}000$; cf. reference (31)} of −3.3 ± 1.3‰ for $C_{18:2}$ and −0.6 ± 1.4‰ for ergosterol. The isotopic composition of $C_{18:2}$ and ergosterol from the labeled incubation ($AT\%_{DIC}$ = 10%) displayed slightly higher $\delta^{13}C$ values, ranging from −29.2‰ to −23.3‰ and from −25.1‰ to −19.9‰, respectively. The apparent isotope effect of lipid biosynthesis therefore increased, yielding average $\varepsilon_{lipids/glucose}$ values of +0.3 ± 2.2‰ for $C_{18:2}$ and +3.8 ± 2.2‰ for ergosterol, roughly 4‰ higher than the non-labeled treatment.

The $\delta^{13}C$ values of fungal biomarkers $C_{18:2}$ and ergosterol produced under natural cultivation conditions with glutamic acid ranged from −20.8‰ to −17.0‰ and from −18.4‰ to −13.9‰, respectively. Lipids were consistently depleted in ^{13}C relative to glutamic acid ($\delta^{13}C_{glutamic\ acid}$ = −12.7‰), with an isotope effect ($\varepsilon_{lipids/glutamic\ acid}$) of −6.2 ± 1.9‰ for $C_{18:2}$ and −3.9 ± 1.7‰ for ergosterol. The $\delta^{13}C$ values of $C_{18:2}$ and ergosterol from the labeled incubations ($AT\%_{DIC}$ = 10%) were higher, ranging from −14.8‰ to −10.3‰ and from −14.9‰ to −9‰, respectively, and yielding $\varepsilon_{lipids/glutamic\ acid}$ values (+0.7‰ ± 2.5‰ for $C_{18:2}$ and +1.7% ± 3.3‰ for ergosterol) that were roughly 6‰ higher than non-labeled incubations.

The inorganic C incorporation into fungal lipids (Fig. 3) was calculated after Equation 1 .

$$IC_{(\text{assimilation})} = \frac{F^{13C}_{\text{lipids labeled}} - F^{13C}_{\text{lipids control}}}{F^{13C}_{DIC(\text{medium})} - F^{13C}_{\text{substrate}}}$$

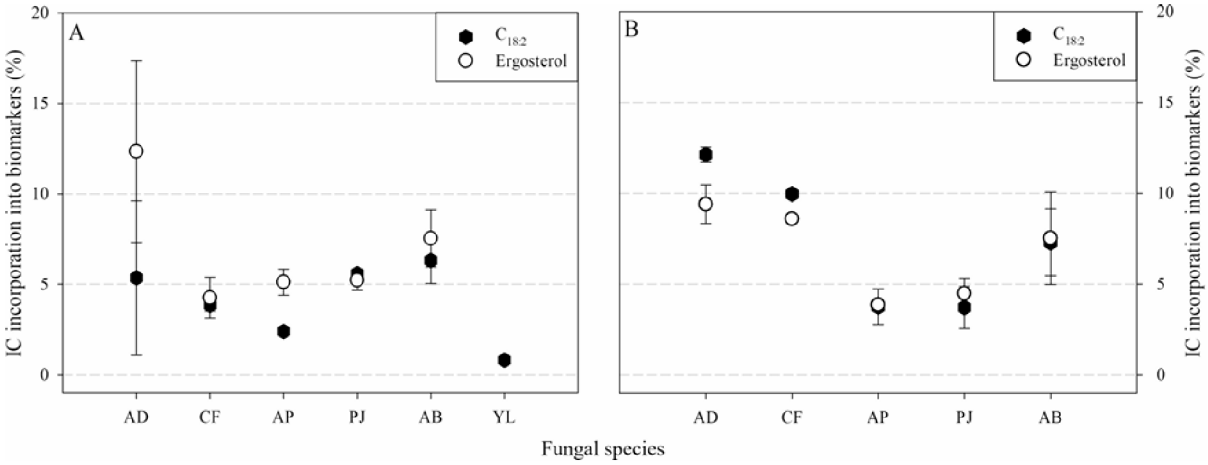

FIG 3 IC assimilation (*y*-axis) by fungal species (*x*-axis) into the specific biomarker fatty acid $C_{18:2}$ and ergosterol incubated with glucose (A) and glutamic acid (B). Data are shown only for conventional GC-IRMS analyses following lipid extraction and purification (see Lipid Extraction and Chemical Preparation). AB, *Aspergillus brasiliensis*; AD, *Aspergillus dimorphicus*; AP, *Acremonium polychromum*; CF, *Cordyceps farinosa*; IC, inorganic carbon; PJ, *Penicillium janczewskii*; YL, *Yarrowia lipolytica*.

Equation 1

Inorganic carbon (IC) assimilation was calculated as the difference in the fraction of ^{13}C [$F^{13C} = (^{13}C) / (^{13}C + {}^{12}C)$] of the lipids harvested from the labeling experiment compared to the natural (control), normalized by the difference in F^{13C} of the DIC measured at the end of the incubation and the F^{13C} of the substrate. F was calculated as $F^{13}C = (R^{13C/12C}) / (R^{13C/12C} + 1)$, where *R* is calculated from the $\delta^{13}C$ ratios as measured with the IRMS equipment using the reverse of the δ notations ($\delta^{13}C = ([^{13}C/^{12}C]_{sample} / [^{13}C/^{12}C]_{ref} - 1) \times 1{,}000$ [modified after references (28, 32)].

For fungi growing on glucose, the average incorporation of inorganic C into $C_{18:2}$ and ergosterol was 4.7% ± 1.6% and 6.9% ± 3.3%, respectively. When growing on glutamic acid, the average inorganic C incorporations into $C_{18:2}$ and ergosterol were 7.4% ± 3.7% and 6.8% ± 2.5%.

Hydrogen isotopes

The contribution of water-hydrogen to lipid biosynthesis was estimated in triplicate for fungi growing in natural MilliQ (−66‰ ± 1‰) and three different enrichment treatments (+107‰ ± 21‰, +209‰ ± 18‰, and +411‰ ± 11‰). A linear regression was then used to constrain the fractional abundance of ^{2}H (^{2}F) between the medium water and the lipids, yielding a slope that represents the "net" contribution of water-derived H to lipid H, known as the water hydrogen assimilation factor α_W (Fig. 4) (22, 26). The α_W values for fungal biomarkers $C_{18:2}$ and ergosterol harvested from glucose incubations ranged from 0.58 ± 0.03 to 0.67 ± 0.03 and from 0.46 ± 0.03 to 0.75 ± 0.03, respectively. $C_{18:2}$ harvested from the yeast strain (YL) growing on glucose exhibited unusually low α_W value of 0.32 ± 0.03 (Fig. 4); these data are excluded from subsequent calculations. The α_W values for fungal biomarker $C_{18:2}$ and ergosterol from glutamic acid incubations ranged from 0.75 ± 0.02 to 1.15 ± 0.10 and from 0.54 ± 0.02 to 0.74 ± 0.02, respectively. The average α_W value for $C_{18:2}$ was significantly higher with glutamic acid as the C substrate (0.90 ± 0.02; $n = 58$) versus glucose (0.62 ± 0.01, $n = 42$, $P < 0.005$), whereas the average α_W values for ergosterol were very similar between glutamic acid (0.68 ± 0.08) and glucose (0.64 ± 0.13).

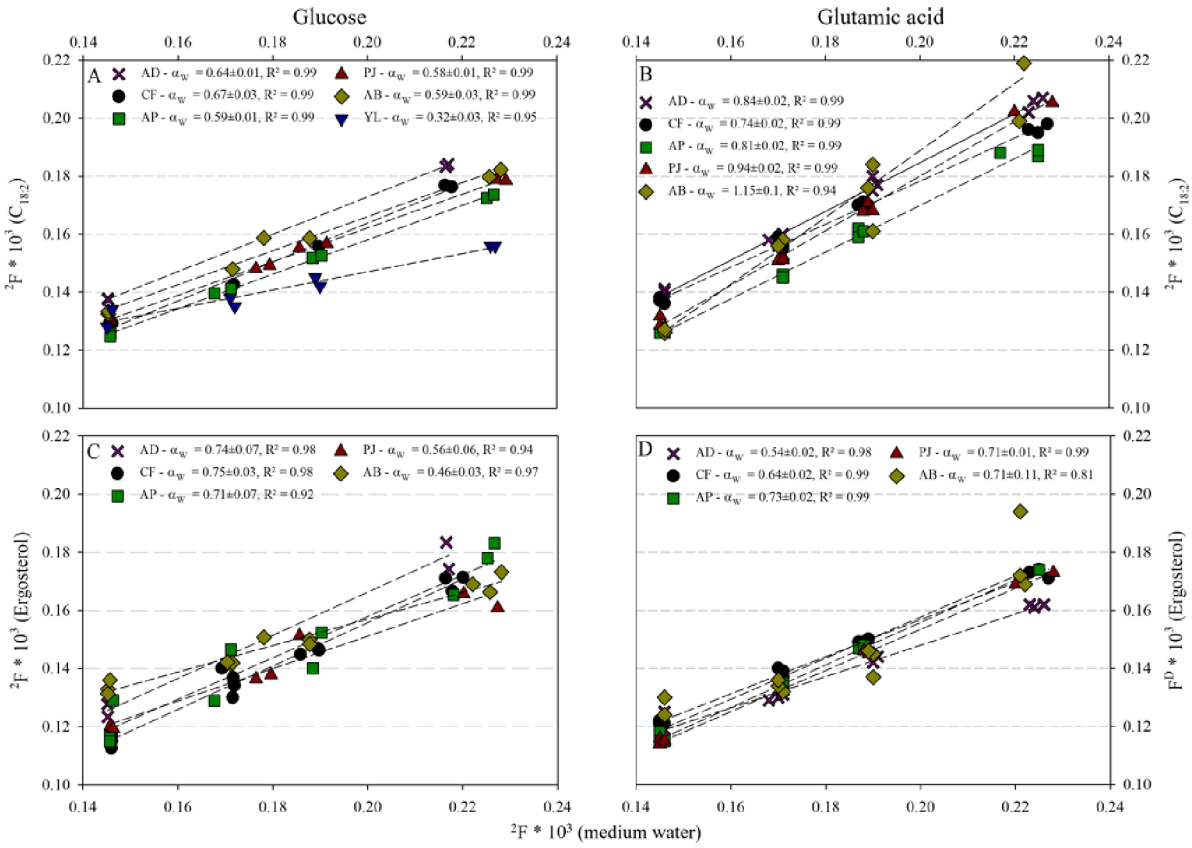

FIG 4 The water hydrogen assimilation factor (α_W values) estimated as the slope of the fractional $^{2/1}$H abundance ($^2F \times 10^3$) in lipids (*y*-axis) versus medium water (*x*-axis). Data are shown for fungal biomarkers $C_{18:2}$ (A and B) and ergosterol (C and D) extracted from the different fungal species grown on glucose (A and C) or glutamic acid (B and D) using the conventional GC-IRMS method (see Lipid Extraction and Chemical Preparation in Materials and Methods). AB, *Aspergillus brasiliensis*; AD, *Aspergillus dimorphicus*; AP, *Acremonium polychromum*; CF, *Cordyceps farinosa*; PJ, *Penicillium janczewskii*; YL, *Yarrowia lipolytica*.

Analysis of fungal biomass by Pyr-GC-FID/MS/IRMS

Four dual-SIP experiments were selected to compare inorganic C incorporation and α_W values determined via the extraction-free, pyrolysis approach [pyrolysis-gas chromatography-isotope ratio mass spectrometry (Pyr-GC-IRMS); n = 24 analyses] to the well-established, wet chemistry approach (GC-IRMS, n = 48 analyses). This included the species CF and AP grown on glucose and AD and CF grown on glutamic acid (Fig. 5; Table S2). The inorganic C incorporation into the fungal biomarkers $C_{18:2}$ and ergosterol from the glucose experiments were on average 3.1% ± 1% and 4.6% ± 0.6% (GC) versus 1.9% ± 0.5% and 4.5% ± 0.4% (Pyr). For the glutamic acid experiment, the average inorganic C incorporation into $C_{18:2}$ and ergosterol were 11.1% ± 1.5% and 9.0% ± 0.6% (GC) versus 8.1% ± 0.9% and 8.1% ± 0.8% (Pyr), respectively. The α_W values for $C_{18:2}$ and ergosterol from the glucose experiment were on average 0.63 ± 0.05 and 0.73 ± 0.02 (GC) versus 0.62 ± 0.01 and 0.39 ± 0.03 (Pyr). For the glutamic acid experiment, the average α_W values for $C_{18:2}$ and ergosterol were 0.79 ± 0.05 and 59.0 ± 0.07 (GC) versus 0.81 ± 0.06 and 0.48 ± 0.06 (Pyr).

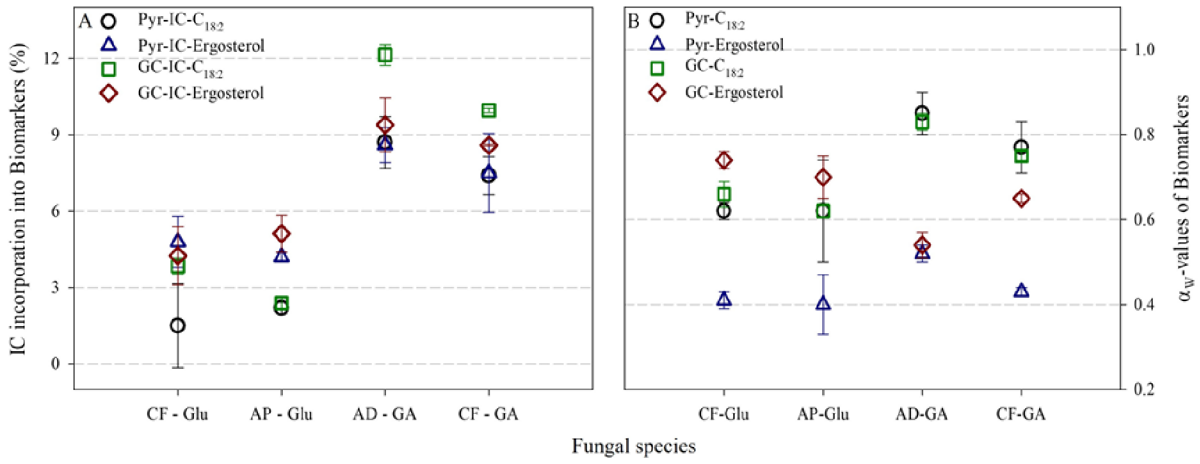

FIG 5 Comparison between pyrolysis and conventional GC-IRMS analysis of fungal biomarkers to determine IC incorporation (A) and water assimilation factor (α_W) (B). AD, *Aspergillus dimorphicus*; AP, *Acremonium polychromum*; CF, *Cordyceps farinosa*.

DISCUSSION

We have generated complementary data sets of inorganic C and water H incorporation into fungal lipids using two different approaches. The interpretation of these estimates in the sections below are based on data determined via classical GC analysis, following extraction, purification, and transesterification of lipids as described in Lipid Extraction and Chemical Preparation in Materials and Methods and thus comparable with previous studies that have used this approach [e.g., see references (22, 26, 33)]. We further compare these values with those derived from direct analysis of fungal biomass via pyrolysis-GC (cf. Pyrolysis GC in Materials and Methods), as this approach may promote higher throughput for lipid analyses and thereby may help to constrain inorganic C and water H assimilation factors across more species and carbon substrates.

Inorganic C assimilation into fungal lipids

CO_2 assimilation by heterotrophic organisms is reported to be a measure of both anabolic processes and the catabolic status of the cell, with assimilation, anaplerotic, biosynthesis, and redox balancing reactions playing important roles to ensure the provision of energy and to replenish intermediates in the TCA cycle that have been released for biosynthesis (16, 34, 35). The by-fixation of inorganic C via anaplerotic pathways typically varies between 1% and 8% of the biomass C, depending on central metabolic pathways, and could further increase to assimilate C substrates that are more reduced than the biomass, as various carboxylase enzymes are employed to match the redox state of the substrate with that of the biomass (16). Whereas inorganic C assimilation by fungi was previously reported to amount to roughly 1%, based primarily on radiocarbon uptake into whole cells (20, 36, 37), our results suggest that ^{13}C-labeled inorganic C accounted for 2%–12% of C assimilated into fungal membrane lipid biomarkers, when grown on minimum medium with glucose or glutamic acid as the main C source. Both glucose and glutamic acid are slightly more reduced [degree of reduction (DOR) = 4.0 and 3.6, respectively (38)] than expected for biomass [DOR = 4.25 (19)], suggesting that assimilatory carboxylation should not contribute as strongly as anaplerotic or biosynthesis reactions to inorganic C by-fixation during growth on these substrates. Our findings indicate that inorganic ^{13}C incorporation into the $C_{18:2}$ biomarker was slightly lower during growth on glucose substrate (4.7% ± 1.6%) versus glutamic acid (7.4% ± 3.7%, Fig. 3), which may have involved more carboxylation reactions to replenish central metabolites. For example, during growth on glutamic acid,

relatively more carboxylase reactions may be required to replenish acetyl-CoA, thereby increasing the conduit for by-fixation of inorganic C. Consistent with this notion, growth on glutamic acid was slower than glucose across fungal species (Fig. 1).

In contrast to the observations for $C_{18:2}$, inorganic ^{13}C incorporation into ergosterol was similar for both substrates (6.9% ± 3.3% and 6.8% ± 2.5%, Fig. 3). The different patterns of inorganic C incorporation into $C_{18:2}$ versus ergosterol are likely due to their different biosynthetic pathways, where both products start from acetyl-CoA. For fatty acids, acetyl-CoA molecules are merged to malonyl-CoA, and other acetyl-CoA molecules are added repeatedly until the desired chain length for the fatty acid is attained. Ergosterol is synthesized from squalene (C_{30}), which is produced by merging C_5 intermediates of the mevalonate pathway (e.g., isopentenyl-pyrophosphate). Each C_5 unit of squalene stems from the merger of three acetyl-CoA molecules in a decarboxylation reaction. Squalene further undergoes cyclization to form lanosterol, the main precursor for sterols, through the subsequent removal of three methyl groups (39, 40). Before the final ergosterol molecule is produced, another methyl group is added to the backbone (39, 40). The removal and/or replacement of acetyl-CoA-derived C during ergosterol biosynthesis may thus make this biomarker less sensitive than fatty acids to the inorganic ^{13}C incorporation via assimilation or anaplerotic pathways.

Water hydrogen incorporation into fungal lipids

Previous studies have demonstrated that the regression slope between hydrogen isotopes of water medium and microbial lipids (i.e., α_W) varies with the type of metabolism used during growth, and different organisms may exhibit similar fractionation or α_W values when grown on the same substrate (26, 41, 42). Variability in fatty acid hydrogen isotopic composition is suggested to be a function of the isotope effects of hydrogen transporters and electron acceptors (NADPH and NADH), as they are the main portals for hydrogen incorporation in FA biosynthesis pathways (accounting for around 50%), with the remaining coming directly from environmental water (~25%) and acetyl-CoA (~25%) (24, 26, 42). In the current study, the water-derived hydrogen contribution to membrane lipids was consistent among fungal species grown on the same substrate and similar to the patterns observed for inorganic C incorporation, with the average α_W value of the $C_{18:2}$ fatty acid biomarker harvested from glucose incubations being significantly lower than glutamic acid incubations (0.62 ± 0.04 versus 0.90 ± 0.16, $P < 0.005$). This finding indicates that the central metabolism of glutamic acid resulted in a higher contribution of H from environmental water to $C_{18:2}$. This finding may be explained by the metabolic pathway, where glutamic acid is converted to α-ketoglutarate by transamination, which leads to an exchange of functional groups between the amino acid and the carboxyl acid as well as the addition of water molecules and the involvement of NADP and NADPH before entering the TCA cycle as α-ketoglutarate (43). The contribution of H from the glutamic acid substrate to fatty acids would thereby be lower and replaced by water-derived H, explaining the higher α_W value. For ergosterol, α_W values for glucose and glutamic acid incubations were not significantly different (0.64 ± 0.13 and 0.68 ± 0.08, respectively), suggesting that ergosterol is less sensitive to H contributions from water in the growth medium. For the synthesis of ergosterol from squalene, at least 10 intermediate steps are needed, which include several steps involving desaturase enzymes (44) which remove hydrogen atoms from the molecule. This might explain the insensitive response of ergosterol to the different metabolic pathways presented in this study. In the context of previously reported α_W values for the three domains of life, fungal lipids are more comparable to those of bacteria (0.4–0.9) (24) than those of eukaryotes (0.7–1.2), although only phyto- and zooplankton α_W values are reported so far for that domain [see reference (45) and references within].

Dual-SIP approach

Dual-SIP experiments with deuterated water (HDO) and ^{13}C-DIC have been applied to distinguish autotrophic versus heterotrophic modes of C assimilation for pure cultures

of bacteria and archaea (26, 27) and have also been used to track microbial activity in marine sediments (21, 33, 46, 47). The main objective of this study was to develop the dual-SIP assay to determine inorganic ^{13}C (^{13}IC) and ^{2}H incorporation into fungal lipid biomarkers (ratio ^{13}IC:α_W), which could be further applied to more comprehensively explore the patterns derived from different functional and/or taxonomic groups of fungi. The average ^{13}IC:α_W ratios for $C_{18:2}$ were 0.076 ± 0.026 and 0.11 ± 0.057 for glucose and glutamic acid, respectively. This first evidence defines distinct spaces for fungal growth on the different substrates in the ratio plot (Fig. 6) and supports the use of the dual-SIP assay to distinguish the different metabolic modes employed by fungi for growth on sugars versus amino acids. For ergosterol, the ^{13}IC and α_W values determined for both carbon sources could not be distinguished in the ratio plot (Fig. 6), suggesting poor potential for ergosterol to serve as a biomarker of metabolic mode. More data and studies of additional taxa and C substrates are needed to fully exploit the potential of this approach.

Pyr-GC-MS/IRMS

An additional objective of this study was to test the potential of using Pyr-GC-IRMS to determine the isotopic composition of the fungal biomarker $C_{18:2}$ and ergosterol for a rapid analysis that eliminates time- and solvent-consuming wet chemistry steps. The application of Pyr-GC-MS for the analysis of whole cells was previously reported for fatty acid quantification (48), which relies on thermal-assisted hydrolysis and methylation via a derivatization agent to enhance detection. In the current study, we used trimethylsulfonium hydroxide (TMSH) as a derivatization agent because it was reported that it does not cause any isomerization and/or degradation as observed for other TMH solutions (49, 50).

For the dual-SIP experiments selected for both analyses, the patterns of ^{13}IC incorporation and α_W values determined by the conventional GC-IRMS protocol were generally redundant with results from the Pyr-GC-IRMS analysis, with the exception of α_W values calculated for ergosterol (Fig. 5; Table S2). The average IC incorporation determined for ergosterol was consistent between traditional GC-IRMS and Pyr-GC-IRMS protocols, and while the incorporation trends were consistent, ^{13}IC incorporation into $C_{18:2}$ determined via the traditional GC analyses was mostly higher than their pyrolysis counterparts. This may be due to the improved chromatographic separation between $C_{18:1}$ and $C_{18:2}$ fatty acid methyl esters (FAMEs) achieved by the longer 120-m column employed for traditional GC-IRMS analyses and/or the greater number of replicates analyzed via this protocol. α_W values calculated from the Pyr-GC-IRMS for ergosterol

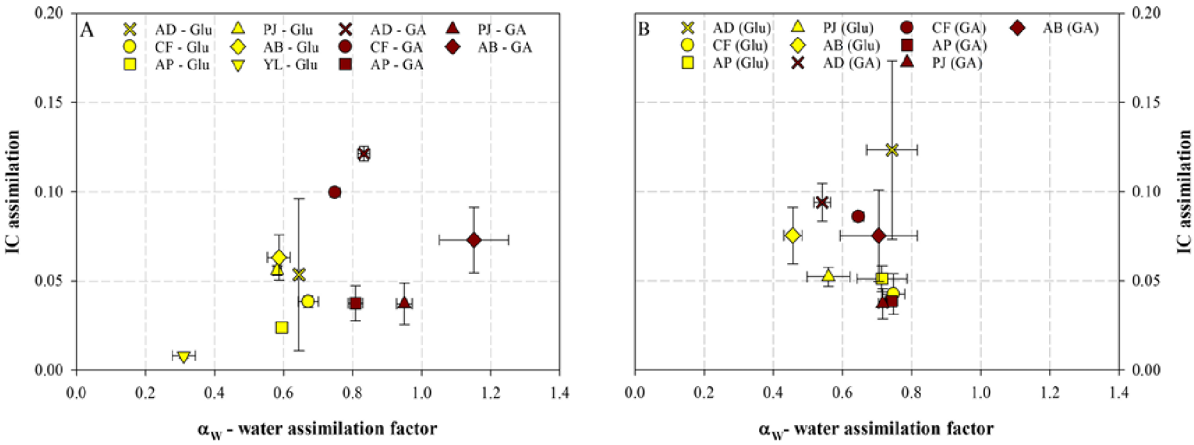

FIG 6 IC and α_W value ratio plots for $C_{18:2}$ (A) and ergosterol (B). The power of the dual-SIP approach for fungal biomarkers shows distinguished groupings for glucose (yellow) versus glutamic acid (red) for $C_{18:2}$, whereas these groups overlap for ergosterol. IC, inorganic carbon.

are inconsistent with their GC-IRMS counterparts and might be due to the lower signal for ergosterol detected via Pyr-GC-IRMS (Fig. 7) compared to the single, typically large peak observed with traditional GC-IRMS (not shown). Overall, our findings suggest that the Pyr-GC-IRMS protocol for determining stable C and H isotopic composition of $C_{18:2}$ represents a robust and fast alternative to the conventional GC-IRMS analysis.

The advantage of the Pyr-GC-IRMS approach was the tandem measurement of fatty acids and ergosterol in the same analytical injection (Fig. 7), which reduced the time of analysis but required high pyrolysis and GC temperatures for optimal detection (51). On the other hand, Pyr-GC analyses required the use of a shorter separation column (30 m) and thus poorer peak resolution because the pyrolysis unit could not withstand the higher backpressure of the 120-m column used for optimal separation of FAMEs. Nevertheless, the IL60 column achieved decent baseline resolution for $C_{18:2}$ and allowed for detection of ergosterol in the same injection and negligible interference of other compounds in fungal biomass samples, owing to the high maximum operation temperature for this column (300°C), which is a limitation for most polar columns (maximum temperature around 260°C–280°C).

Conclusion and future perspective

The purpose of this work was to apply the dual-SIP approach for determining heterotrophic CO_2 fixation and water H assimilation into fungal lipid biomarkers when grown on labile substrates (glucose and glutamic acid) available in soil systems. Our findings suggest that fungi solicit distinguishable isotope effects during the incorporation of ^{13}C-DIC and HDO into their membrane lipids when growing on glucose versus glutamic acid as the C substrate. We could show that the heterotrophic inorganic C incorporation into fungal biomarkers was within the expected range of 2%–8% (35), and we report for the first time the water H assimilation factor values for fungal biomarkers, which range between 0.58 and 1.15 and are broadly consistent with α_W values reported for

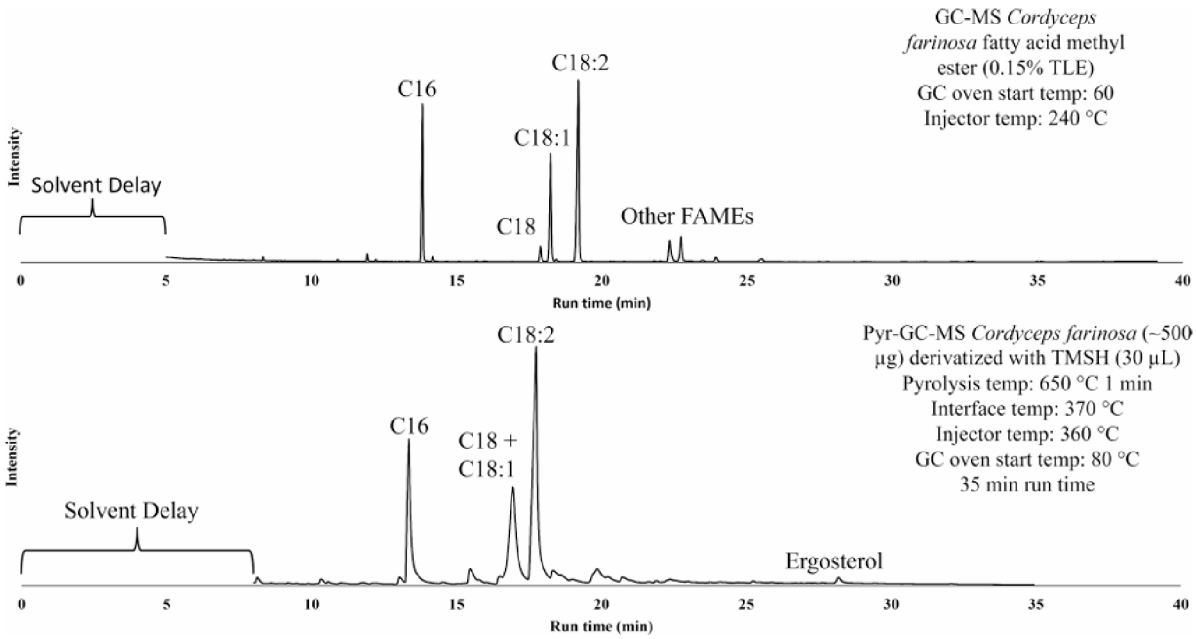

FIG 7 Typical flame ionization detector chromatogram of a *Cordyceps farinosa* FAME/lipid measurement with conventional GC-MS (top) and Pyr-GC-MS (bottom). Separation of FAMEs for the fungal biomarker $C_{18:2}$ was successfully achieved with both methods. Advantage of the Pyr-GC method includes the measurement of both FAMEs and ergosterol in the dry biomass, whereas for the conventional method, sterol and FAME analyses are pre-extracted and analyzed separately. TLE, total lipid extract.

heterotrophic bacteria. Ergosterol was less informative as a fungal biomarker in these studies in comparison to the more distinguishable signals exhibited by $C_{18:2}$; however, it may serve as a potential marker for a distinction between labile and more stable (recalcitrant) C sources. Future application of this dual-SIP assay to explore fungal activity in environmental settings has the advantages that both isotope labels can be added to environmental incubations with minimal alteration of the natural habitat; fungal lipid production can be estimated by HDO incorporation alone; and the $^{13}IC/\alpha_W$ ratio can inform which C substrates support their growth. Environmental case studies applying the dual-SIP assay described here should also choose an appropriate label dose for each isotope: $^{2}/^{1}H$-water label strength should be commensurate with the expected production of the biomarker over the fossil pool and may range up to H_2O values of +8,000‰; similarly, the dose of $^{13}/^{12}C$-DIC must consider background DIC levels and heterotrophic production during the incubation. For this study, estimates of ^{13}C incorporation into fungal lipids were calculated based on ^{13}F-DIC values at the end of the incubation. Furthermore, maintaining ^{13}C-enrichment of the DIC pool also requires a closed headspace and especially requires that oxygen levels are monitored during aerobic, dual-SIP incubations.

Additional growth experiments that more comprehensively define $^{13}IC:\alpha_W$ ratios imparted during growth on more stable forms of soil organic carbon (e.g., lignin) across a larger diversity of fungal taxa are needed to better constrain the interpretive ability of isotope fractionation signals and evaluate the potential of this approach for environmental studies. This effort will be supported by the applicability of pyrolysis coupled with GC-MS and IRMS for direct analysis of fungal biomass demonstrated in this study.

MATERIALS AND METHODS

Cultivation and harvesting

Pure cultures of microscopic fungi (Table S1), AD strain BCCO 20_2442, CF strain BCCO 20_1579, PJ strain BCCO 20_0265, AP strain BCCO 20_1588, AB strain CCM 8222, and one yeast species YL strain MUCL 054012 were incubated at 25°C in the dark in pre-combusted 2-L Schott bottles containing 50 mL of a autoclaved modified minimum media Czapek-Dox broth (30). The fungal inocula were prepared using sterile ultrapure water for sampling the spores, which were washed and centrifuged with sterile MilliQ water three times before being inoculated (1 mL) with approximately 10^6 spores/mL under a biological safety cabinet using sterile utensils and solutions. The growth medium contained per liter: 4-g organic C source ($C_6H_{12}O_6$, glucose and $C_5H_9NO_4$, glutamic acid, tested separately); 3-g $NaNO_3$; 1-g K_2HPO_4; 0.5-g $MgSO_4$; 0.5-g KCl; 0.01-g $FeSO_4$; and 0.09-g $NaHCO_3$. The pH was adjusted to 7.3. Dual-SIP experiments were performed using ^{13}C-bicarbonate (^{13}C-DIC and $NaH^{13}CO_3$) and D_2O according to Table 1, which were added to the medium after 0.2-µm sterile filtration. Each fungal species was grown in triplicate with non-labeled substrates (treatment 1), with δ^2H of the medium water adjusted to (i) 100‰ δ^2H and 10% of ^{13}C-DIC (treatment 2), (ii) 200‰ δ^2H and 10% ^{13}C -DIC (treatment 3), and (iii) 400‰ δ^2H and 10% ^{13}C-DIC (treatment 4). The Schott bottles were kept closed to prevent the labeled ^{13}C-DIC from outgassing. Headspace samples for CO_2 analysis (2 mL) were collected every 2–3 days from each bottle into helium-flushed (10 min at 100 mL/min) 12-mL exetainer vials (Exetainer; Labco Limited, UK) to monitor fungal growth and ensure O_2 availability. For the experiments with the species AD and CF growing on

TABLE 1 Incubation setup of fungal species for SIP experiments with ^{13}C-bicarbonate (^{13}C-DIC) and deuterated water (D_2O)

Treatment	Replicates	δ^2H of water (label strength)	$\delta^{13}C$-DIC (label strength)
1	3	Natural	Natural
2	3	100‰	10%
3	3	200‰	10%
4	3	400‰	10%

glucose, 1-L bottles were used, and neither CO_2 concentration nor isotopic composition were measured for AD.

At the end of the experiment, the mycelia were filtered from the growth medium using an autoclaved sterile miracloth placed on a sterile funnel on a sterile 50-mL falcon tube. The mycelia on the miracloth were washed three times with sterile MilliQ water, then the mycelia were dried by first placing the miracloth on dry paper, then transferring to pre-weighed 50-mL falcon tubes. The biomass of the fresh (wet) weight was recorded, and samples were stored at −20°C until lyophilization, after which the dry weight of each sample was determined and stored at −20°C until further analysis.

Growth monitoring

Headspace CO_2 of fungal incubations (1 mL) were measured for CO_2 concentration on a Hewlett Packard HP 5890 Series II GC (Agilent Technologies, Inc, Santa Clara, USA) coupled with a thermal conductivity detector (TCD) equipped with a 30-m HP-PLOT/Q (polystyrene-divinylbenzene, 0.53-mm ID, 0.40-µm df; Agilent Technologies, Inc). The detector temperature was set to 130°C; the oven was set to 70°C; and the system was operated with helium at a flow rate of 1 mL/min.

Lipid extraction and chemical preparation

Bligh and Dyer

Lyophilized fungal biomass was extracted using a modified Bligh and Dyer protocol (52). Samples were sonicated for 10 min in four steps with a mixture of dichloromethane (DCM)-methanol (MeOH)-water (1.0:2.0:0.8, vol/vol/vol) by using 30-mL solvent per extraction step. A phosphate buffer (8.7-g/L KH_2PO_4, pH 7.4) was used for the first two steps, and a trichloroacetic acid buffer (50-g/L CCl_3COOH, pH 2) was used for the final two steps. After each extraction step, the samples were centrifuged at 1,250 rpm for 5 min, and the supernatants were collected in a pre-combusted separation funnel. Phase separation was induced by addition of DCM and MilliQ, and the organic phase was drawn off and collected in a pre-combusted Schott bottle. The aqueous phase was washed three more times with DCM, and then the pooled organic phase was washed three more times with de-ionized MilliQ water. Finally, the organic phase was collected as the total lipid extract (TLE) and was evaporated under a stream of argon and stored at −20°C. All vials used for sample handling and storage were pre-combusted at 450°C for 6 h, and syringes for sample transfer were pre-rinsed with DCM:MeOH (5:1 vol/vol).

Saponification

Thirty percent of the TLE was dried and saponified for fatty acid analysis, using 1 mL 6% KOH in MeOH for 3 h at 80°C (53). After cooling, 1 mL of 0.05 KCl was added. Neutral lipids were extracted four times using 1-mL n-hexane. The rest of the solution was treated with 10% HCl to reach a pH value of 1, and then free fatty acids were extracted four times using 1-mL n-hexane. Following that, all extracts were dried, mixed with 1-mL 20% BF_3 in MeOH and heated at 70°C for 1 h to convert free fatty acids into FAMEs. The solutions were extracted four times with 1-mL n-hexane. The combined extracts were evaporated under argon and stored at −20°C until further analysis.

Measurements

HDO isotope analysis

Liquid samples were transferred into 1.5-mL glass vials (32 × 11.6 mm, Fisher Scientific) and then measured using Triple Liquid Water Isotope Analyzer (Los Gatos Research), which is based on the principle of high-resolution laser absorption spectroscopy. Samples were dispensed into the instrument using an autosampler (PAL3 LSI, ABB company) and a 1.2-µL syringe (Hamilton). Samples were measured and evaluated against prepared laboratory standards of known isotopic composition.

The isotopic ratios of these laboratory standards were verified by measuring against international standards (VSMOW2 and SLAP2). To check the quality control, the measurements of the samples were also interspersed with periodic measurements of the prepared verification samples with known isotopic composition. The final isotopic composition (δ^2H) was determined using LIMS software. Analytical error in case of δ^2H was <1.5‰.

Substrate analysis

Substrates (~100 µg) were weighed into tin capsules (8 × 5 mm; Sercon, Crewe, UK) and placed in a helium-flushed carousel autosampler, then introduced to an Elemental Analyzer IsoLink IRMS system (EA IsoLink; Thermo Scientific, Bremen, Germany) equipped with a CHN/NC/N EA combustion/reduction reactor (Sercon) heated to 1,020°C. A pulse of oxygen was introduced to the reactor simultaneously with the sample. The sample gases were quantified via a TCD and then introduced to a MAT 253 Plus IRMS (Thermo Scientific) via the open split of a Conflo IV interface, with helium as the carrier gas. The isotopic composition was determined using Isodat version 3.0 software against the corresponding CO_2 working gas (−4.191‰ for δ^{13}C), and the values were corrected for linearity and normalized to the Vienna Pee Dee Belemnite (VPDB) scale using an international IAEA-600 (−27.771‰ for δ^{13}C) standard. The analytical error was <0.04‰.

DIC and CO_2 isotopic analyses

Medium water samples (2 mL) or CO_2 headspace (2 mL) gas was injected into a helium-flushed 12-mL exetainer vial (Exetainer, Labco Limited). Water samples were acidified with 0.1-mL 85% H_3PO_4 and left to equilibrate for at least 24 h before measurement. Headspace CO_2 was purged using a double-holed needle with helium into a 250-µL sample loop then separated via a Carboxen PLOT 1010 (0.53-mm ID; Supelco, Bellefonte, USA) held at 70°C with a flow rate of 0.75 bar and then introduced into the MAT253 Plus IRMS (Thermo Scientific) via a Conflo IV interface. Each sample was injected three times during one analysis. The isotopic composition was determined using Isodat version 3.0 software against the corresponding CO_2 working gas (−4.191‰ for δ^{13}C). The values were corrected for linearity and normalized to the VPDB scale using internal house standards and international standards IAEA-603 and IAEA-303A (2.46‰ and 93.3‰ for δ^{13}C, respectively). The analytical error was <0.2‰.

FAME analysis

FAMEs were measured using a GC Trace1310 gas chromatograph equipped with an SSL injector, a double gooseneck Topaz splittless liner (Restek, Bellefonte, USA) and a TR-FAME column (70% cyanopropyl polysilphenylene-siloxane; 120 m, 0.25-mm ID, 0.25-µm df; Thermo Scientific). The samples were injected in splitless mode, with the injector temperature at 310°C. The GC oven was held at 60°C for 1 min, then ramped to 150°C at 10°C/min and to 250°C at 4°C/min, then held at 250°C for 15 min. Helium was used as carrier gas with a constant flow of 1.5 mL/min. The column was coupled via a multichannel device splitting the flow to a flame ionization detector (FID) and a mass spectrometer (MS), enabling both peak quantification and identification from one injection. The FID was set to 300°C with flows of air at 350 mL/min, H_2 at 35 mL/min, and N_2 makeup gas at 40 mL/min. The MS (ISQ QD, Thermo Scientific) ion source was set to electron impact ionization (EI) mode at 70 eV and a scan range of *m/z* 50–500 with a scan time of 0.2 s. The transfer line temperature was set to 280°C, and the ion source was set to 230°C. The scan was started 15 min after the injection to avoid ionization of the solvent peak in the MS.

For FAME identification, the fragmentation patterns and mass spectra were compared to the National Institute of Standards and Technology (NIST) Spectral Library. Quantification was determined from the FID trace, according to the response of the internal standard (2-methyloctadecanoic acid) and following Equation 2 :

$$\text{Compound concentration}\left(\frac{ng}{g(\text{sample})}\right) = \frac{\frac{\text{PeakArea}}{\text{PeakSTD}} \times STD(ng)}{\%(\text{injected}) \times g(\text{sample})}$$

Equation 2

The final concentration is calculated with PeakArea being the integrated area of the unknown compound, PeakSTD being the integrated area of the given standard, and STD as the known concentration of the standard in nanogram, and the percentage of the injected TLE and the mass of the extracted sample in gram (52).

Stable carbon and hydrogen isotope compositions of FAMEs were determined by splitting the flow from the GC column to a GC-Isolink II reactor, coupled with a MAT253 Plus IRMS via a Conflo IV interface; values are expressed in standard delta notation ($\delta^{13}C$ and $\delta^{2}H$). MS information was simultaneously acquired by using the multichannel device described above. For conversion of FAMEs and ergosterol to CO_2, the combustion reactor (nickel oxide tube with CuO, NiO, and Pt wires) was set to 1,000°C. For conversion of FAMEs and ergosterol to H_2, the pyrolysis reactor (aluminum tube) was set to 1,420°C. FAMEs were identified by their retention times and fragmentation patterns. The isotopic composition was determined using Isodat version 3.0 software against the corresponding CO_2 or H_2 working gas (−4.191‰ for $\delta^{13}C$ and −239.5‰ for $\delta^{2}H$). Isotope corrections for instrument drifts, linearity, and normalization to the VPDB or Vienna standard mean ocean water (VSMOW)/standard light Antarctic precipitation (SLAP) scales were performed according to the response of USGS70 (−30.53‰ for $\delta^{13}C$, −183.9‰ for $\delta^{2}H$) and USGS72 (−1.54‰ for $\delta^{13}C$ and 348.3‰ for $\delta^{2}H$) reference standards. The analytical error was <0.5‰ and <3.1‰ for $\delta^{13}C$ and $\delta^{2}H$, respectively.

Pyrolysis GC

The pyrolysis unit Shimadzu 3030D (Shimadzu, Kyoto, Japan/Frontier Laboratories, Fukushima, Japan) was installed on top of the GC Trace1310 gas chromatograph SSL injector (Thermo Scientific), and the GC was equipped with an SLB-IL60 column [non-bonded; 1,12-di(tripropylphosphonium)dodecane bis(trifluoromethanesulfonyl)imide phase, 30 m, 0.25-mm ID, 0.20-µm df; Supelco]. Due to the high restriction and thus backpressure from the 120-m FAME column, a different shorter analytical column (30 m) was used with the pyrolysis injector, which resulted in co-elution of $C_{18:0}$ and $C_{18:1}$ peaks (Fig. 1). The furnace temperature was set to 650°C, and the interface temperature was set to 370°C. The injector temperature was set to 360°C, and the GC oven was held at 80°C for 1 min then ramped to 175°C at 15°C/min, then ramped to 195°C at 2°C/min and then ramped to 300°C at 10°C/min and held for 7 min at 300°C. Helium was used as carrier gas with a constant flow of 1.5 mL/min and a split flow of 40 mL/min. The column was coupled via a multichannel device to enable simultaneous FID and MS acquisition from one injection. The GC-MS (ISQ QD, Thermo Scientific) ion source was set to EI mode at 70 eV and a scan range of *m/z* 50–500 with a scan time of 0.2 s was applied. MS scanning started after 8 min to avoid ionization of the solvent peak in the MS. Transfer line temperature was set to 300°C, and the ion source was set to 250°C. The samples (lyophilized biomass, 80 µg–1.5 mg) were weighed into an ultraclean stainless steel Eco-Cup LF (Frontier Laboratories), which were burned with a torch before usage to remove contaminants. FAMEs and ergosterol were detected in the same analytical run. Immediately prior to the measurement, 10–40 µL of TMSH was added on the sample to increase the volatization of the FAME and ergosterol and to improve measurement sensitivity. Identification was performed using fragmentation patterns and the NIST 14 library. Quantification was performed with a calibration regression (0.5–400.0 ng) using an external standard (nonadecanoic acid, C_{19}) for FAMEs and ergosterol (5–20 ng) for ergosterol. The same setup and method were also used to acquire stable carbon and hydrogen isotope composition of FAMEs and ergosterol via a GC-Isolink II device, as explained above. The column flow was split via a multichannel device to acquire MS and

isotopic data simultaneously. The analytical error was <0.6‰ and <3.3‰ for $\delta^{13}C$ and $\delta^{2}H$, respectively.

ACKNOWLEDGMENTS

We thank Ljubov Polaková for the support of the stable isotope measurements and laboratory protocols; the Collection of Microscopic Fungi of the Institute of Soil Biology BC CAS for providing the fungal species *Aspergillus dimorphicus* strain BCCO 20_2442, *Cordyceps farinosa* strain BCCO 20_1579, *Penicillium janczewskii* strain BCCO 20_0265, and *Acremonium polychromum* strain BCCO 20_1588; and the Czech Collection of Microorganisms (CCM) for kindly providing the *Aspergillus brasiliensis* strain CCM 8222. The authors declare no conflict of interest in the performance and publication of this research.

This project was funded by the Czech Science Foundation GACR nr. 20–223805 (FUNSIF) and supported by MEYS CZ grant LM2015075 Projects of Large Infrastructure for Research, Development and Innovations, as well as the European Regional Development Fund Project: Research of Key Soil-Water Ecosystem Interactions at the SoWa Research Infrastructure (no. CZ.02.1.01/0.0/0.0/16_013/0001782).

AUTHOR AFFILIATIONS

[1]Department of Ecosystem Biology, Faculty of Science, University of South Bohemia, České Budějovice, Czechia
[2]Institute of Soil Biology and Biochemistry, Biology Centre CAS, České Budějovice, Czechia
[3]Institute of Hydrobiology, Biology Centre CAS, České Budějovice, Czechia
[4]Institute of Microbiology CAS, Praha, Czechia

PRESENT ADDRESS

Wesley d. M. Rangel, Programa de Pós-Graduação em Irrigação no Cerrado, Instituto Federal Goiano (IF Goiano), Ceres, Goiás, Brazil

AUTHOR ORCIDs

Stanislav Jabinski http://orcid.org/0009-0002-4748-6151
Wesley d. M. Rangel http://orcid.org/0000-0002-0587-0908
Jan Jansa http://orcid.org/0000-0002-0331-1774
Travis B. Meador http://orcid.org/0000-0001-8255-5883

FUNDING

Funder	Grant(s)	Author(s)
Grantová Agentura České Republiky (GAČR)	20-223805	Travis B. Meador
Ministerstvo Školství, Mládeže a Tělovýchovy (MŠMT)	LM2015075	Travis B. Meador
EC | European Regional Development Fund (ERDF)	CZ.02.1.01/0.0/0.0/16_013/0001782	Travis B. Meador

AUTHOR CONTRIBUTIONS

Stanislav Jabinski, Conceptualization, Data curation, Formal analysis, Investigation, Methodology, Software, Validation, Visualization, Writing – original draft, Writing – review and editing | Wesley d. M. Rangel, Investigation, Methodology, Resources, Writing – review and editing | Marek Kopáček, Formal analysis, Methodology, Resources, Validation, Writing – review and editing | Veronika Jílková, Resources, Writing – review and editing | Jan Jansa, Conceptualization, Validation, Writing – review and editing |

Travis B. Meador, Conceptualization, Data curation, Formal analysis, Funding acquisition, Investigation, Methodology, Project administration, Resources, Software, Supervision, Validation, Visualization, Writing – original draft, Writing – review and editing

DATA AVAILABILITY

Cultivation and stable isotope composition data have been submitted to the Fractome database of biological isotope fractionations (https://fractome.caltech.edu/).

ADDITIONAL FILES

The following material is available online.

Supplemental Material

Text S1, Tables S1 and S2 (AEM02065-23-s0001.docx). Overview of supplemental material, iable of fungal strains used in this study, table of isotope incorporation values.
Tables S3 and S4 (AEM02065-23-s0002.xlsx). Raw data of isotope atom % values for fungal lipids and calculated incorporation factors.

REFERENCES

1. Schmidt MWI, Torn MS, Abiven S, Dittmar T, Guggenberger G, Janssens IA, Kleber M, Kögel-Knabner I, Lehmann J, Manning DAC, Nannipieri P, Rasse DP, Weiner S, Trumbore SE. 2011. Persistence of soil organic matter as an ecosystem property. Nature 478:49–56. https://doi.org/10.1038/nature10386
2. Lehmann J, Kleber M. 2015. The contentious nature of soil organic matter. Nature 528:60–68. https://doi.org/10.1038/nature16069
3. Han L, Sun K, Jin J, Xing B. 2016. Some concepts of soil organic carbon characteristics and mineral interaction from a review of literature. Soil Biol Biochem 94:107–121. https://doi.org/10.1016/j.soilbio.2015.11.023
4. Lv J, Huang Z, Luo L, Zhang S, Wang Y. 2022. Advances in molecular and microscale characterization of soil organic matter: current limitations and future prospects. Environ Sci Technol 56:12793–12810. https://doi.org/10.1021/acs.est.2c00421
5. Ciais P, Dolman AJ, Bombelli A, Duren R, Peregon A, Rayner PJ, Miller C, Gobron N, Kinderman G, Marland G, et al. 2014. Current systematic carbon-cycle observations and the need for implementing a policy-relevant carbon observing system. Biogeosciences 11:3547–3602. https://doi.org/10.5194/bg-11-3547-2014
6. Lindahl BD, Tunlid A. 2015. Ectomycorrhizal fungi–potential organic matter decomposers, yet not saprotrophs. New Phytol 205:1443–1447. https://doi.org/10.1111/nph.13201
7. Hart KM, Kulakova AN, Allen CCR, Simpson AJ, Oppenheimer SF, Masoom H, Courtier-Murias D, Soong R, Kulakov LA, Flanagan PV, Murphy BT, Kelleher BP. 2013. Tracking the fate of microbially sequestered carbon dioxide in soil organic matter. Environ Sci Technol 47:5128–5137. https://doi.org/10.1021/es3050696
8. San-Emeterio LM, Zavala LM, Jiménez-Morillo NT, Pérez-Ramos IM, González-Pérez JA. 2023. Effects of climate change on soil organic matter C and H isotope composition in a Mediterranean Savannah (*Dehesa*): an assessment using Py-CSIA. Environ Sci Technol 57:13851–13862. https://doi.org/10.1021/acs.est.3c01816
9. Frey SD. 2019. Mycorrhizal fungi as mediators of soil organic matter dynamics. Annu Rev Ecol Evol Syst 50:237–259. https://doi.org/10.1146/annurev-ecolsys-110617-062331
10. Snajdr J, Cajthaml T, Valášková V, Merhautová V, Petránková M, Spetz P, Leppänen K, Baldrian P. 2011. Transformation of Quercus petraea litter: successive changes in litter chemistry are reflected in differential enzyme activity and changes in the microbial community composition. FEMS Microbiol Ecol 75:291–303. https://doi.org/10.1111/j.1574-6941.2010.00999.x
11. Kirk TK, Farrell RL. 1987. Enzymatic" combustion": the microbial degradation of lignin. Annu Rev Microbiol 41:465–505. https://doi.org/10.1146/annurev.mi.41.100187.002341
12. Fioretto A, Di Nardo C, Papa S, Fuggi A. 2005. Lignin and cellulose degradation and nitrogen dynamics during decomposition of three leaf litter species in a Mediterranean ecosystem. Soil Biol Biochem 37:1083–1091. https://doi.org/10.1016/j.soilbio.2004.11.007
13. Baldrian P, Voříšková J, Dobiášová P, Merhautová V, Lisá L, Valášková V. 2011. Production of extracellular enzymes and degradation of biopolymers by saprotrophic microfungi from the upper layers of forest soil. Plant Soil 338:111–125. https://doi.org/10.1007/s11104-010-0324-3
14. Högberg P, Nordgren A, Buchmann N, Taylor AF, Ekblad A, Högberg MN, Nyberg G, Ottosson-Löfvenius M, Read DJ. 2001. Large-scale forest girdling shows that current photosynthesis drives soil respiration. Nature 411:789–792. https://doi.org/10.1038/35081058
15. Smith SE, Read D. 2008. Mineral nutrition, toxic element accumulation and water relations of arbuscular mycorrhizal plants. Mycorrhizal symbiosis 3:145–148. https://doi.org/10.1016/B978-012370526-6.50007-6
16. Kornberg HL. 1965. Anaplerotic sequences in microbial metabolism. Angew Chem Int Ed Engl 4:558–565. https://doi.org/10.1002/anie.196505581
17. Romanenko VI. 1964. Heterotrophic assimilation of CO_2 by bacterial flora of water. Mikrobiologiia 33:679–683.
18. Roslev P, Larsen MB, Jørgensen D, Hesselsoe M. 2004. Use of heterotrophic CO_2 assimilation as a measure of metabolic activity in planktonic and sessile bacteria. J Microbiol Methods 59:381–393. https://doi.org/10.1016/j.mimet.2004.08.002
19. Braun A, Spona-Friedl M, Avramov M, Elsner M, Baltar F, Reinthaler T, Herndl GJ, Griebler C. 2021. Reviews and syntheses: heterotrophic fixation of inorganic carbon–significant but invisible flux in environmental carbon cycling. Biogeosciences 18:3689–3700. https://doi.org/10.5194/bg-18-3689-2021
20. Sorokin JI. 1966. On the carbon dioxide uptake during the cell synthesis by microorganisms. Z Allg Mikrobiol 6:69–73. https://doi.org/10.1002/jobm.3630060107
21. Kellermann MY, Wegener G, Elvert M, Yoshinaga MY, Lin Y-S, Holler T, Mollar XP, Knittel K, Hinrichs K-U. 2012. Autotrophy as a predominant mode of carbon fixation in anaerobic methane-oxidizing microbial communities. Proc Natl Acad Sci U S A 109:19321–19326. https://doi.org/10.1073/pnas.1208795109
22. Kopf SH, McGlynn SE, Green-Saxena A, Guan Y, Newman DK, Orphan VJ. 2015. Heavy water and ^{15}N labelling with NanoSIMS analysis reveals growth rate-dependent metabolic heterogeneity in chemostats. Environ Microbiol 17:2542–2556. https://doi.org/10.1111/1462-2920.12752
23. Huguet A, Meador TB, Laggoun-Défarge F, Könneke M, Wu W, Derenne S, Hinrichs K-U. 2017. Production rates of bacterial tetraether lipids and fatty acids in peatland under varying oxygen concentrations. Geochim

Cosmochim Acta 203:103–116. https://doi.org/10.1016/j.gca.2017.01.012
24. Caro TA, McFarlin J, Jech S, Fierer N, Kopf S. 2023. Hydrogen stable isotope probing of lipids demonstrates slow rates of microbial growth in soil. Proc Natl Acad Sci U S A 120:e2211625120. https://doi.org/10.1073/pnas.2211625120
25. Hoefs J. 2018. Stable isotope geochemistry. Springer International Publishing AG, part of Springer Nature.
26. Zhang X, Gillespie AL, Sessions AL. 2009. Large D/H variations in bacterial lipids reflect central metabolic pathways. Proc Natl Acad Sci U S A 106:12580–12586. https://doi.org/10.1073/pnas.0903030106
27. Osburn MR, Sessions AL, Pepe-Ranney C, Spear JR. 2011. Hydrogen-isotopic variability in fatty acids from Yellowstone National Park hot spring microbial communities. Geochim Cosmochim Acta 75:4830–4845. https://doi.org/10.1016/j.gca.2011.05.038
28. Wegener G, Bausch M, Holler T, Thang NM, Prieto Mollar X, Kellermann MY, Hinrichs K-U, Boetius A. 2012. Assessing sub - seafloor microbial activity by combined stable isotope probing with deuterated water and ^{13}C - bicarbonate. Environ Microbiol 14:1517–1527. https://doi.org/10.1111/j.1462-2920.2012.02739.x
29. Wu W, Meador TB, Könneke M, Elvert M, Wegener G, Hinrichs KU. 2020. Substrate - dependent incorporation of carbon and hydrogen for lipid biosynthesis by *Methanosarcina barkeri*. Environ Microbiol Rep 12:555–567. https://doi.org/10.1111/1758-2229.12876
30. Thom C, Raper KB. 1945. A manual of the aspergilli. Vol. 60. LWW.
31. Hayes JM. 2004. An introduction to isotopic calculations. Woods Hole Oceanographic Institution, Woods Hole, MA.
32. Boschker HTS, Middelburg JJ. 2002. Stable isotopes and biomarkers in microbial ecology. FEMS Microbiol Ecol 40:85–95. https://doi.org/10.1111/j.1574-6941.2002.tb00940.x
33. Wu W, Meador T, Hinrichs K-U. 2018. Production and turnover of microbial organic matter in surface intertidal sediments. Org Geochem 121:104–113. https://doi.org/10.1016/j.orggeochem.2018.04.006
34. Dijkhuizen L, Harder W. 1985. Microbial metabolism of carbon dioxide. In Comprehensive biotechnology: the principles, applications, and regulations of biotechnology in industry, agriculture, and medicine/editor-in-chief, Murray Moo-Young
35. Erb TJ. 2011. Carboxylases in natural and synthetic microbial pathways. Appl Environ Microbiol 77:8466–8477. https://doi.org/10.1128/AEM.05702-11
36. Schinner F, Concin R. 1981. Carbon dioxide fixation by wood - rotting fungi. Eur J For Pathol 11:120–123. https://doi.org/10.1111/j.1439-0329.1981.tb00077.x
37. Schinner F, Concin R, Binder H. 1982. Heterotrophic CO_2 fixation by fungi in dependence on the concentration of the carbon source. Paper presented at the Phyton; annales rei botanicae
38. Shuler ML, Kargi F. 2002. Bioprocessing engineering: basic concepts. Prentice-Hall Inc, NJ: Upper Saddle River.
39. Dupont S, Lemetais G, Ferreira T, Cayot P, Gervais P, Beney L. 2012. Ergosterol biosynthesis: a fungal pathway for life on land? Evolution 66:2961–2968. https://doi.org/10.1111/j.1558-5646.2012.01667.x
40. Eisenkolb M, Zenzmaier C, Leitner E, Schneiter R. 2002. A specific structural requirement for ergosterol in long-chain fatty acid synthesis mutants important for maintaining raft domains in yeast. Mol Biol Cell 13:4414–4428. https://doi.org/10.1091/mbc.e02-02-0116
41. Valentine DL. 2009. Isotopic remembrance of metabolism past. Proc Natl Acad Sci U S A 106:12565–12566. https://doi.org/10.1073/pnas.0906428106
42. Wijker RS, Sessions AL, Fuhrer T, Phan M. 2019. $^2H/^1H$ variation in microbial lipids is controlled by NADPH metabolism. Proc Natl Acad Sci U S A 116:12173–12182. https://doi.org/10.1073/pnas.1818372116
43. Cooper AJL, Kuhara T. 2014. α-Ketoglutaramate: an overlooked metabolite of glutamine and a biomarker for hepatic encephalopathy and inborn errors of the urea cycle. Metab Brain Dis 29:991–1006. https://doi.org/10.1007/s11011-013-9444-9
44. Hu Z, He B, Ma L, Sun Y, Niu Y, Zeng B. 2017. Recent advances in ergosterol biosynthesis and regulation mechanisms in *Saccharomyces cerevisiae*. Indian J Microbiol 57:270–277. https://doi.org/10.1007/s12088-017-0657-1
45. Wu W. 2018. Microbial activity in marine sediment constrained via lipid-based stable isotope probing PhD Thesis, Universität Bremen
46. Kellermann MY, Yoshinaga MY, Wegener G, Krukenberg V, Hinrichs K-U. 2016. Tracing the production and fate of individual archaeal intact polar lipids using stable isotope probing. Org Geochem 95:13–20. https://doi.org/10.1016/j.orggeochem.2016.02.004
47. Wegener G, Kellermann MY, Elvert M. 2016. Tracking activity and function of microorganisms by stable isotope probing of membrane lipids. Curr Opin Biotechnol 41:43–52. https://doi.org/10.1016/j.copbio.2016.04.022
48. Holzer G, Bourne TF, Bertsch W. 1989. Analysis of *in situ* methylated microbial fatty acid constituents by curie-point pyrolysis—gas chromatography—mass spectrometry. J Chromatogr A 468:181–190. https://doi.org/10.1016/S0021-9673(00)96315-5
49. Ishida Y, Wakamatsu S, Yokoi H, Ohtani H, Tsuge S. 1999. Compositional analysis of polyunsaturated fatty acid oil by one-step thermally assisted hydrolysis and methylation in the presence of trimethylsulfonium hydroxide. J Anal Appl Pyrolysis 49:267–276. https://doi.org/10.1016/S0165-2370(98)00095-3
50. Blokker P, Pel R, Akoto L, Brinkman UAT, Vreuls RJJ. 2002. At-line gas chromatographic–mass spectrometric analysis of fatty acid profiles of green microalgae using a direct thermal desorption interface. J Chromatogr A 959:191–201. https://doi.org/10.1016/s0021--9673(02)00463-6
51. Parsi Z, Górecki T. 2006. Determination of ergosterol as an indicator of fungal biomass in various samples using non-discriminating flash pyrolysis. J Chromatogr A 1130:145–150. https://doi.org/10.1016/j.chroma.2006.07.045
52. Wörmer L, Lipp JS, Hinrichs K-U. 2017. Comprehensive analysis of microbial lipids in environmental samples through HPLC-MS protocols, p 289–317. In Hydrocarbon and lipid microbiology protocols: petroleum, hydrocarbon and lipid analysis
53. Elvert M, Boetius A, Knittel K, Jørgensen BB. 2003. Characterization of specific membrane fatty acids as chemotaxonomic markers for sulfate-reducing bacteria involved in anaerobic oxidation of methane. Geomicrobiol J 20:403–419. https://doi.org/10.1080/01490450303894

Manuscript II

Fungi present distinguishable isotopic signals when grown on glycolytic versus tricarboxylic acid cycle intermediates

Stanislav Jabinski, Vítězslav Kučera, Marek Kopáček, Jan Jansa, Travis B. Meador

(Submitted to Biogeoscience (2024))

Fungi present distinguishable isotopic signals when grown on glycolytic versus tricarboxylic acid cycle intermediates

Stanislav Jabinski[1,2] Vítězslav Kučera[3,4], Marek Kopáček[1,5], Jan Jansa[4], Travis B. Meador[1,2,5*]

[1]University of South Bohemia, Faculty of Science, Department of Ecosystem Biology, Branišovská 1760, 370 05 České Budějovice, Czechia

[2]Institute of Soil Biology and Biochemistry, Biology Centre CAS, Na Sádkách 7, 370 05 České Budějovice, Czechia

[3]Charles University, Faculty of Sciences, Albertov 6, 128 00 Praha, Czechia

[4]Institute of Microbiology CAS, Vídeňská 1083, 142 20 Praha, Czechia

[5]Institute of Hydrobiology, Biology Centre CAS, Na Sádkách 7, 370 05 České Budějovice, Czechia

Correspondence to: Travis B. Meador (travis.meador@bc.cas.cz)

Abstract

Microbial activity in soils controls both the size and turnover rates of large carbon (C) inventories stored in the subsurface, having important consequences for the partitioning of C between terrestrial and atmospheric reservoirs as well as the recycling of mineral nutrients such as nitrogen or phosphorus (often bound to the C) that support plant growth. Fungi are major decomposers of soil organic matter (SOM); however, uncertainty in the predominant C substrates that fuel respiration confound models of fungal production and SOM turnover. To further define the signals of microbial heterotrophic activity, we applied a dual hydrogen (H) and C stable isotope probing (SIP) approach on pure fungal cultures representing the phyla Ascomycetes, Basidiomycetes, and Zygomycetes growing on monomeric (glucose, succinate) or complex substrates (tannic acid, β-cyclodextrin). Our findings demonstrate that the investigated species incorporated only minor amounts of inorganic C (provided as carbonate) into their membrane lipids, amounting to < 3% of lipid-C, with no consistent patterns observed between species or growth substrates. The net incorporation of water-derived H (i.e., α_W) into lipids also did not differ significantly between incubations with monomeric versus complex substrates; however, growth on succinate solicited significantly higher α_W values than glucose or β-cyclodextrin. This finding suggests that environmental ^{2}H-SIP assays have the potential to distinguish between microbial communities supported predominantly by substrates that are catabolized by the tricarboxylic acid cycle versus glycolytic pathway. Furthermore, the average α_W value of heterotrophic fungal incubations [0.69 ± 0.03 (SEM)] is consistent with that observed for bacterial heterotrophs and may be applied for upscaling lipid-based estimates of fungal production in environmental assays.

1. Introduction

Soil organic matter (SOM) is the major reservoir of carbon (1580×10^{15} g C) in the biosphere, and active microbial populations act to redistribute this C to other reactive reservoirs, such as atmosphere (Carson et al., 2001; Grinhut et al., 2007). Major uncertainties in modeling C and climate dynamics stem from insufficient knowledge on the

controls of SOM degradation and transformation (Ciais et al., 2014; Lindahl and Tunlid 2015). Saprotrophic soil fungi are one of the major decomposers in soils, who are known to degrade naturally occurring complex molecules such as lignin (Kirk & Farrell, 1987; Fioretto et al., 2005; Baldrian et al., 2011), cellulose (Šnajdr et al., 2011) and humic substances (Grinhut et al., 2007), but are also reported to compete for accessible plant photosynthate excreted by roots (De Boer et al., 2005; Högberg et al., 2001; Smith & Read, 2008). Despite the unique and important fungal niche in biogeochemical cycles, their contributions to SOM cycling remains poorly constrained (Frey 2019; Grinhut et al., 2007). Furthermore, heterotrophic organisms feeding on organic substrates to gain energy and build biomass are also known to fix a variable amount of inorganic C, in order to replenish intermediates in the tricarboxylic acid (TCA) cycle (Kornberg 1965). It has been suggested that 2 - 8% of the biomass C in heterotrophs originates from inorganic C incorporated through anaplerotic carboxylation reactions (Romanenko 1964; Roslev et al., 2004; Braun et al., 2021). Although, the awareness of these processes has existed for decades (Kornberg 1965; Sorotkin 1966), the relevance and the metabolic controls on heterotrophic inorganic C fixation remains poorly understood, partly due to the lack of reliable estimates for most organisms and habitats (Braun et al., 2021).

Advanced analytical techniques now allow linking microbial taxa to specific processes in environmental studies by measuring the incorporation of stable isotopes into biomarkers (Boschker et al., 1998; Dumont and Murrell, 2005; Kreuzer-Martin, 2007), such as fungal and bacterial membrane lipid fatty acids (Treonis et al., 2004; Willers et al., 2015) or other biomarkers (Boschker and Middelbourg, 2002). Previous studies have demonstrated that variability in the $^{2/1}H$ composition of microbial lipids is redundant with that of environmental water (Hoefs, 2018; Kopf et al., 2015), and stable isotope probing (SIP) assays applying enrichments in $^{2}H_2O$ have proven to be a useful tracer of microbial activity in a diverse range of environments (Fischer et al., 2013; Kellermann et al., 2012; Wegener et al., 2016; Wu et al., 2018). Large H-isotope fractionations, yielding $\delta^{2}H$-values between −400‰ and +200‰, have been observed during biosynthetic incorporation of water hydrogen (water-H) into individual compounds within a single cell or total biomass, which can be indicative of metabolic processes (Osborn et al., 2011; Sachse et al., 2012; Zhang et al., 2009). To fully exploit the potential of SIP experiments, a dual-SIP approach was developed to track total microbial production by adding heavy water ($^{2}H_2O$) together with ^{13}C-labeled inorganic C (IC), enabling simultaneous estimates of total and autotrophic metabolism, respectively (Wegener et al., 2012; Wu et al., 2020). Recently, Jabinski et al. (2024) validated an innovation of the dual-SIP assay by using rapid pyrolysis of fungal biomass to determine the stable C and H isotopic composition of fungal lipids, and demonstrated that water-H and IC assimilation signatures could successfully distinguish between fungal ecotypes growing on glucose or glutamic acid as the C source.

The aim of the current study was to further assess the controls on water-H and inorganic C incorporation into lipids and expand our knowledge for interpreting environmental signals by applying the dual-SIP assay on a broader range of pure fungal cultures and growth substrates, including labile monomers versus more complex, high molecular weight molecules. We hypothesized that I) the incorporation of inorganic C and water-H into the fungal fatty acid biomarker $C_{18:2}$ will be similar for fungal species growing on the same substrate, and II) that inorganic C and water-H incorporation will distinguish between growth on labile versus more complex C substrates.

2. Methods

2.1 Cultivation & Harvesting

Fungal pure cultures of two Basidiomycetes (Paxillus involutus (PI, strain SB-22); Phanerodontia chrysosporium (PC, strain CCM8074)), two Zygomycetes (Mortierella (MO, strain RK-38); Umbelopsis (UM, strain RK-43)) and two Ascomycetes (Penicillium jancewskii (PJ, strain BCCO20_0265); Paecilomyces lilacinus (PL, strain DP-23)) were incubated at 25 °C in the dark in 500 mL Schott bottles containing 50 mL of a mineral media described previously (Bukovská et al 2018) with the vitamins left out, which was inoculated with approximately 10^6 spores or a hyphal block < 0.5 cm^3 (Basidiomycetes) recovered from a previous culture using the same cultivation medium solidified with agar (1.5%).

The growth medium contained per liter: 4 g organic C in various forms ($C_6H_{12}O_6$ glucose; $C_4H_6O_4$ succinic acid; $C_{42}H_{70}O_{35}$ β-Cyclodextrin or $C_{76}H_{52}O_{46}$ tannic acid), 0.01 g $FeSO_4$ * $7H_2O$, 2 g KH_2PO_4, 0.5 g $MgSO_4$ * $7H_2O$, 0.1 g NaCl, 0.1 g CaCl, 2.5 g $(NH_4)_2SO_4$, 0.45 g $NaHCO_3$ and 1 mL of a mixed solution (per liter: 0.5 g H_3BO_3, 0.04 g $CuSO_4$ * $5H_2O$, 0.1 g KI, 0.4 g $MnSO_4$ * $5H_2O$, 0.2 g $NaMoO_4$ * $2H_2O$, 0.4 g $ZnSO_4$ * $7H_2O$). The pH of the medium was adjusted to 4.5 before inoculation.

Dual-SIP experiments were performed using ^{13}C-bicarbonate (^{13}C-DIC, $NaH^{13}CO_3$) and deuterated water (D_2O). Each fungal strain was grown in triplicate with non-labeled substrates (Treatment I), with δ^2H of the medium water adjusted to 100‰ and 10% of ^{13}C-DIC (Treatment II), 200‰ δ^2H and 10% ^{13}C -DIC (Treatment III), and 400‰ δ^2H and 10% ^{13}C -DIC (Treatment IV). The Schott bottles were closed with a rubber stopper in order to keep the labeled ^{13}C-DIC from outgassing, and ample headspace was provided to maintain oxic conditions throughout the growth experiment. Fungal growth was monitored via the accumulation of CO_2 in the headspace, and we aimed to harvest when CO_2 levels reached 10%; however, without preliminary knowledge of the fungal growth dynamics, some cultivations exceeded this level more quickly than they could be sampled and analyzed.

Mycelia were separated from the growth medium via filtration through 5 µm Isopore polycarbonate filters (47 mm diam, Merck catalogue number TMTP04700) using vacuum filtration device allowing to collect the cultivation medium into sterile 50 mL tube. Thereafter, the mycelium was washed with ample MilliQ water, transferred to pre-weighed, sterile 50 mL tubes, fresh weight of the biomass was recorded, and the samples were frozen at -80 °C until lyophilization. A subsample of the cultivation medium was also frozen at -80 °C and the rest was used to determine pH post-incubation. After lyophilization, the dry weight of each sample was determined and stored at -20 °C until further analysis.

2.2 Measurements

2.2.1 Headspace CO_2 concentration and isotope composition

Samples of headspace (0.3 mL) were collected weekly from each bottle into helium flushed 12 mL exetainer vials (Exetainer, Labco Limited, UK) and analyzed for their CO2 concentration and 13C/12C isotopic ratio using Gasbench II equipped with a single cryo-trap connected to Delta V Advantage isotopic ratio mass spectrometer (IRMS) via Conflow IV (Thermo Scientific, Bremen, Germany). Ambient air (with the CO2 concentration

measured using LiCor 850 gas analyzer previously) was used as standard for CO2 concentration measurements, whereas laboratory cylinder with CO2 gas (δ13C = -2.86 ‰) was used as a standard for the isotopic composition of the C. The analytical error was below 1‰. Data was analyzed and exported using the Isodat 3.0 software.

2.2.2 Medium water (^2H_2O)

Liquid samples were transferred into 1.5 ml glass vials (32 x 11.6 mm, Fischer Scientific) and then measured using Triple Liquid Water Isotope Analyzer (Los Gatos Research), which is based on the principle of high-resolution laser absorption spectroscopy. Samples were dispensed into the instrument using an autosampler (PAL3 LSI, ABB company) and a 1.2 µL syringe (Hamilton). Samples were measured and evaluated against prepared laboratory standards of known isotopic composition. The isotopic ratios of these laboratory standards were verified by measuring against international standards (VSMOW2, SLAP2) made by the IAEA. For quality control purposes, the measurements of the samples were also interspersed with periodic measurements of the prepared verification samples with known isotopic composition. The final isotopic composition (δ^2H) was determined using LIMS software. Analytical error of δ^2H was <1.5‰.

Water sampled from incubations with tannic acid could not be measured using the laser, as described above, due to its high organic carbon content, and was rather measured via a GasBench II system (Thermo Scientific, Bremen, Germany; Application Note: 30049). Medium water samples (200 µL) were added with a platinum catalyst to a 12 mL exetainer vials (Exetainer, Labco Limited, UK). The headspace was flushed with 1% H_2 in He at approximately 100 mL min-1 with for 6 min. After an equilibration time of over 40 min, the samples were measured by purging the exetainer using a double-holed needle with helium into a 250 µL sample loop. The sample was then injected and separated via a Carboxen PLOT 1010 (0.53 mm ID; Supelco, Bellefonte, USA) held at 90 °C with a flow rate of 0.75 bar, and then introduced into the MAT253 Plus IRMS via a Conflo IV interface. Each sample was injected three times during one analysis. The isotopic composition was determined using Isodat 3.0 software against the corresponding H_2 working gas (-239‰ for δ^2H) and the values were corrected and normalized using international standards VSMOW2 (0‰ for δ^2H), SLAP2 (-427.5‰ for δ^2H), USGS53 (+40.2‰ for δ^2H) and GFLES-2 (159.9‰ for δ^2H). The analytical error was around 1‰.

2.2.3 Carbon ($\delta^{13}C$) substrate analysis

Substrates (~100 µg) were weighed into tin capsules (8 * 5 mm, Sercon, Crewe, UK) and placed in a helium-flushed carousel autosampler, then introduced to an Elemental Analyzer IsoLink device (EA IsoLink CNSOH, Thermo Scientific, Bremen, Germany) equipped with a CHN/NC/N EA combustion/reduction reactor (Sercon, Crewe, UK) heated to 1020 °C. A pulse of oxygen was introduced to the reactor simultaneously with the sample. The sample gases were quantified via a thermal conductivity detector (TCD) and then introduced to a MAT 253 Plus isotope ratio mass spectrometer (IRMS; Thermo Scientific; Bremen, Germany) via the open split of a Conflo IV interface, with helium as the carrier gas. The isotopic composition was determined using Isodat 3.0 software against the corresponding CO2 working gas (-4.191‰ for δ13C), and the values were corrected for linearity and normalized to the VPDB scale using international reference material IAEA-600 (-27.771‰ for δ13C). The analytical error was <0.04‰.

2.2.3 Pyrolysis GC for lipid analysis

The pyrolysis unit Shimadzu 3030D (Shimadzu, Kyoto, Japan/ Frontier Laboratories, Fukushima, Japan) was installed on top of the GC Trace1310 gas chromatograph SSL injector (Thermo Scientific, Bremen, Germany) and the GC was equipped with an SLB-IL60 column (non-bonded; 1,12-Di(tripropylphosphonium)dodecane bis(trifluoromethanesulfonyl)imide phase, 30 m, 0.25 mm ID, 0.20 µm df, Supelco, Bellefonte, USA). The furnace temperature was 650 °C and the interface temperature was 370 °C. The injector temperature was 360 °C and the GC oven was held at 80 °C for 1 min then ramped to 175 °C at 15 °C min^{-1}, then ramped to 195 °C at 2 °C min^{-1}, then ramped to 300 °C at 10 °C min^{-1}, and finally held at 300 °C for 7 min. Helium was used as carrier gas with a constant flow of 1.5 mL min^{-1} with a split ratio of 40 and a split flow of 26.7 mL min^{-1}. The column flow was split via a multichannel device to acquire MS and isotopic data simultaneously from one injection. The GC-MS (ISQ QD; Thermo Scientific, Bremen, Germany) ion source was set to electron impact ionization mode (EI) at 70 eV and a scan range of m/z 50 – 500 with a scan time of 0.2 sec^{-1} was applied. Scan started after 8 min to avoid the solvent peak in the MS. Transfer line temperature was set to 300 °C and the Ion source was set to 250 °C.

The samples (freeze-dry biomass, 0.1 mg – 1.3 mg) were weighed into an ultra-clean stainless steel Eco-Cup LF (Frontier Laboratories, Fukushima, Japan) which were burned with a torch before usage to ensure no contamination. FAMEs signals were acquired in the same run. Immediately prior to the measurement, 30 µL of trimethyl sulfonium hydroxide (TMSH) was added on the sample to increase the volatilization of the fatty acids and improve measurement sensitivity. Identification was performed using fragmentation patterns and the NIST 14 library.

Stable carbon and hydrogen isotope compositions of FAMEs were determined by splitting the flow from the GC column to a GC-Isolink II reactor, coupled to a MAT253 Plus IRMS via a Conflo IV interface. Values are expressed in standard delta notation ($\delta^{13}C$ and $\delta^{2}H$). MS information was simultaneously acquired by use of the multi-channel device described above. For conversion of FAMEs and ergosterol to CO_2, the combustion reactor (nickel oxide tube with CuO, NiO, and Pt wires) was set to 1000 °C. For conversion of FAMEs and ergosterol to H_2, the pyrolysis reactor (aluminum tube) was set to 1420 °C. FAMEs were identified by their retention times and fragmentation patterns. The isotopic composition was determined using Isodat 3.0 software against the corresponding CO_2 or H_2 working gas (-4.191‰ for $\delta^{13}C$, -239.5‰ for $\delta^{2}H$). Isotope corrections for instrument drifts, linearity, and normalization to the VPDB or VSMOW scales were performed according to the response of USGS70 (-30.53‰ for $\delta^{13}C$, -183.9‰ for $\delta^{2}H$) and USGS72 (-1.54‰ for $\delta^{13}C$, 348.3‰ for $\delta^{2}H$) reference standards. The analytical error was <0.5‰ and <10‰ for $\delta^{13}C$ and $\delta^{2}H$, respectively.

3. Results

3.1 Fungal growth and CO_2 production

All fungal species were pure cultures, which were incubated in a mineral medium with either glucose, succinate, β-cyclodextrin, or tannic acid serving as the sole organic C source. Growth was monitored by the evolution of CO_2 into the headspace, which ranged from 0.36% (no respiration of substrate) to a maximum of 35%, after incubation times ranging from 5 to 160 days (Fig. 1). The pH of the media in all incubations ranged from 2 to 5.5

at the time of harvest, with a general trend of decreasing pH with increasing CO_2; however, the trend was opposite when succinate was the carbon source, with pH increasing from 4 to 5.5. For samples that produced sufficient biomass, the dry biomass of harvested fungal hyphae ranged up to 250 mg, and at least 30 µg dry biomass was used to analyze fungal membrane fatty acids by Pyr-GC-IRMS. Only the Ascomycetes species PL and PJ grew sufficiently on each tested substrate to produce enough biomass for stable isotope analysis. Incubations of Zygomycetes species with glucose or succinate also yielded sufficient dry biomass, and only UM and not MO was able to grow on β-cyclodextrin; Zygomycetes species produced neither CO_2 nor biomass when incubated with tannic acid. The Basidiomycetes typically exhibited the slowest growth, and both species (PI and PC) only produced enough biomass when grown on glucose. The CO2 levels in Basidiomycetes incubations with succinate increased to a maximum of ~ 2%, but only PI yielded sufficient biomass for analysis. PC grew sufficiently on β-cyclodextrin, with CO_2 levels increasing to a maximum of 3%, while CO_2 remained < 0.6% in PI incubations.

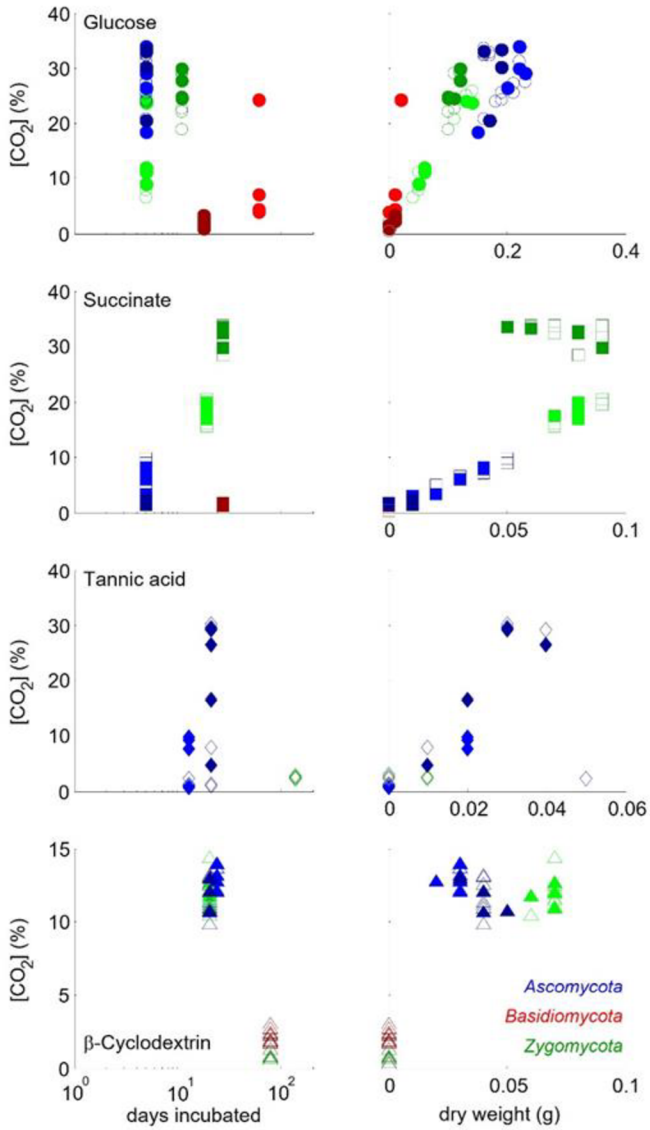

Figure 1. Growth of fungal species on each substrate as indicated by production of CO_2 versus days of incubation (left panels) or dry biomass (right panels). Filled symbols indicate samples for which the $C_{18:2}$ biomarker was measured by Pyr-GC-IRMS. Colors represent the Ascomycetes species PJ (dark blue) and PL (light blue), Zygomycetes species MO (dark green) and UM (light green), and Basidiomycetes species PC (dark red) and PI (light red). The symbols denote incubations with glucose (circles), succinate (squares), tannic acid (diamonds), or b-cyclodextrin (triangles).

Fungal respiration of the growth substrates led to decreasing $\delta^{13}C$-CO_2 values as fungal biomass was produced, which followed a hyperbolic trend expected for the mixing of CO_2 from two different sources (Text S1; c.f., Kendall and Caldwell, 1998). The atom % ^{13}C in control incubations with no fungal inoculum was measured at the latest time of harvest of inoculated incubations and stayed below 0.4% except tannic acid which ranged from 2-3%; the δ13C values of the substrates were glucose = -26.5‰; succinate = -28.3‰, tannic acid = -27.4‰, β-cyclodextrin = -10.6‰. The mixing relationship was modeled using all CO_2 data, across all incubations, and integrated to approximate the mixing-weighted average $F^{13}C$ value of inorganic C for each incubation (cf., Text S1, Fig. S2), which was finally applied in the denominator of Eq. 1 to estimate the fraction of lipid-C derived from inorganic C. For incubations that produced sufficient fungal biomass for stable C isotopic analysis, the weighted average $\delta^{13}C$ values of inorganic C that were applied in Eq. 1 ranged from 200 to 1400 ‰ (i.e., ~ 1.3 to 2.6 AT% ^{13}C).

3.2 Stable isotopic composition of fungal lipids

3.2.1 Carbon isotopes

The $\delta^{13}C$ values of fungal biomarker $C_{18:2}$ was determined as described in section 2.2.4 and is reported in this section as standard delta values (‰). The inorganic C incorporation into the biomarker was calculated based on the following equation 1:

$$\%IC_{(assimilation)} = \frac{F^{13C}{}_{lipids\ labeling} - F^{13C}{}_{lipids\ control}}{F^{13C}{}_{DIC(medium)} - F^{13C}{}_{substrate}} \times 100\% \qquad \text{(Eq. 1)}$$

Equation 1: Inorganic carbon (IC) assimilation was calculated as the difference in the ^{13}C atom fraction (F^{13C}) of lipids from the labeling experiment compared to the natural (control), relative to the difference between the mixing-weighted average F^{13C} of dissolved inorganic C (DIC, cf. Text S1) and the F^{13C} of the substrate. F was calculated as $F^{13}C = (R^{13C/12C})/(R^{13C/12C} + 1)$, where R is calculated from the $\delta^{13}C$ ratios as measured with the IRMS equipment using the reverse of the δ notations ($\delta^{13}C = ([^{13}C/^{12}C]_{sample}/[^{13}C/^{12}C]_{ref} - 1) * 1000$ (modified after Boschker & Middelburg 2002; Wegener et al., 2012).

The $\delta^{13}C$ values of fungal biomarkers $C_{18:2}$ (Table 1) produced under natural cultivation conditions with glucose (i.e., non-labeled; $AT\%_{DIC}$ ~ 1%) ranged from -24.1‰ to -21.2‰ across all strains (n = 6 species). As expected, $C_{18:2}$ harvested from the labeled incubations exhibited slightly higher $\delta^{13}C$ values (up to +11‰; PC grown on glucose) than the corresponding experiment amended with natural bicarbonate, likely owing to the incorporation of labeled inorganic C into the $C_{18:2}$ fatty acid.

Table 1. $\delta^{13}C$ values of fungal biomarker $C_{18:2}$ harvested from incubations with non-labeled substrates (nat) or those amended with ^{13}C-labeled bicarbonate. Incorporation of inorganic C (%IC) was calculated based on Eq.1. Not all fungal species grew on all substrates, and some did not give enough biomass for analysis (n.d*) and therefore no inorganic C incorporation was calculated (n.d). Errors represent the standard deviation of replicate incubations.

Species	**Glucose $\delta^{13}C$ (‰)**		**IC (%)**	**Succinate $\delta^{13}C$ (‰)**		**IC (%)**	**Tannic acid $\delta^{13}C$ (‰)**		**IC (%)**	**β-cyclodextrin $\delta^{13}C$ (‰)**		**IC (%)**
	Nat	+		nat	+		nat	+		nat	+	
Paxillus involutus (PI)	-21.5	-16.7	0.6 (±0.2)	n.d*	n.d*	n.d	n.d*	n.d*	n.d	n.d*	n.d*	n.d

Phanerodontia chrysosporium (PC)	-24.1	-15.9	0.9 (±0.3)	-27.3	-23.5	0.3 (±0.1)	n.d*	n.d*	n.d	n.d*	n.d*	n.d
Mortierella (MO)	-21.9	-20.7	0.5 (±0.1)	-31.7	-31.5	0.1 (±0.1)	n.d*	n.d*	n.d	n.d*	n.d*	n.d
Umbelopsis (UM)	-21.2	-21.1	0.1 (±0.0)	-30.6	-28.2	0.7 (±0.2)	n.d*	n.d*	n.d	-21.7	-18.1	0.8 (±0.3)
Penicillium jancewskii (PJ)	-23.2	-22.1	0.5 (±0.2)	-30.1	-27.8	0.2 (±0.0)	-25.9	-20.5	2.2 (±0.5)	-20.7	-20.1	0.1 (±0.2)
Paecilomyces lilacinus (PL)	-23.0	-23.5	n.d	-30.8	-29.9	0.1 (±0.0)	-25.4	-25.0	0.1 (±0.0)	-19.1	-17.6	0.7 (±0.4)

The estimated incorporation of IC into $C_{18:2}$ (%IC) typically ranged up to 1%; only PJ grown on tannic acid exhibited higher %IC values, which ranged up to 2.2% (Fig. 2). There were no general trends observed in %IC with other measured or estimated parameters, including CUE; however, for the two species that were able to grow on tannic acid, %IC was positively correlated with the amount of CO_2 and biomass produced during the incubation ($R^2 > 0.85$, $n = 5$, $p < 0.01$).

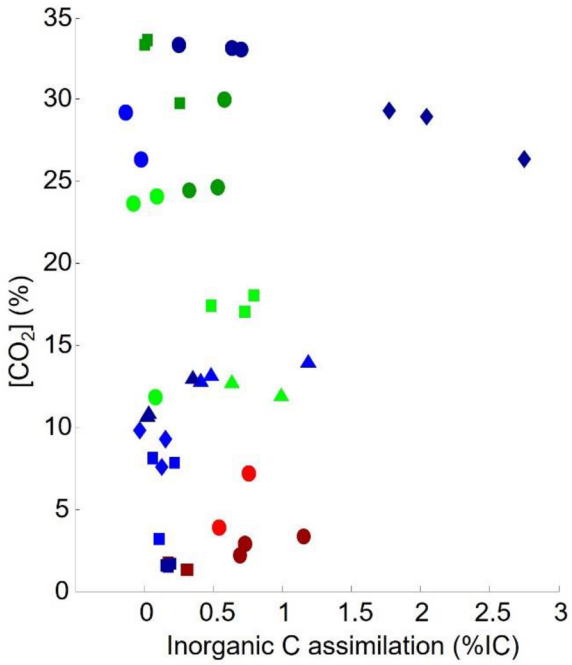

Figure 2. %IC values for fungal species respiring glucose (circles), succinate (squares), tannic acid (diamonds), or b-cyclodextrin (triangles). Colors represent fungal phyla as described in Fig. 1.

3.2.2 Water assimilation factor (α_W)

The "net" contribution of water hydrogen to lipid H is reported as the water hydrogen assimilation factor α_W (Kopf et al., 2015), and was estimated based on the slope of the linear regression line between H isotopic composition of lipid versus growth medium water (Fig. 3), which ranged from natural MilliQ (δ^2H = -45‰ ± 10‰) to the labeled treatments (65‰ ± 4‰; 166‰ ± 10‰; 368‰ ± 27‰). The α_W values for the fungal

biomarker $C_{18:2}$ grown on glucose ranged from 0.37 ± 0.03 to 0.75 ± 0.06 with an average value of 0.60 ± 0.05 (n = 6 species; ±SEM). When grown on succinic acid, the α_W values for $C_{18:2}$ harvested from individual species ranged from 0.78 ± 0.01 to 0.96 ± 0.02 with an average value of 0.83 ± 0.04 (n = 4 species; ±SEM). When grown on tannic acid, the α_W values for $C_{18:2}$ harvested from individual species ranged from 0.74 ± 0.06 to 0.77 ± 0.03, and when grown on β-cyclodextrin the α_W values for $C_{18:2}$ ranged from 0.46 ± 0.03 to 0.68 ± 0.04 with an average value of 0.58 ± 0.06 (n = 4 species; ±SEM). The average α_W values for $C_{18:2}$ for all substrates and species was 0.67 ± 0.04 (±SEM).

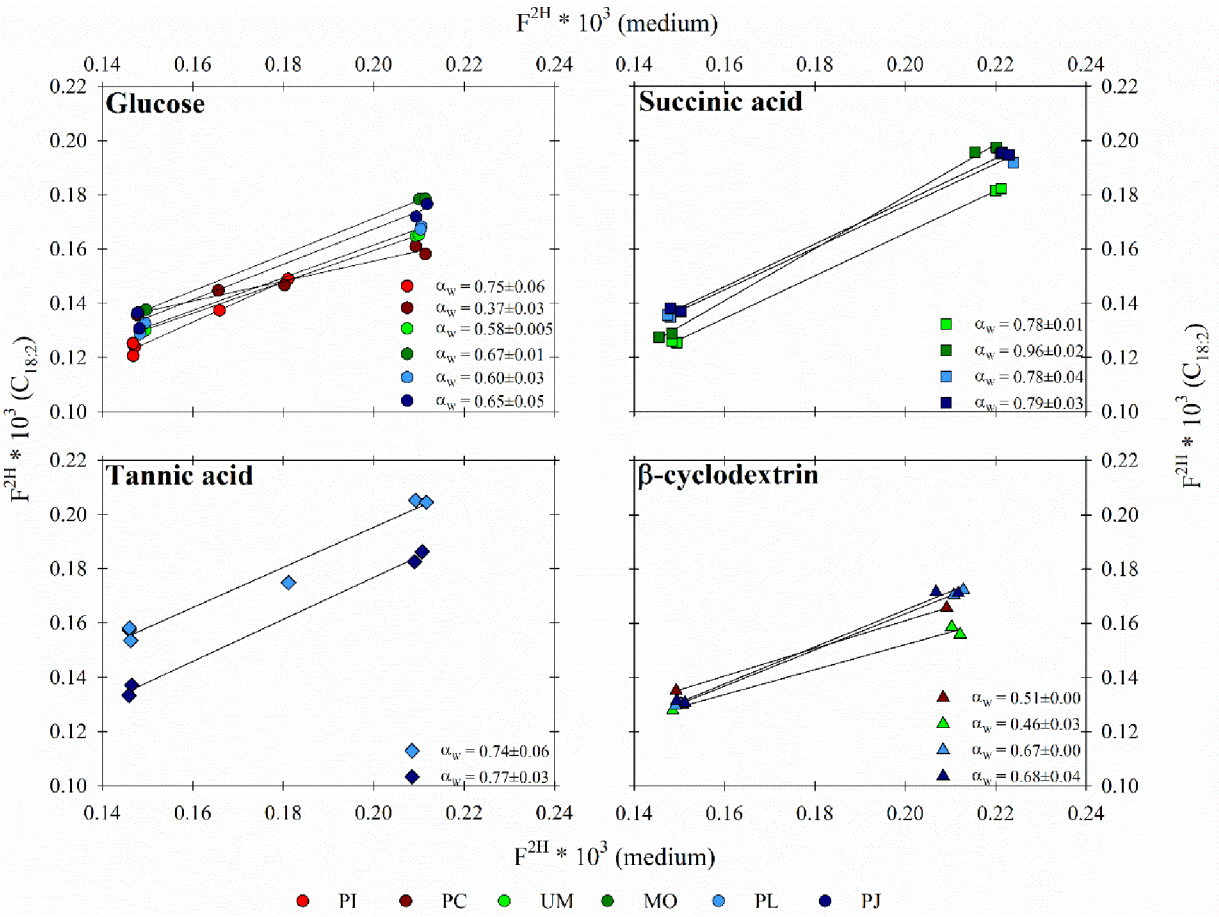

Figure 3. The water hydrogen assimilation factor (αW values) is estimated as the slope of the fractional $^{2/1}H$ abundance (F^{2H}) in lipids (y-axis) versus medium water (x-axis). Data are shown for fungal biomarker $C_{18:2}$ produced during growth on the different substrates (glucose, succinic acid, tannic acid and β-cyclodextrin) and harvested from the different fungal species [Paxillus involutus (PI), Phanerodontia chrysosporium (PC), Mortierella (MO), Umbelopsis (UM), Penicillium jancewskii (PJ) and Paecilomyces lilacinus (PL)]. R^2 values for all slopes were > 0.97.

4. Discussion

4.1 Fungal growth dynamics

Collectively, the fungal incubation experiments included a total of six species representing three different phyla, and exhibited a large range in the relative amounts of CO_2 and biomass produced, with the estimated carbon use efficiency [CUE = biomass-C / (CO_2 + biomass-C)] ranging from 0.2 to 0.6 (Fig. 4). The incubations were initiated under atmospheric, oxic conditions, such that fungi were able to respire the substrate aerobically. While oxic conditions likely prevailed during most of the incubation period, it is probable that some incubations turned

anoxic when CO_2 levels exceeded 21%, which occurred primarily in incubations with glucose or *Mortierella*. This was an unintended consequence of performing the incubations in closed bottles, which was required to prevent the escape of ^{13}C-labeled inorganic C. Nevertheless, such alteration between oxic and anoxic conditions is common in natural environments, and the measured inorganic C assimilation into fungal lipids was consistently low (<3%; Fig. 2), regardless of the implied anoxia.

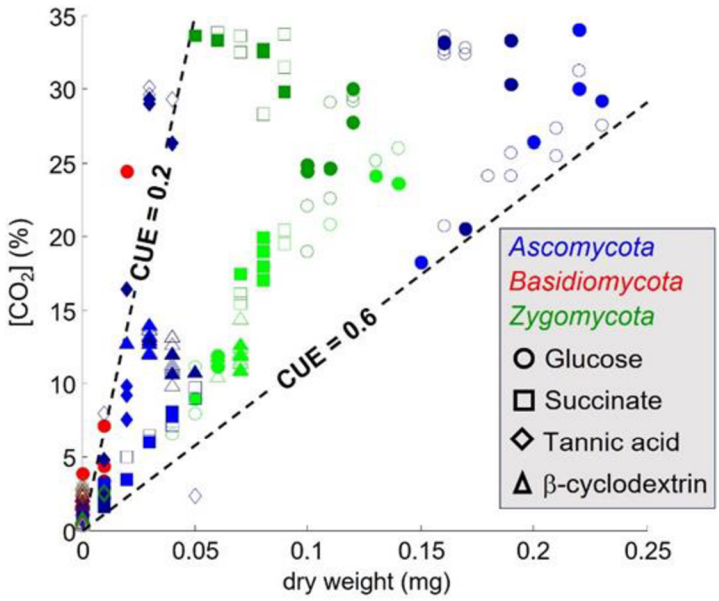

Figure 4. Carbon use efficiency of fungal species from three phyla growing on monomers or complex substrates. Colors and symbols are consistent with Fig. 1.

4.2 Fungal IC assimilation into lipids

A fundamental process in nature and basis for ecological food webs is the fixation of inorganic C via photosynthesis and chemosynthesis by autotrophic organisms. Inorganic C assimilation by heterotrophic organisms also plays an important role in ensuring the provision of energy and to replenish intermediates in the TCA cycle that have been released for biosynthesis (Kornberg 1965). Therefore, inorganic C assimilation is a measure of both anabolic processes and the catabolic status of the cell, influenced by assimilation, biosynthesis, anaplerotic reactions and redox balancing reactions (Braun et al., 2021; Erb 2011). Previous reports on the by-fixation of inorganic C (%IC) via anaplerotic pathways into heterotrophic biomass varied between 1 - 8% (Dijkhuizen & Harder, 1985; Feisthauer et al., 2008; Romanenko 1964; Roslev et al., 2004), whereas for fungi it was previously reported to amount to roughly 1% (Sorokin 1961; Schinner & Concin, 1981; Schinner et al., 1982), and was recently shown to vary between 2 – 12% for Ascomycetes when grown on glucose or glutamic acid (Jabinski et al., 2024). Our results demonstrate a low range in %IC for all different substrates and species tested in this study (0 - 3%), with the Ascomycetes (0 - 2%) assimilating relatively less inorganic C then previously reported species (4.6% ± 1.6%; Jabinski et al., 2024). The highest incorporation was 2.8% by *Penicillium jancewskii* (PJ) when grown on tannic acid (Table 1; Fig. 3); notably, this experiment yielded high production of CO_2 and biomass, suggesting that increased assimilation of inorganic C may promote the ability to respire the complex substrate. The high CO_2 levels also suggest that the incubations of PJ with tannic acid may have turned anoxic, which may also explain the higher inorganic C incorporation in these incubations.

4.3 Water hydrogen derived Lipid synthesis

As demonstrated previously, the regression slope between hydrogen isotopic composition of water medium and microbial lipids (i.e., α_W) varies with the type of metabolism (Zhang et al., 2009; Valentine, 2009; Wijker et al., 2019; Jabinski et al., 2024). For fatty acid biosynthesis, H incorporation is suggested to be a function of transporters and electron acceptors (NADPH and NADH), with contributions accounting for around half of all lipid hydrogen. The remaining comprises equal contributions of H obtained directly from environmental water or acetyl-CoA (Valentine, 2009; Zhang et al., 2009; Caro et al., 2023). The consensus from previous studies that investigated the lipids of heterotrophic bacteria is that microbial heterotrophs exhibit α_W values ranging from 0 to 1.2, with a mean of 0.71±0.17 (e.g., Caro et al., 2023). Jabinski et al. (2024) demonstrated that five species of heterotrophic Ascomycetes exhibit similar α_W values (0.62 ± 0.04) for the fungal biomarker $C_{18:2}$ during growth on glucose. In the current study, α_W values for the fungal biomarker $C_{18:2}$ during growth on glucose (0.60 ± 0.05) were agreeable with Jabinski et al. (2024), but more variable, likely owing to the broader phylogenetic coverage of the current study. However, significant differences in α_W values were observed both between and within the different phyla and substrates tested.

Ascomycetes species exhibited the most consistent α_W values when grown on each of the four different substrates [0.63 ± 0.03 (Glu); 0.78 ± 0.01 (SA); 0.76 ± 0.02 (TA); 0.67 ± 0.01 (BC)]. Basidiomycetes only produced enough biomass for isotopic analysis when grown on glucose and β-cyclodextrin, and showed high variability in α_W between species. For example, during growth on glucose, *P. involutus* exhibited much higher α_W values than *P. chrysosporium* (0.75 ± 0.06 versus 0.37 ± 0.03, respectively), and both of these values were beyond the more confined range of α_W values determined for Zygomycetes and Ascomycetes species. Growth on β-cyclodextrin, which consists of seven glucopyranose units ($C_6H_{12}O_6$), exhibited similar α_W values (0.58 ± 0.06) as growth on glucose (0.60 ± 0.05), suggesting that the catabolism of glucose subunits via glycolysis overprints signals of water-H incorporation that may derive during degradation of β-cyclodextrin. Succinate yielded significantly higher α_W values (0.83 ± 0.05), which was more similar to that reported previously for glutamic acid (0.90 ± 0.07; Jabinski et al., 2024). A one-way analysis of variance (ANOVA; Holm-Sidak method; SigmaPlot v11) confirmed the significant difference between glucose and glutamic acid ($p < 0.001$), glutamic acid and β-cyclodextrin ($p < 0.001$), succinate and glucose ($p < 0.003$) and succinate and β-cyclodextrin ($p < 0.005$). It also confirmed that there was no significant difference between the other substrate combinations ($p > 0.005$). Notably, glutamic acid and succinate are thought to be introduced into the TCA cycle through coupled metabolites, where succinate is a direct metabolite inside the TCA cycle and glutamic acid is converted to α-ketoglutarate intermediate by transamination before entering the TCA cycle, which is only 2 steps from succinate (Cooper et al., 2014). Also, being acids, these substrates may have a greater capacity than saccharides to exchange H with ambient water at experimental pH (typically $2 < pH < 5.2$), especially glutamic acid, which also comprises an amino moiety. Tannic acid (0.76 ± 0.02) yielded no significant differences ($p > 0.005$) from the other substrates, and is reported to be degraded to different subunits including gallic acid and glucose (Banerjee and Mahapatra, 2012; Lekha and Lonsane, 1997 and references within). Aromatic degradation pathways employed by fungi generate intermediates that go through the β-ketoadipate pathway (Mäkelä et al., 2015) before entering the TCA cycle as a succinyl-CoA

metabolite (Lekha and Lonsane, 1997). The α_W values induced by degradation of TA suggest that it integrates both the low α_W signature of glycolysis and high α_W signature of the TCA cycle (Fig. 5).

Together, our incubation experiments suggest that α_W values determined for the fungal biomarker $C_{18:2}$ could not distinguish between fungal growth on relatively labile monomers (i.e., glucose and succinate; requiring as few as 5 days of cultivation) versus larger, less-labile substrates (i.e., β-cyclodextrin and tannic acid; requiring 20 to 183 days of cultivation). However, with the exception of Basidiomycetes, α_W values of fungal lipid biomarkers may be indicative of fungi employing primarily glycolytic or TCA pathways. Environmental assays that quantify fungal lipid production via the incorporation of ambient water-H (i.e., the lipid-SIP approach) may upscale to total production estimates by applying our calculated mean α_W value of 0.69 ± 0.03 [n = 27; ± (SEM)], which is consistent with the α_W value of 0.71 recommended for soil microbial communities (Caro et al., 2023).

4.4 Dual-SIP approach

Dual-SIP experiments with ^2H_2O and ^{13}C-dissolved IC previously highlighted the potential to track microbial activity and distinguish heterotopic vs autotrophic metabolic modes within environmental settings and pure cultures (Kellerman et al., 2012, 2016; Wegener et al., 2012; Huguet et al., 2017; Wu et al., 2018, 2020). This approach was also previously applied to investigate fungal pure cultures (Jabinski et al., 2024), in which the plot of assimilation of inorganic C versus water-H into the fungal biomarker $C_{18:2}$ could distinguish five Ascomycetes species growing on glucose or glutamic acid, with α_W values explaining most of the variability. While calculated IC:α_W are useful to distinguish autotrophic from heterotrophic growth, all calculated values in this study remained near zero, with %IC ranging up to 3% and α_W values ranging from 0.6 to 0.8. This pure culture study therefore suggests that fungal assimilation of inorganic C is low and less insightful than the more distinguishable α_W values for identifying fungal phylotypes or ecotypes in environmental assays.

5. Conclusion

The purpose of this work was to apply the dual-SIP assay on pure fungal cultures to define the effect of different carbon substrates on incorporation of water-H and inorganic C into their membrane lipids. Although heterotrophic C fixation by microbes may range up to 8% of biomass C, inorganic C assimilation into the fungal biomarker $C_{18:2}$ harvested from six species representing Ascomycetes, Basidiomycetes, and Zygomycetes did not vary consistently between species or substrate, and remained below 3%. However, *Penicillium jancewskii*, the species that was most successful at respiring tannic acid, also exhibited the highest %IC value of all incubations (Fig. 1; Fig. 5), suggesting that fungal degradation of similarly complex substrates may rely in part on the assimilation of inorganic C (e.g., via anaplerotic reactions).

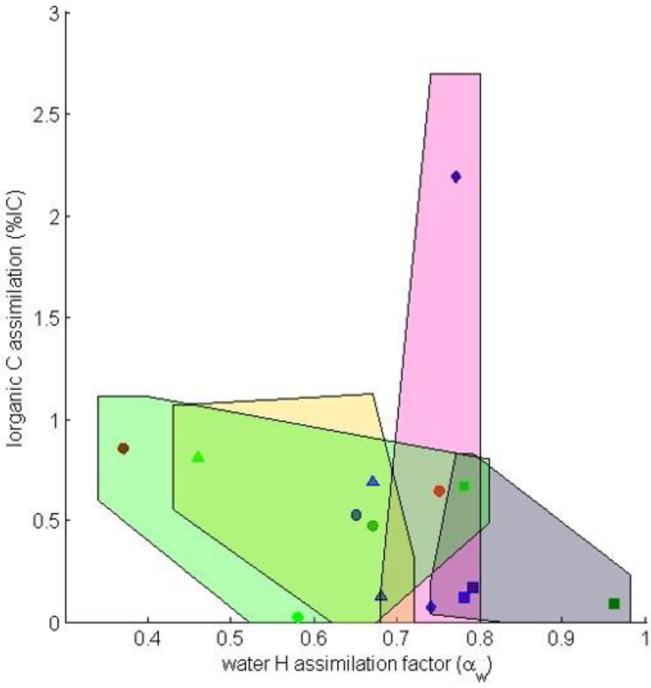

Figure 5. %IC and α_W value scatter plot for $C_{18:2}$ identifying the grouping of glucose (circles, green shape), succinic acid (squares, grey shape), tannic acid (diamonds, pink shape) and b-cyclodextrin (triangles, yellow shape) incubations with Ascomycetes, Basidiomycetes, and Zygomycetes. Refer to Fig. 1. Caption for further details.

In contrast to %IC, we conclude that substrates that activated the glycolysis pathway yielded significantly lower α_W values than those catabolized as TCA intermediates. The expanded dataset provided by this study indicates that inorganic C assimilation by heterotrophic fungi accounts for < 3% of lipid carbon, and fungal production estimated by ^{2}H-lipid SIP experiments can be adjusted by an average α_W value of 0.69, to provide a more accurate estimate of total lipid production. Furthermore, determination of α_W values in environmental ^{2}H-SIP assays may be useful to identify the prevalence of fungal ecotypes that rely on C substrates fueling glycolysis (e.g., leaf litter) versus those that are fed primarily by TCA intermediates (e.g., root exudate).

Author contribution

Stanislav Jabinski, Conceptualization, Data curation, Formal analysis, Investigation, Methodology, Software, Validation, Visualization, Writing – original draft, Writing – review and editing

Vítězslav Kučera, Investigation, Methodology, Resources, Writing – review and editing

Marek Kopáček, Formal analysis, Methodology, Resources, Validation,

Jan Jansa, Conceptualization, Formal analysis, Methodology, Resources, Validation, Writing – review and editing

Travis B. Meador, Conceptualization, Data curation, Formal analysis, Funding acquisition, Investigation, Methodology, Project administration, Resources, Software, Supervision, Validation, Visualization, Writing – original draft, Writing – review and editing

Competing interests

The authors declare that they have no conflict of interest.

Acknowledgements

We thank Ljubov Polaková for the support of the stable isotope measurements and laboratory protocols; the Collection of Microscopic Fungi of the Institute of Soil Biology BC CAS for providing the fungal species Penicillium janczewskii strain BCCO20_0265 and the Institute of Institute of Microbiology CAS for providing the fungal species Paxillus involutus strain SB-22; Phanerodontia chrysosporium strain CCM8074, Mortierella strain RK-38; Umbelopsis strain RK-43 and Paecilomyces lilacinus strain DP-23.

This Project was funded by the Czech Science Foundation GACR nr. 20-223805 (FUNSIF) and supported by MEYS CZ grant LM2015075 Projects of Large Infrastructure for Research, Development and Innovations as well as the European Regional Development Fund-Project: research of key soil-water ecosystem interactions at the SoWa Research Infrastructure (No. CZ.02.1.01/0.0/0.0/16_013/0001782).

References

Baldrian, P., Voříšková, J., Dobiášová, P., Merhautová, V., Lisá, L., & Valášková, V. (2011). Production of extracellular enzymes and degradation of biopolymers by saprotrophic microfungi from the upper layers of forest soil. *Plant and Soil, 338*(1-2), 111-125.

Banerjee, D., & Mahapatra, S. (2012). Fungal tannase: A journey from strain isolation to enzyme applications. *Dynamic Biochemistry, Process Biotechnology and Molecular Biology, 6*(2), 49-60.

Boer, W. D., Folman, L. B., Summerbell, R. C., & Boddy, L. (2005). Living in a fungal world: Impact of fungi on soil bacterial niche development. *FEMS Microbiology Reviews, 29*(4), 795-811.

Boschker, H. T. S., & Middelburg, J. J. (2002). Stable isotopes and biomarkers in microbial ecology. *FEMS Microbiology Ecology, 40*, 85-95.

Boschker, H. T. S., Nold, S. C., Wellsbury, P., Bos, D., De Graaf, W., Pel, R., & Cappenberg, T. E. (1998). Direct linking of microbial populations to specific biogeochemical processes by 13C-labelling of biomarkers. *Nature, 392*(6678), 801-805.

Braun, A., Spona-Friedl, M., Avramov, M., Elsner, M., Baltar, F., Reinthaler, T., Herndl, G. J., & Griebler, C. (2021). Reviews and syntheses: Heterotrophic fixation of inorganic carbon—significant but invisible flux in environmental carbon cycling. *Biogeosciences, 18*, 3689–3700.

Bukovská, P., Bonkowski, M., Konvalinková, T., Beskid, O., Hujslová, M., Püschel, D., et al. (2018). Utilization of organic nitrogen by arbuscular mycorrhizal fungi - is there a specific role for protists and ammonia oxidizers? *Mycorrhiza, 28*(3), 269-283.

Carlson, C. A., Bates, N. R., Hansell, D. A., & Steinberg, D. K. (2001). Carbon Cycle. In J. Steele, S. Thorpe, & K. Turekian (Eds.), *Encyclopedia of Ocean Science* (2nd ed., pp. 477-486). Academic Press.

Caro, T. A., McFarlin, J., Jech, S., Fierer, N., & Kopf, S. (2023). Hydrogen stable isotope probing of lipids demonstrates slow rates of microbial growth in soil. *Proceedings of the National Academy of Sciences, 120*(16), e2211625120.

Ciais, P., Dolman, A. J., Bombelli, A., Duren, R., Peregon, A., Rayner, P. J., & Marland, G. (2014). Current systematic carbon-cycle observations and the need for implementing a policy-relevant carbon observing system. *Biogeosciences, 11*(13), 3547-3602.

Cooper, A. J. L., & Kuhara, T. (2014). α-Ketoglutaramate: An overlooked metabolite of glutamine and a biomarker for hepatic encephalopathy and inborn errors of the urea cycle. *Metabolic Brain Disease, 29*, 991-1006.

Dijkhuizen, L., & Harder, W. (1985). Microbial metabolism of carbon dioxide. In M. Moo-Young (Ed.), *Comprehensive Biotechnology: The Principles, Applications, and Regulations of Biotechnology in Industry, Agriculture, and Medicine*.

Dumont, M. G., & Murrell, J. C. (2005). Stable isotope probing—linking microbial identity to function. *Nature Reviews Microbiology, 3*(6), 499-504.

Erb, T. J. (2011). Carboxylases in natural and synthetic microbial pathways. *Applied and Environmental Microbiology, 77*, 8466-8477.

Feisthauer, S., Wick, L. Y., Kästner, M., Kaschabek, S. R., Schlömann, M., & Richnow, H. H. (2008). Differences of heterotrophic 13CO2 assimilation by *Pseudomonas knackmussii* strain B13 and *Rhodococcus opacus* 1CP and potential impact on biomarker stable isotope probing. *Environmental Microbiology, 10*(6), 1641-1651.

Fioretto, A., Di Nardo, C., Papa, S., & Fuggi, A. (2005). Lignin and cellulose degradation and nitrogen dynamics during decomposition of three leaf litter species in a Mediterranean ecosystem. *Soil Biology and Biochemistry, 37*(6), 1083-1091.

Fischer, C. R., Bowen, B. P., Pan, C., Northen, T. R., & Banfield, J. F. (2013). Stable-isotope probing reveals that hydrogen isotope fractionation in proteins and lipids in a microbial community are different and species-specific. *ACS Chemical Biology, 8*(8), 1755-1763.

Frey, S. D. (2019). Mycorrhizal fungi as mediators of soil organic matter dynamics. *Annual Review of Ecology, Evolution, and Systematics, 50*, 237-259.

Grinhut, T., Hadar, Y., & Chen, Y. (2007). Degradation and transformation of humic substances by saprotrophic fungi: Processes and mechanisms. *Fungal Biology Reviews, 21*(4), 179-189.

Hoefs, J. (2018). Stable isotope geochemistry. *Springer International Publishing AG*, part of Springer Nature.

Högberg, P., Nordgren, A., Buchmann, N., Taylor, A. F., Ekblad, A., Högberg, M. N., & Read, D. J. (2001). Large-scale forest girdling shows that current photosynthesis drives soil respiration. *Nature, 411*(6839), 789-792.

Huguet, A., Meador, T. B., Laggoun-Défarge, F., Könneke, M., Wu, W., Derenne, S., & Hinrichs, K.-U. (2017). Production rates of bacterial tetraether lipids and fatty acids in peatland under varying oxygen concentrations. *Geochimica et Cosmochimica Acta, 203*, 103-116.

Jabinski, S., Rangel, W. D. M., Kopáček, M., Jílková, V., Jansa, J., & Meador, T. B. (2024). Constraining activity and growth substrate of fungal decomposers via assimilation patterns of inorganic carbon and water into lipid biomarkers. *Applied and Environmental Microbiology, 90*(4), e02065-23.

Kellermann, M. Y., Wegener, G., Elvert, M., Yoshinaga, M. Y., Lin, Y.-S., Holler, T., & Hinrichs, K.-U. (2012). Autotrophy as a predominant mode of carbon fixation in anaerobic methane-oxidizing microbial communities. *Proceedings of the National Academy of Sciences, 109*(47), 19321-19326.

Kellermann, M. Y., Yoshinaga, M. Y., Wegener, G., Krukenberg, V., & Hinrichs, K.-U. (2016). Tracing the production and fate of individual archaeal intact polar lipids using stable isotope probing. *Organic Geochemistry, 95*, 13-20.

Kirk, T. K., & Farrell, R. L. (1987). Enzymatic combustion: The microbial degradation of lignin. *Annual Reviews in Microbiology, 41*(1), 465-501.

Kopf, S. H., McGlynn, S. E., Green-Saxena, A., Guan, Y., Newman, D. K., & Orphan, V. J. (2015). Heavy water and (15)N labelling with NanoSIMS analysis reveals growth rate-dependent metabolic heterogeneity in chemostats. *Environmental Microbiology, 17*(7), 2542-2556.

Kornberg, H. L. (1965). Anaplerotic sequences in microbial metabolism. *Angewandte Chemie International Edition in English, 4*, 558-565.

Kreuzer-Martin, H. W. (2007). Stable isotope probing: Linking functional activity to specific members of microbial communities. *Soil Science Society of America Journal, 71*(2), 611-619.

Lekha, P. K., & Lonsane, B. K. (1997). Production and application of tannin acyl hydrolase: State of the art. *Advances in Applied Microbiology, 44*, 215-260.

Lindahl, B. D., & Tunlid, A. (2015). Ectomycorrhizal fungi–potential organic matter decomposers, yet not saprotrophs. *New Phytologist, 205*(4), 1443-1447.

Osburn, M. R., Sessions, A. L., Pepe-Ranney, C., & Spear, J. R. (2011). Hydrogen-isotopic variability in fatty acids from Yellowstone National Park hot spring microbial communities. *Geochimica et Cosmochimica Acta, 75*(17), 4830-4845.

Romanenko, V. I. (1964). Heterotrophic assimilation of CO2 by bacterial flora of water. *Mikrobiologiia, 33*, 679-683.

Roslev, P., Larsen, M. B., Jørgensen, D., & Hesselsoe, M. (2004). Use of heterotrophic CO2 assimilation as a measure of metabolic activity in planktonic and sessile bacteria. *Journal of Microbiological Methods, 59*, 381-393.

Sachse, D., Billault, I., Bowen, G. J., Chikaraishi, Y., Dawson, T. E., Feakins, S. J., & Kahmen, A. (2012). Molecular paleohydrology: Interpreting the hydrogen-isotopic composition of lipid biomarkers from photosynthesizing organisms. *Annual Review of Earth and Planetary Sciences, 40*, 221-249.

Schinner, F., Concin, R., & Binder, H. (1982). Heterotrophic CO2 fixation by fungi in dependence on the concentration of the carbon source. *Paper presented at the Phyton; Annales Rei Botanicae.*

Schinner, F., & Concin, R. (1981). Carbon dioxide fixation by wood-rotting fungi. *European Journal of Forest Pathology, 11*, 120-123.

Smith, S. E., & Read, D. (2008). Mineral nutrition, toxic element accumulation and water relations of arbuscular mycorrhizal plants. *Mycorrhizal Symbiosis, 3*, 145-148.

Šnajdr, J., Cajthaml, T., Valášková, V., Merhautová, V., Petránková, M., Spetz, P., & Baldrian, P. (2011). Transformation of *Quercus petraea* litter: Successive changes in litter chemistry are reflected in differential enzyme activity and changes in the microbial community composition. *FEMS Microbiology Ecology, 75*(2), 291-303.

Sorokin, J. I. (1966). On the carbon dioxide uptake during the cell synthesis by microorganisms. *Zeitschrift für allgemeine Mikrobiologie, 6*(1), 69-73.

Sorokin, Y. I. (1961). Heterotrophic carbon dioxide assimilation by microorganisms. *Zhurnal Obshchei Biologii, 22*(4), 265-272.

Treonis, A. M., Ostle, N. J., Stott, A. W., Primrose, R., Grayston, S. J., & Ineson, P. (2004). Identification of groups of metabolically-active rhizosphere microorganisms by stable isotope probing of PLFAs. *Soil Biology and Biochemistry, 36*(3), 533-537.

Valentine, D. L. (2009). Isotopic remembrance of metabolism past. *Proceedings of the National Academy of Sciences, 106*(31), 12565-12566.

Wegener, G., Bausch, M., Holler, T., Thang, N. M., Prieto Mollar, X., Kellermann, M. Y., & Boetius, A. (2012). Assessing sub-seafloor microbial activity by combined stable isotope probing with deuterated water and 13C-bicarbonate. *Environmental Microbiology, 14*(6), 1517-1527.

Wegener, G., Kellermann, M. Y., & Elvert, M. (2016). Tracking activity and function of microorganisms by stable isotope probing of membrane lipids. *Current Opinion in Biotechnology, 41*, 43-52.

Wijker, R. S., Sessions, A. L., Fuhrer, T., & Phan, M. (2019). 2H/1H variation in microbial lipids is controlled by NADPH metabolism. *Proceedings of the National Academy of Sciences, 116*(25), 12173-12182.

Willers, C., Jansen van Rensburg, P. J., & Claassens, S. (2015). Phospholipid fatty acid profiling of microbial communities–a review of interpretations and recent applications. *Journal of Applied Microbiology, 119*(5), 1207-1218.

Wu, W., Meador, T. B., & Hinrichs, K.-U. (2018). Production and turnover of microbial organic matter in surface intertidal sediments. *Organic Geochemistry, 121*, 104–113.

Wu, W., Meador, T. B., Könneke, M., Elvert, M., Wegener, G., & Hinrichs, K. U. (2020). Substrate-dependent incorporation of carbon and hydrogen for lipid biosynthesis by *Methanosarcina barkeri*. *Environmental Microbiology Reports, 12*(5), 555-567.

Zhang, X., Gillespie, A. L., & Sessions, A. L. (2009). Large D/H variations in bacterial lipids reflect central metabolic pathways. *Proceedings of the National Academy of Sciences, 106*(31), 12580-12586

Additional information

Text S1. Mixing model

$\delta^{13}C$-CO_2 was proportional to inverse of CO_2 concentration in the headspace, as expected for stable isotopic mixing models (cf. Kendall and Caldwell, 1998). In our case, the labeled bicarbonate amendment could contribute

to a total CO_2 concentration ([CO_2]) of ~ 0.3 %, which mixed with CO_2 released from respiration of the substrates during the incubation; this assumption neglects the known fractionation of CO2 exchange between the headspace and medium, which we assume to be minimal given the high label (target AT% ^{13}C = 10%). Data from all incubations plotted along a hyperbolic curve, which was modeled as a simple inverse relationship:

$$d^{13}C_{CO2} = (929 \times 1/[CO_2]) + d^{13}C_{subs} \qquad \textit{Equation S1}$$

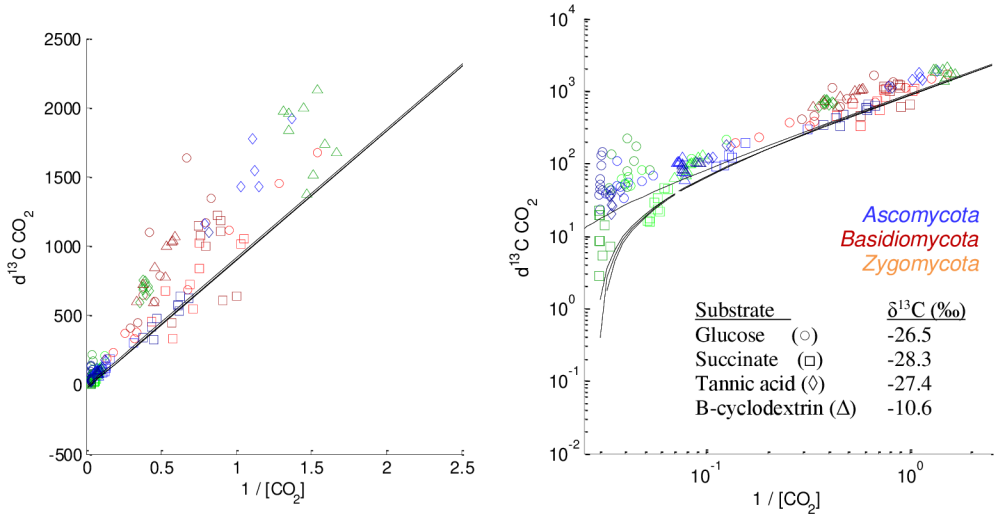

Figure S1. Hyperbolic evolution of $\delta^{13}C$-CO_2 with increasing [CO2] released from respiration, for incubations of Ascomycota (blue), Basidiomycota (red), or Zygomycota (green) with glucose (circles), succinate (squares), tannic acid (diamonds), or b-cyclodextrin (triangles). Panel B is the log-log plot of panel A, indicating the expected mixing lines for respiration of each substrate.

The fit gave an R^2 of 0.8047 and RMSE of 251. These values improved when considering only incubations in which CO_2 levels increased above 1% (i.e., those that yielded sufficient biomass).

Because fungal lipid production occurred during the hyperbolic evolution of $\delta^{13}C$-CO_2, the accuracy of the %IC calculation (Eq. 1, main text) can be improved by estimating the weighted average $\delta^{13}C$ of inorganic C that could have been incorporated into lipids during the incubation as respired CO_2 accumulated. The weighted average stable C isotope composition of CO_2 that fungi were exposed to during the incubation can be approximated by the integral of the hyperbolic curve, normalized by [CO_2] at harvest. The resulting integral is a logarithmic

$$d^{13}C_{CO2} = (a / (1 + [CO_2]) + b$$

function of [CO_2]. Because we are considering incubations in which [CO_2] approached 1%, where the integral function approaches zero (i.e., LN 1 = 0), the data were rather fitted by a hyperbolic curve described by the function:

Furthermore, the trend was more accurately approximated by plotting against ^{13}F-CO_2 rather than $\delta^{13}C$-CO_2, with improved R^2 of 0.8472 and RMSE of 0.0016, and coefficients a = 0.02478 ± 0.00167 and b = 0.01054 ± 0.00037 (Fig. S2). Thus, the weighted average equation becomes:

Weighted average $^{13}F_{CO2} = (0.02478 \times LN(1+[CO_2]) + (0.01054 \times [CO_2])$ *Equation S2*

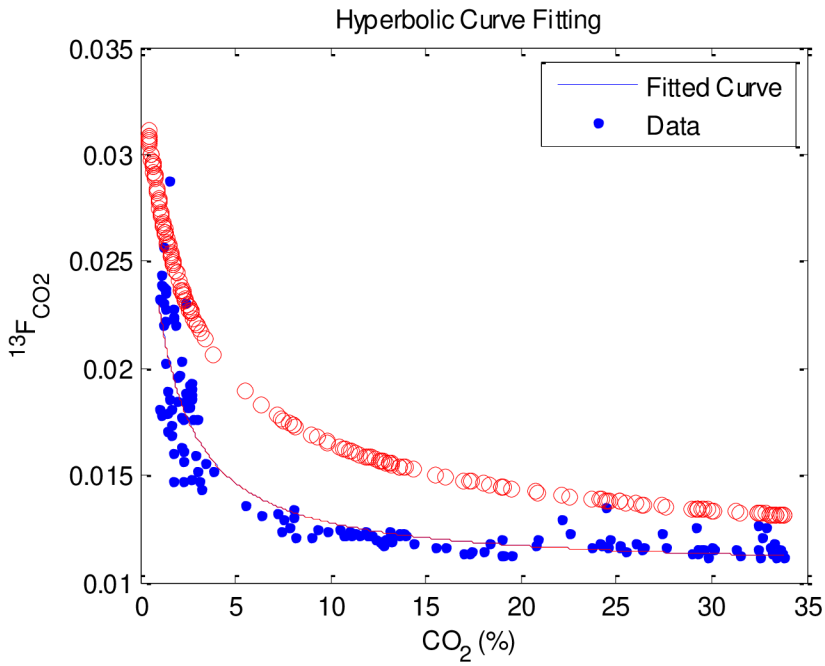

Figure S2. Hyperbolic curve of decreasing $^{13}F_{CO2}$ with increasing CO_2 in headspace during fungal respiration of substrates (filled blue circles). The fitted curve representing Eq. S2 is shown in pink. The weighted average $^{13}F_{CO2}$ during fungal production in each incubation (open red circles) was estimated as the integral of the fitted curve normalized by the CO_2 concentration at harvest.

Finally, the estimated weighted average $^{13}F_{CO2}$ was used to calculate the heterotrophic incorporation of inorganic C into lipids (%IC) via Eq. 1 of the main text, which amounted to < 3% for all experimental incubations. Sensitivity analysis of the fitted coefficients (i.e., 95% confidence intervals) indicated a coefficient of variation of the reported %IC values of up to 30%, with the highest reported fungal %IC values (i.e., *Penicillium jancewskii* grown on tannic acid) ranging from 1.8 to 2.8%.

Literature cited

Kendall, C., Caldwell, E. A. (1998). Fundamentals of isotope geochemistry. *In Isotope tracers in catchment hydrology* (pp. 51-86). Elsevier.

Manuscript III

Microbial production and turnover times in roots and horizons of natural forest soils

Stanislav Jabinski, Veronika Jilkova, Marek Kopacek, Travis B. Meador
(2024)

Seasonal accounts of microbial production and turnover forest soil horizons

***Stanislav Jabinski*[1,2*], *Veronika Jílková*[2], *Marek Kopáček*[1,3], *Travis B. Meador*[1,2,3]**

[1] University of South Bohemia, Faculty of Science, Department of Ecosystem Biology, Branišovská 1760, 370 05 České Budějovice, Czechia

[2] Institute of Soil Biology and Biochemistry, Biology Centre CAS, Na Sádkách 7, 370 05 České Budějovice, Czechia

[3] Institute of Hydrobiology, Biology Centre CAS, Na Sádkách 7, 370 05 České Budějovice, Czechia

* Corresponding author: stanislav.jabinski@bc.cas.cz

Key words: Lipid-SIP, microbial fatty acids, Soil incubation, microbial production, hydrogen isotopes

Abstract

Atmospheric CO_2 cycles through terrestrial vegetation, into higher trophic levels, and eventually to decomposers and the underlying soils, where the portion that is not respired back to the atmosphere accumulates as soil organic matter (SOM). This key flux is controlled primarily by the soil fauna and is important for the functioning of the ecosystem. As soils are very sensitive to climate change, estimating the reactivity of soil organic matter is important to constrain future climate scenarios. To investigate microbial activity/production and turnover times of microbial communities and fungal contribution we incubated roots, A and O Horizon of the Blansky les in spring and autumn and applied a stable isotope probing assay utilizing heavy water (^2H_2O) in combination with fatty acid extractions. Our results could demonstrate that Fungi dominated the abundance and production profiles of Root incubations, with relatively high mean CUE values ranging up to 0.44. Bacterial groups exhibited higher production rates and turnover times in A and O Horizons in spring but it reversed in autumn, when fungi were dominant. The fluxes derived from the SIP assay applied in this study serve to constrain the turnover and C demand of the forest soil microfauna community.

1. Introduction

Soil organic matter (SOM) is one of the largest carbon pools on earth and contains more carbon than atmosphere and terrestrial vegetation together. Due to its high sensitivity to climate and environmental change, understanding the dynamics of organic matter degradation and turnover in soils is key for determining terrestrial C budgets as well as the interactions among climate, ecosystems, and humans (Tian et al., 2015). Reducing the uncertainty in projecting soil responses to climate change requires new datasets and methods that constrain the effects of various drivers on SOM (Beillouin et al., 2022).

One approach to addressing this knowledge gap is to grasp how microbial life shapes SOM and how microbial population dynamics, trophic relationships, and microbial interactions shape soil biogeochemistry. Because organisms must adapt their membrane lipid structures, which are major cellular components with a large verity

of structural and functional diverse compounds, to environmental changes, the chemical signatures of these molecules may reveal both the dominant metabolic pathways and activity of microbial populations. Indeed, microbial membrane lipid biomarkers and their compound-specific stable isotopic compositions provide an effective tool for identification of microbial communities and metabolic activities (e.g., Boschker et al., 1998). Phospholipid fatty acids (PLFA) are commonly used to describe soil microbial communities, offering the advantage that upon cell death, PLFA rapidly degrade and therefore thought to function as a biomarker of living cells. Another advantage is the accurate estimation of microbial biomass and shifts in community composition (i.e., diversity). The combination of PLFA and the application of stable isotope probing (SIP) to determine functionally active components of microbial communities is also becoming increasingly used in soil microbial ecology studies (Kreuzer-Martin, 2007). This allows researchers to assess growth/turnover rates in soils, where biomass pools vary widely.

Hydrogen (H) SIP has been shown to be a useful tracer of microbial community activity in a diverse range of environments (Caro et al., 2023; Wu et al., 2018; Huguet et al., 2017). Because all organisms require water, the incorporation of ^{2}H from $^{2}H_2O$ into membrane lipids during biosynthesis can track growth without altering environmental conditions and allowing for measurements of microbial growth in natural conditions without substrate addition. Due to very low abundance of ^{2}H relative to ^{1}H in nature, the method offers high sensitivity; the required incubation times are relatively short because only a small amount of newly synthesized lipids is required. Moreover, all microorganisms synthesize lipids regardless of their stage in the cell cycle or metabolic activity. In contrast, nucleic acids and proteins, which are also used in SIP experiments, may be synthesized for cellular maintenance and repair, even without cell growth. Hence, lipids are less likely to require repair and thus provide a more specific measurement of membrane and cell growth (Caro et al., 2023). In this study, we applied ^{2}H-SIP to investigate fatty acid production in the Blanský Les protected forest to (I) quantify and compare the microbial production between different soil layers and (II) to quantify the role and contribution of fungi in this ecosystem.

2. Materials and Methods

2.1. Field sampling

The Blanský Les Nature Reserve in Southern Bohemia (Czech Republic; N48° 55‘ E14° 12′, 629 m a.s.l.), is very well-preserved area in the lower parts of the Šumava mountains. Blanský Forest is a highland with its peak Kleť Mountain (1084 m a. s. l,). Soils were collected from the surface with a corer (di 46 mm) to a depth of 1 m and divided between the mineral horizon (A horizon) and the humus horizon (O Horizon). For each of the three different stations 5 replicate sediment cores were acquired and mixed into a 3 L Ziplock bag to gain enough material for further analysis. In the laboratory the freshly collected soils were sieved with a 2-mm sieve for the A Horizon and 4-mm sieve for the O Horizon, where roots were also manually collected and separately stored. 1 g triplicates of each station of A and O horizon soils (n = 18 samples) were taken for determining the water content, by drying the soils at 60 °C overnight. Soil pH was mixed with a 1:10 soil water suspension, vortexed for 2 min

and then measured with a pH meter. Soils were stored at 4 °C until further analysis. Samples were taken in June and October of 2021.

2.2 Incubation setup

5 g of horizon A, horizon O and roots were filled into 500 mL Schott bottles and kept close. A total of 36 incubations were used for each season. One bottle per soil type were incubated without addition of labeled substrates (natural), triplicates were incubated with the addition of heavy water ^2H_2O in different label strengths ranging from ^2F = 10000 ppm, 5000 ppm and 2000 ppm (δ^2H = 63849‰, 31261‰ and 11865‰ vs. VSMOW, respectively). Samples were incubated for 14 days in the dark at 12 °C and were monitored every 2 – 3 days for oxygen consumption via oxygen sensors which were attached inside selected bottles to ensure aerobic conditions (Figure 1).

Figure 1. Incubation setup for the June and October incubations with sample code X.Y.Z with X = Location, Y = type of soil (1 = A horizon; 2 = roots, 3 = O horizon) and Z = labeling strength (1 = 63849‰, 2 = 31261‰ and 3 = 11865‰ δ^2H vs. VSMOW). The black stars represent the samples with an oxygen sensor.

After 14 days of incubation, samples were transferred from the Schott bottles into 50 mL falcon tubes. 10 mL of Qlarivia water (^2F = 18 ppm; δ^2H = -884‰,) was mixed with the samples and vortexed. The water was then retrieved with the porewater from the soils and filtered with nylon 0.2 µm syringe filters for hydrogen water isotopic measurements. The soils were frozen overnight, lyophilized and stored at -20°C until further analysis.

2.3 Extraction & FA methylation

Lyophilized samples (0.5 g) were extracted using a modified Bligh and Dyer protocol (Wörmer et al., 2017). 2-methlyoctadecanoic acid (2-MOA) was added as an extraction standard at the start of the extraction. Samples were sonicated for 10 min in four steps with a mixture of dichloromethane (DCM) methanol (MeOH) water (1.0:2.0:0.8, vol/vol/vol) by using 30 mL solvent per extraction step. A phosphate buffer (8.7 g L^{-1} KH_2PO_4, pH 7.4) was used for the first two steps, and a trichloroacetic acid buffer (50 g L^{-1} CCl_3COOH, pH 2) was used for the final two steps. After each extraction step, the samples were centrifuged at 1250 rpm for 5 min, and the supernatants were collected in a pre-combusted separation funnel. Phase separation was induced by addition of DCM and MilliQ, and the organic phase was drawn off and collected in a pre-combusted Schott bottle. The aqueous phase was washed three more times with DCM, and then the pooled organic phase was washed three

more times with de-ionized MilliQ water. Finally, the organic phase was collected as the total lipid extract (TLE) and was evaporated under a stream of argon and stored at -20 °C. All vials used for sample handling and storage were pre-combusted at 450°C for 6 h, and syringes for sample transfer were pre-rinsed with DCM:MeOH (5:1 vol/vol).

Thirty percent of the TLE was dried and saponified for fatty acid analysis, using 1 mL 6% KOH in MeOH for 3 h at 80 °C (Elvert et al., 2003). After cooling, 1 mL of 0.05 KCl was added. Neutral lipids were extracted four times using 1 mL n-hexane. The rest of the solution was treated with 10% HCl to reach a pH value of 1, and then free fatty acids were extracted four times using 1 mL n-hexane. Following that, all extracts were dried, mixed with 1 mL 20% BF_3 in MeOH and heated at 70 °C for 1 h to convert free fatty acids into FAMEs. The solutions were extracted four times with 1 mL n-hexane. The combined extracts were evaporated under argon and stored at -20 °C until further analysis.

2.4 Measurements

2.4.1 Heavy water (D_2O) isotope analysis

Liquid samples were transferred into 1.5 mL glass vials (32 × 11.6 mm, Fisher Scientific) and then measured using Triple Liquid Water Isotope Analyzer (Los Gatos Research), which is based on the principle of high-resolution laser absorption spectroscopy. Samples were dispensed into the instrument using an autosampler (PAL3 LSI, ABB company) and a 1.2 µL syringe (Hamilton). Samples were measured and evaluated against prepared laboratory standards of known isotopic composition. The isotopic ratios of these laboratory standards were verified by measuring against international standards (VSMOW2 and SLAP2). To check the quality control, the measurements of the samples were also interspersed with periodic measurements of the prepared verification samples with known isotopic composition. The final isotopic composition (δ^2H) was determined using LIMS software. Analytical error in case of δ^2H was <1‰.

2.4.2 CO_2 analysis

Headspace CO_2 (2 mL) gas were injected into a helium-flushed 12 mL exetainer vial (Exetainer, Labco Limited, UK). Headspace CO_2 was purged using a double-holed needle with helium into a 250 µL sample loop then separated via a Carboxen PLOT 1010 (0.53 mm ID; Supelco, Bellefonte, USA) held at 70 °C with a flow rate of 0.75 bar and were introduced into the MAT253 Plus IRMS (Thermo Scientific, Bremen, Germany) via a Conflo IV interface. Each sample was injected three times during one run. The concentration was calculated based on a one-point calibration using a 0.3% CO2 gas in He standard.

2.4.3 FAME quantification and isotope analysis

FAMEs were measured using a GC Trace1310 gas chromatograph equipped with an SSL injector, a double gooseneck Topaz splitless liner (Restek, Bellefonte, USA) and a TR-FAME column (70% cyanopropyl polysilphenylene-siloxane; 120 m, 0.25 mm ID, 0.25 µm df; Thermo Scientific). The samples were injected in

splitless mode, with the injector temperature at 310°C. The GC oven was held at 60 °C for 1 min, then ramped to 150 °C at 10 °C min^{-1} and to 250 °C at 4 °C min^{-1}, then held at 250 °C for 15 min. Helium was used as carrier gas with a constant flow of 1.5 mL min^{-1}. The column was coupled via a multichannel device splitting the flow to a flame ionization detector (FID) and a mass spectrometer (MS), enabling both peak quantification and identification from one injection. The FID was set to 300 °C with flows of air at 350 mL min^{-1}, H_2 at 35 mL min^{-1}, and N_2 makeup gas at 40 mL min^{-1}. The MS (ISQ QD, Thermo Scientific) ion source was set to electron impact ionization (EI) mode at 70 eV and a scan range of m/z 50 – 500 with a scan time of 0.2 s. The transfer line temperature was set to 280 °C, and the ion source was set to 230 °C. The scan was started 15 min after the injection to avoid ionization of the solvent peak in the MS. For FAME identification, the fragmentation patterns and mass spectra were compared to the National Institute of Standards and Technology (NIST) Spectral Library. Quantification was determined from the FID trace, according to the response of the internal standard (2-MOA) and following Equation 1:

$$Compound\ concentration\ \left(\frac{ng}{g(sample)}\right) = \frac{\frac{PeakArea}{PeakSTD} * STD(ng)}{\%(injected) * g(sample)}$$

Equation 1: The final concentration is calculated with PeakArea being the integrated area of the unknown compound, PeakSTD being the integrated area of the given standard, and STD as the known concentration of the standard in nanogram, and the percentage of the injected TLE and the mass of the extracted sample in gram (Wörmer et al., 2017).

Stable hydrogen isotope compositions of FAMEs were determined by splitting the flow from the GC column to a GC-Isolink II reactor, coupled with a MAT253 Plus IRMS via a Conflo IV interface; values are expressed in standard delta notation (δ^2H). MS information was simultaneously acquired by using the multichannel device described above. For conversion of FAMEs H_2, the pyrolysis reactor (aluminum tube) was set to 1420 °C. FAMEs were identified by their retention times and fragmentation patterns. The isotopic composition was determined using Isodat version 3.0 software against the corresponding H_2 working gas (-239.5‰ for δ^2H). Isotope corrections and normalization to Vienna standard mean ocean water (VSMOW) scales were performed according to the response of USGS70 (-183.9‰ for δ^2H) and USGS72 (+348.3‰ for δ^2H) reference standards. The analytical error was <3.1‰ for δ^2H.

3 Results

3.1 Soil incubation parameters

The Blanský Les Nature Reserve samples were divided into A horizon, O horizon and roots which were incubated at 15 °C for 2 weeks. The oxygen sensors recorded no large differences in O_2 concentration between the A horizon and the O horizon, which ranged from 17 to 20% in June and October incubations. The Root incubations exhibited generally higher O_2 consumption, with concentrations dropping to 11-15% in June, and 12-14% in October (Fig 2). Soil humidity was consistent between June and October, with 20 - 30% for A horizon and 40 – 50% for Roots and O horizon. pH was consistent during June for all horizons, with a pH of 3.6 – 3.9 but were different for the A horizon in October, with a pH around 4.2 – 4.5. The pH of O Horizon incubations remained around 3.9. Average CO_2 headspace concentrations were 0.21±0.01% and 0.16±0.04%for A horizon incubations, 4.49±1.02% and 4.4±1.05% for roots, and 1.5±0.4% and 1.15±0.68% or O horizon incubations in June and October, respectively.

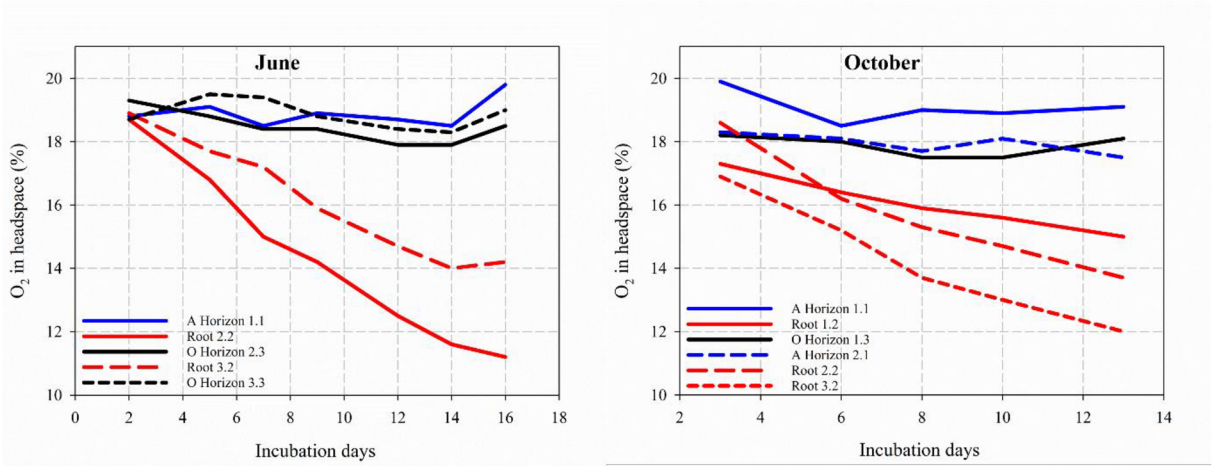

Figure 2. Oxygen concentration measured with oxygen sensors inside the incubation bottles over the 2 weeks of incubation. A and O Horizon exhibited a similar O_2 consumption, but the roots had almost half of the available O_2 consumed.

3.2 Fatty acids methyl ester (FAME) abundance and clustering

The FAME profiles (Fig. 3) included 27 identified FAMEs which ranged from C_{12} to C_{19}. FAMEs were sorted and categorized to presumed microbial sources, according to Zhang et al., 2024, with monounsaturated and cyclopropanoid FAMEs grouped into gram-positive bacteria (C16:1w7, C16:1w9, C16:1w11, C17:1w10, cyc-C17, C18:1 and cyc-C19), iso- and anteiso-FAMEs into gram-negative bacteria (iC14, iC15, aC15, iC16, iC17, aC17, iC18, iC19), C18:2 as the specific biomarker for fungi, methylated FAMEs at the 10th carbon position as Actinobacteria and sulfate reducing bacteria (Me10-C17, Me10-C18, Me10-C19), and saturated straight chain FAMEs categorized as generic fatty acids (C12, C13, C14, C15, C16, C17, C18, C19). FAMEs can be indicative for certain microbial groups, though this approach must be performed with caution because some FAMEs have been reported as having multiple microbial sources (Zelles, 1999). To estimate the total biomass carbon from the FAMEs concentration, a conversion factor of 0.056 g_{Lipids} $g_{biomass}^{-1}$ was assumed for bacterial FA, 0.0033 $g_{C18:2}$ $g_{biomass}^{-1}$ was assumed for fungal FAMEs (Fouilland et al., 2014; Kamer and Baath 2004; Middelburg et al., 2000; Wu et al., 2018).

In June, average FAME concentrations of the different layers were the lowest for A Horizon with 0.09±0.01 mg g^{-1} dry weight (n = 11; ±SEM), O Horizon with 0.6±0.03 mg g^{-1} dry weight (n = 12; ±SEM), and the highest average concentration in the roots with 0.7±0.1 mg g^{-1} dry weight (n = 11; ±SEM). The highest abundant FAME in all horizons was C16 accounting for around 20%, followed by C14, C18:2 and C18:1 with around 12% each. For horizon A, the highest FAMEs were C16 (25%), C18 (18%), C18:1 (15%) and C14 (7%). For the roots the most abundant FAMEs were C18:2 (20%), C16 (18%), C18:1 (13%) and C14 (11%). For the O horizon the highest FAMEs were C14 (19%), C16 (19%), C12 (10%), C18:2 (10%) and C18:1 (10%). The other FAMEs in the different horizons each accounted for < 5%. For comparing bacterial vs fungal contribution to the different horizons, FAMEs were converted to biomass-C, with A horizon having relatively more bacteria (57%), the roots being dominated by fungi (81%) and the O horizon also harboring more fungi (65%).

In October average FAME concentrations of the different horizons were the lowest for A Horizon, with 0.07±0.01 mg g^{-1} dry weight (n = 12; ±SEM), followed by the O horizon with 0.29±0.04 mg g^{-1} dry weight (n = 10; ±SEM), and the Roots exhibited the highest average FAME concentration with 0.66±0.06 mg g^{-1} dry weight (n = 11;

±SEM). The highest abundant FAME in all horizons was C18:1, which accounted for ~ 16%, followed by C16 (15%), C18:2 (13%), and C18 (10%). For Horizon A, the highest FAMEs were C16 (23%), C18:1 (19%) and C18 (14%). For the roots the highest FAMEs were C18:2 (26%), C18:1 (15%) and iC17 (15%). For O horizon the highest FAMEs were C16 (20%), C14 (15%), C18:1 (14%) and C18 (11%). The other FAMEs detected in the different horizons each accounted for lower than 10%. Converting FAMEs abundance to bacterial and fungal biomass C contributions to the different horizons, we estimate that A horizon comprised equal portions of both fungi and bacteria (50%), the Roots and O horizon were dominated by fungi (86% and 61%, respectively). Biomass C estimated from fatty acid abundances in June totaled 2.7±1.1, 28.2±6.7, and 52±18 mg C g^{-1} dry weight in the A and O horizons, and roots, respectively. In October, the totals were 2.3±0.8, 12.5±4.8, and 61±17 mg C g^{-1} dry weight, respectively.

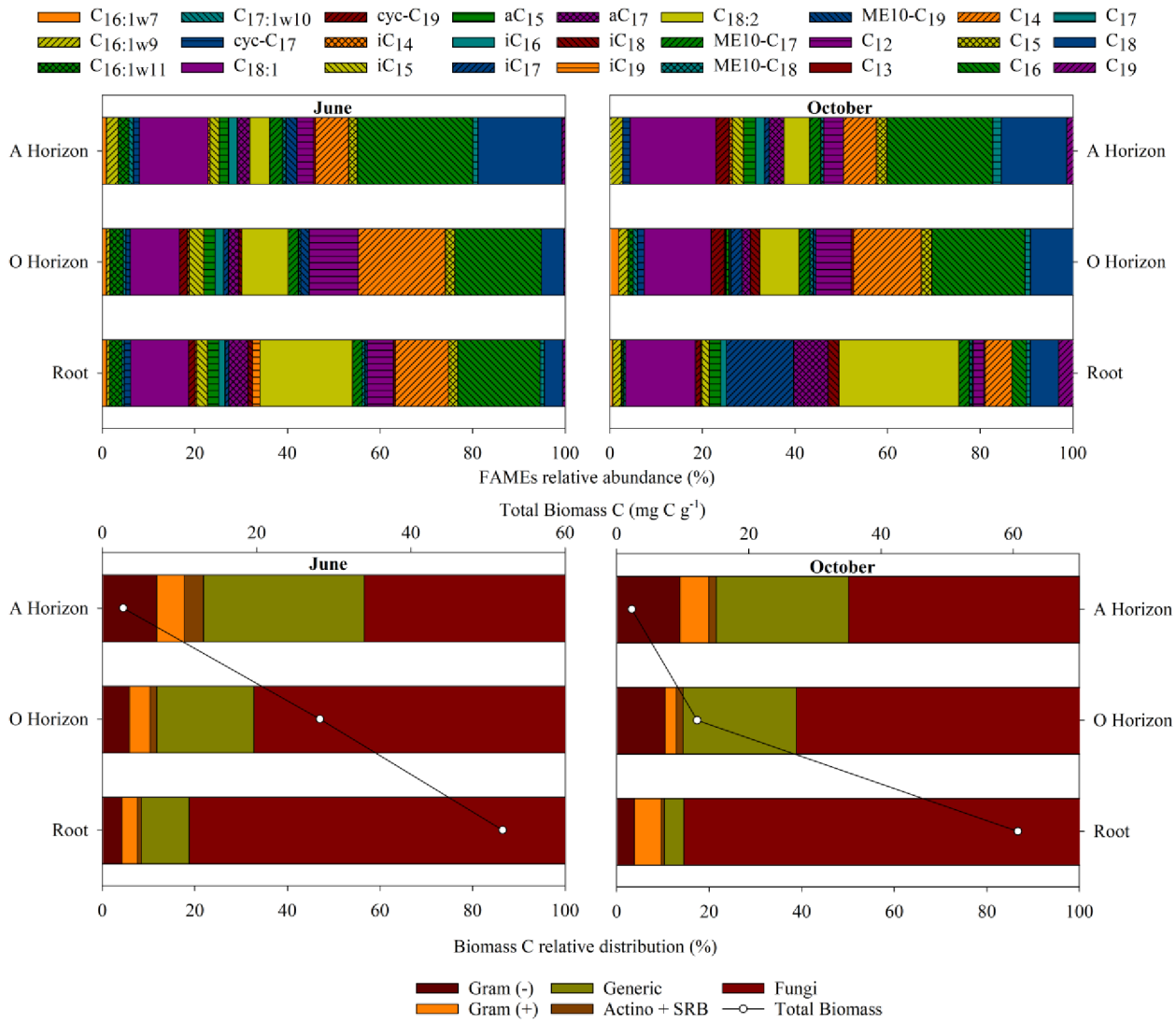

Figure 3. FAMEs relative abundance and corresponding estimated Biomass C of bacterial groups and fungi

3.3 ^{2}H lipid production and turnover rate

Water hydrogen incorporation into FAMEs was calculated based on equation 2 and corrected for the hydrogen water assimilation efficiency with the recently reported water assimilation factors for soil microbes (0.71; Caro et al., 2023) and fungi (0.69; Jabinski et al., 2024, Jabinski et al., unpublished).

$$Produciton_{(Lipids)} = Concentration_{Lipids} * \frac{F^{2H}{}_{lipids\ labeling} - F^{2H}{}_{lipids\ control}}{\left(F^{2H}{}_{medium\ labeling} - F^{2H}{}_{medium\ control}\right) * time}$$

Equation 2: Lipid production (ng L^{-1} yr^{-1}) was calculated using the lipid concentration and multiplying it by the difference of the Fraction of the lipids from the labeling experiment compared to the natural (control), with F^{2H} of the medium subtracted from the F^{2H} of the medium natural (control) and multiplied by the incubation time (cf. Wegener et al., 2012).

In June average FAME production in the different layers were the lowest for A Horizon with 0.14±0.02 mg g^{-1} dry weight (n = 9; ±SEM), O Horizon with 0.28±0.02 mg g^{-1} dry weight (n = 9; ±SEM), and the highest average production in the roots with 1.11±0.15 mg g^{-1} dry weight (n = 8; ±SEM). The highest produced FAMEs in all horizons were C16 with around 34%, followed by C18:1 with around 15%. For horizon A, the highest produced FAMEs were C16 (45%) and C18:1 (10%). For the roots the highest produced FAMEs were C16 (29%), C18:2 (22%) and C18:1 (20%). For the O horizon the highest produced FAMEs were C16 (28%), C18:1 (12%), iC15 (12%) and C18 (10%). The other FAMEs in the different horizons were individually lower than 10%. FAMEs were converted to produced biomass C with A horizon total FAME production of 3.4±2.2 mg C g^{-1} yr^{-1} being dominated by bacteria (69%), the roots total production of biomass C was 91±41 mg C g^{-1} yr^{-1} being dominated by fungi 75±40 mg C g^{-1} yr^{-1} (83%). In the O horizon, total biomass C production of 7.0±2.4 mg C g^{-1} yr^{-1} being dominated by bacteria (75%).

In October average FAME production in the different layers were the lowest for the O horizon with 0.12±0.03 mg g^{-1} dry weight (n = 8; ±SEM), followed by the A horizon with 0.15±0.04 mg g^{-1} dry weight (n = 6; ±SEM). The highest average FAME production was in the roots with 1.54±0.24 mg g^{-1} dry weight (n = 8; ±SEM). The highest produced FAME in all horizons was C18:2 with around 24% followed by C18:1 with around 16%, C16 with 13% and C18 with 11%. For Horizon A, the highest produced FAMEs were C16 (29%), C18:1 (29%) and C19 (12%). The highest produced FAMEs in the roots were C18:2 (48%) and iC17 (19%). For the O horizon the highest produced FAMEs were C18 (18%), C18:2 (16%) and C18:1 (15%). The other FAMEs were individually lower than 10%. FAMEs were converted to produced biomass C with A horizon total Biomass C production of 6.0±3.5 mg C g^{-1} yr^{-1} with highly variable contributions of bacterial and fungal biomass. The root's total production of biomass C was 235±73 mg C g^{-1} yr^{-1} being dominated by fungi 221±72 mg C g^{-1} yr^{-1} (94%), and the O horizon's total biomass C production of 7.4±5.4 mg C g^{-1} yr^{-1} with high variability in bacterial and fungal contributions (1.8±1.3 and 5.6±5.3 mg C g^{-1} yr^{-1}, respectively).

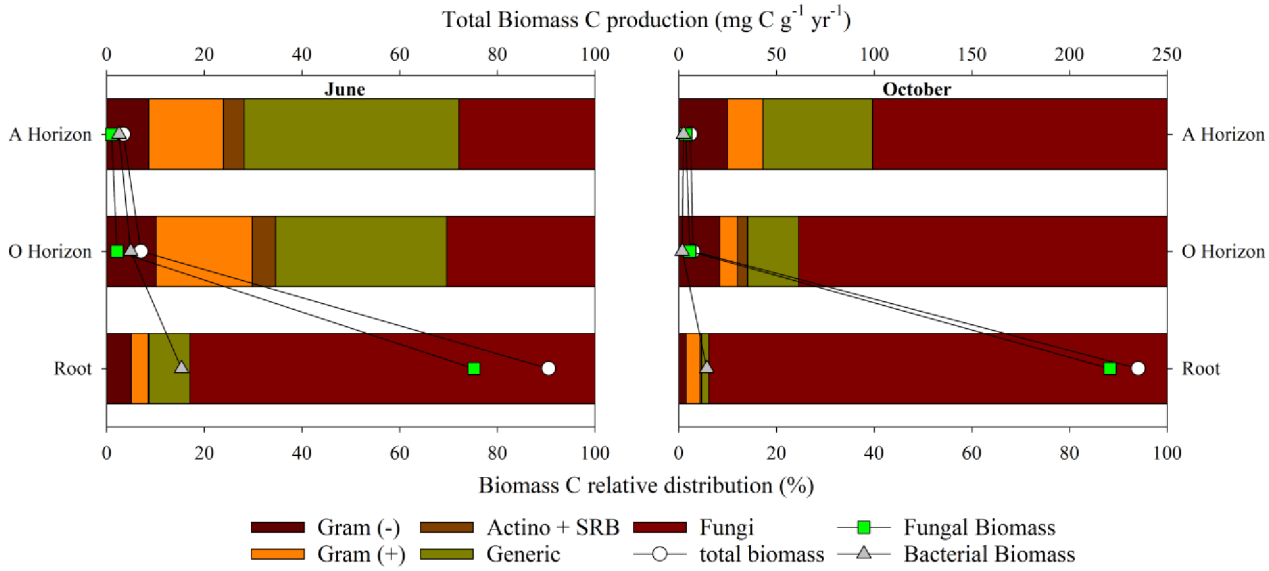

Figure 4. FAMEs and biomass production calculated by the ^2H incorporation into microbial membrane lipids.

To estimate the biomass turnover time, the abundance (mg C g^{-1}) was divided by the production rate (mg C g^{-1} yr^{-1}). For June, total biomass turnover was highest in the roots (0.57±0.32 years) with a turnover time of 0.63±0.30 years for bacteria and 0.56±0.38 years for fungi, followed by A horizon (0.61±0.66 years) with 1.2±0.9 years for bacteria and 0.78±0.59 years for fungi, and O horizon (4.0±1.5 years) with 1.9±0.7 years for bacteria and 8.8±6.4 years for fungi. For October total biomass turnover was again highest in the roots (0.26 years±0.11) with a turnover time of 0.61±0.48 years for bacteria and 0.24±0.11 years for fungi, followed by A horizon (0.38±0.26 years) with 0.48±0.36 years for bacteria and 0.31±0.32 years for fungi, and O horizon (1.6±1.4 years) with 2.6±2.2 years for bacteria and 1.3±1.5 years for fungi.

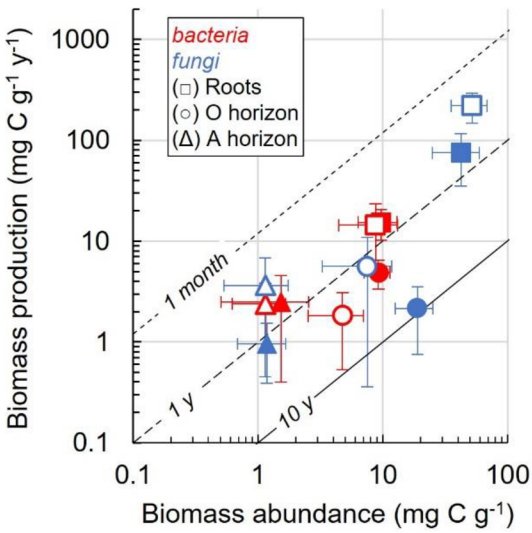

Figure 5. Bacterial (red) and fungal (blue) biomass C turnover in Blanský Les soils in June (filled symbols) and October (open symbols). Biomass C was estimated from fatty acid abundances in roots (squares), O horizon (circles), and A horizon (triangles), and biomass C production was estimated via ^2H incorporation into fatty acids (y-axis).

3.4 Carbon use efficiency

Carbon use efficiency (CUE; [CUE = biomass C / (CO_2 + biomass C)]) was estimated from the freshly produced biomass and measured headspace CO_2 at the end of the incubation, and ranged overall between 0.06 and 0.44. The estimated CUE for A horizon was 0.19±0.12 and 0.35±20, for Roots was 0.23±0.10 and 0.44±0.14 and for O horizon 0.06±0.02 and 0.09±0.06 in June and October, respectively (Fig. 6).

4 Discussion

We have generated a dataset for bacterial and fungal biomass production rates and turnover in a natural spruce/birch forest looking at different soil horizons based on incorporation of labeled H water into membrane lipids. Samples were collected in two different seasons (end of spring and autumn) from roots, and O and A horizons, and incubated for two weeks under dark conditions.

4.1 Microbial fatty acid and biomass production

Total microbial biomass in our incubations varied between 2.7 – 52 mg C g^{-1} dry weight in June and 2.3 – 61 mg C g^{-1} dry weight in October, ranging slightly higher than reported for microbial biomass C in forest soil (2 – 3%; Blagodatskaya and Kuzyakov 2013).

Microbial CUE is important for the determination of carbon cycling in environmental ecosystems where a significant portion of organic matter is assimilated into microbial biomass or is respired by microorganisms to generate energy for cellular processes, which can also be used to distinguish flourishing vs surviving modes (Keiblinger et al., 2010; Pold et al., 2020). Theoretical CUE maxima were reported to be less than 0.8 - 0.6 because microbes need to spend at least 20% of the organic C uptake for energy production by respiration (Gommers et al., 1988; Spohn et al., 2016) but in soil it is thought to hardly ever reach the theoretical maximum because environmental conditions usually require that more energy is invested into respiration (Manzoni et al., 2012; Sinsabaugh et al., 2013). CUE values estimated in this study were lowest in O horizon incubations (0.06±0.02 and 0.09±0.06 in June and October, respectively) and highest in Root incubations (0.23±0.10 and 0.44±0.14, respectively; Fig. 6), demonstrating the alternative growth strategies for the different microbial communities, where fungi dominated production in Root incubations. This finding is consistent with reports of fungi being more efficient in substrate usage than bacteria (Sakamoto and Oba, 1994; Strickland and Rousk, 2010; Adingo et al., 2021). These results are not surprising since roots or the Rhizosphere are considered to be hot-spots for microbial activity (Reinhold-Hurek et al., 2015), where fungal biomass C exceeded that of bacteria by a factor of > 4.3 (F:B ratio); the F:B ratio increased when considering only newly produced biomass (4.9 and 15.3 in June and October incubations, respectively). Fungal biomass C turnover was similar to bacteria in Root incubations in June (6.7±4.5 vs 7.3±3.6 months for bacteria in June) and faster than bacteria in October (2.8±1.3 vs. 7.3±5.8, respectively), which opposes the typical trend of fungal turnover being slower than bacteria (Baath, 1998; Rousk and Baath, 2007). The production of root hairs and sloughed root cells may have also contributed to the high estimates of fungal biomass C in Root incubations, as root biomass is also known to comprise the biomarker $C_{18:2}$ (Denef et al., 2009), which we have ascribed to fungi.

The O horizon incubations contained the humus layer from which roots were removed, and exhibited correspondingly lower biomass C (up to 5-fold in October) and up to 4-fold lower CO_2 accumulation after the 2

weeks of incubation, in comparison to Root incubations. As noted above, CUE for biomass produced during the incubation period was also the lowest in the O horizon. Biomass C turnover time was slower June (4.0±1.5 years) than in October (1.6±1.4 years), with the increase owing mostly to fungi (8.8±6.4 vs 1.3±1.5 years in June and October, respectively), whose contributions to production were highly variable among replicate incubations of the O horizon. This signal could be indicative of fungal populations becoming more reliant on a heterogeneous matrix of humus in the O horizon in autumn, when the pool of fungal biomass C was roughly half of that detected in spring (7.5±4.3 vs 18.9±6.3 mg C g^{-1} dry weight, respectively) and fungal production was larger and highly variable between incubations (5.6±5.3 vs. 2.2±1.4 mg C g^{-1} y^{-1}). Microbial biomass C abundances in the O horizon in June and October were similarly enriched in fungi (67±22% and 61±35%), but bacterial accounted for more of total microbial biomass C production in June (75±22%). This is evidence of rapidly growing bacteria that do not necessarily represent the largest proportion of the soil microbial community (e.g., Caro et al., 2023). In October, the ratio was reversed, with fungal production being dominant but highly variable between replicate incubations (76±71%). The high variability in microbial production and characteristically low CUE observed in O horizon incubations are consistent with an opportunistic heterotrophic community respiring labile, localized hotspots of substrates (e.g., leaf litter) deposited in this top horizon.

Incubations of A horizon exhibited the lowest production of headspace CO_2 production and lowest O_2 consumption (Fig. 1), which was expected for this soil, given its lower C content and greater capacity for minerals to adsorb and protect organic C from degradation. Total biomass C estimates in the A horizon were also roughly ~10-fold lower than in the O horizon in June, and 5-fold lower in October. Interestingly, CUE values were higher than the O horizon in both seasons, and exhibited a similar pattern as observed in Root incubations, with CUE lower in June (0.19±0.12) than in October (0.35±0.20). Total microbial biomass C in the A horizon comprised roughly equal portions of bacteria and fungi in both June and October, and mean microbial turnover times of < one year were more similar to that observed in Root rather than O horizon incubations. However, the trend in A and O horizons were similar, with relatively slower turnover (9.4±7.1 months) and variable production (3.4±2.2 mg C g^{-1} y^{-1}) dominated by bacteria (72±61%) in June, and relatively faster turnover (4.6±3.1 months) and higher production (6.0±3.5 mg C g^{-1} y^{-1}) in October. Although microbial abundance and production was lowest in the A horizon, turnover time was > 4-fold faster and CUE was > 3-fold higher in the A vs. O horizon. The faster turnover times could be attributed, in part, to fatty acids belonging to gram positive bacteria, which accounted for 27% and 12% of biomass C production in June and October, respectively, and exhibited among the fastest turnover observed in the dataset (4.2±1.8 and 4.0±0.9 months, respectively). Our results suggest that, on average, the microbes inhabiting the A horizon are “generalists” who are collectively lower in abundance but relatively more active than the “opportunists” found the organic-rich O horizon.

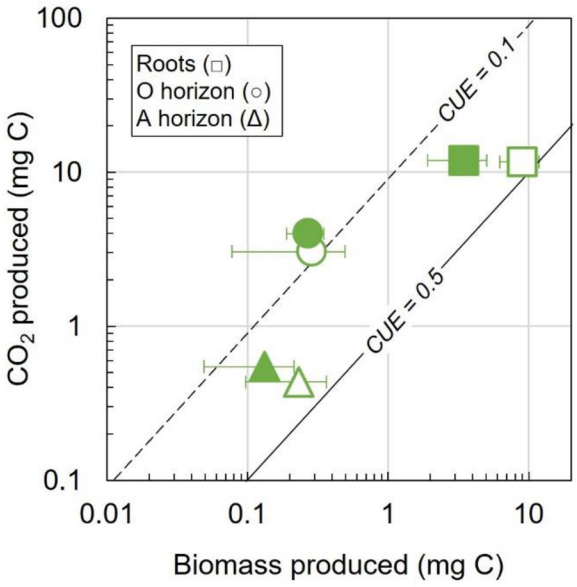

Figure 6. Carbon use efficiency of soil microbial communities in Roots (squares), O horizon (circles), or A horizon (triangles) incubated in June (filled symbols) or October (open symbols; cf. Section 3.4). The lines indicate trajectories of CUE = 0.1 (dashed) or 0.5 (solid) corresponding to proportional production of biomass C and CO_2.

5. Conclusion

Blanský Les soil incubated with heavy water (^2H_2O) revealed unique patterns of fatty acid production among the microbial communities inhabiting roots, and the O and A horizons. Fungi apparently dominated the abundance and production profiles of Root incubations, where CUE was characteristically high and ranged up to 0.44±0.14 in October (Fig. 6). Biomass C production in the Root incubations was on the order of hundreds of mg C g^{-1} y^{-1} and much higher than in O or A horizons (typically < 10 mg C g^{-1} y^{-1}); this may have been supported by additional production of the "fungal" C18:2 biomarker by root tissue. Fungi also exhibited consistently faster turnover times in October vs June incubations (Fig. 5), suggesting alternate growth strategies as substrate input varies across the seasons. Although the A horizon was characterized by the lowest average microbial abundance (< 3 mg C g^{-1} dry weight) and production rates (< 6 mg C g^{-1} y^{-1}), the bulk microbial community was relatively more active in the A vs. O horizon, as implied by the faster turnover times (i.e., months vs. years, respectively), with evident contributions of both fungi and gram-positive bacteria. The microbial fatty acid production fluxes and CUE estimates reported here may help to constrain the formation processes and reactivity of SOM. By assuming the fluxes determined in spring and autumn represent an average for Blanský Les soils, yearly inputs of 465, 100, and 18 mg C g^{-1} dry weight must be delivered to the roots, O, and A horizons soils to satisfy the respective C demands of the heterotrophic microbial communities.

Acknowledgements

The research was supported by the Czech Science Foundation GACR nr. 20-223805 (FUNSIF) and supported by MEYS CZ grant LM2015075 Projects of Large Infrastructure for Research, Development and Innovations as well as the European Regional Development Fund-Project: research of key soil-water ecosystem interactions at the SoWa Research Infrastructure (No. CZ.02.1.01/0.0/0.0/16_013/0001782).

References

Adingo, S., Yu, J. R., Xuelu, L., Li, X., Jing, S., & Xiaong, Z. (2021). Variation of soil microbial carbon use efficiency (CUE) and its influence mechanism in the context of global environmental change: a review. *PeerJ*, 9, e12131.

Bååth, E. (1998). Growth rates of bacterial communities in soils at varying pH: a comparison of the thymidine and leucine incorporation techniques. *Microbial Ecology*, 36, 316-327.

Beillouin, D., Cardinael, R., Berre, D., Boyer, A., Corbeels, M., Fallot, A., ... & Demenois, J. (2022). A global overview of studies about land management, land-use change, and climate change effects on soil organic carbon. *Global Change Biology*, 28(4), 1690-1702.

Blagodatskaya, E., & Kuzyakov, Y. (2013). Active microorganisms in soil: critical review of estimation criteria and approaches. *Soil Biology and Biochemistry*, 67, 192-211.

Boschker, H. T. S., Nold, S. C., Wellsbury, P., Bos, D., De Graaf, W., Pel, R., ... & Cappenberg, T. E. (1998). Direct linking of microbial populations to specific biogeochemical processes by 13C-labelling of biomarkers. *Nature*, 392(6678), 801-805.

Caro, T. A., McFarlin, J., Jech, S., Fierer, N., & Kopf, S. (2023). Hydrogen stable isotope probing of lipids demonstrates slow rates of microbial growth in soil. *Proceedings of the National Academy of Sciences*, 120(16), e2211625120.

Denef, K., Roobroeck, D., Wadu, M. C. M., Lootens, P., & Boeckx, P. (2009). Microbial community composition and rhizodeposit-carbon assimilation in differently managed temperate grassland soils. *Soil Biology and Biochemistry*, 41(1), 144-153.

Elvert, M., Boetius, A., Knittel, K., & Jørgensen, B. B. (2003). Characterization of specific membrane fatty acids as chemotaxonomic markers for sulfate-reducing bacteria involved in anaerobic oxidation of methane. *Geomicrobiology Journal*, 20(4), 403-419.

Fouilland, E., Tolosa, I., Bonnet, D., Bouvier, C., Bouvier, T., Bouvy, M., ... & Vidussi, F. (2014). Bacterial carbon dependence on freshly produced phytoplankton exudates under different nutrient availability and grazing pressure conditions in coastal marine waters. *FEMS Microbiology Ecology*, 87(3), 757-769.

Gommers, P. J. F., Van Schie, B. J., Van Dijken, J. P., & Kuenen, J. G. (1988). Biochemical limits to microbial growth yields: an analysis of mixed substrate utilization. *Biotechnology and Bioengineering*, 32(1), 86-94.

Huguet, A., Meador, T. B., Laggoun-Défarge, F., Könneke, M., Wu, W., Derenne, S., & Hinrichs, K. U. (2017). Production rates of bacterial tetraether lipids and fatty acids in peatland under varying oxygen concentrations. *Geochimica et Cosmochimica Acta*, 203, 103-116.

Jabinski, S., d. M. Rangel, W., Kopáček, M., Jílková, V., Jansa, J., & Meador, T. B. (2024). Constraining activity and growth substrate of fungal decomposers via assimilation patterns of inorganic carbon and water into lipid biomarkers. *Applied and Environmental Microbiology*, 90(4), e02065-23.

Keiblinger, K. M., Hall, E. K., Wanek, W., Szukics, U., Hämmerle, I., Ellersdorfer, G., ... & Zechmeister-Boltenstern, S. (2010). The effect of resource quantity and resource stoichiometry on microbial carbon-use-efficiency. *FEMS Microbiology Ecology*, 73(3), 430-440.

Klamer, M., & Bååth, E. (2004). Estimation of conversion factors for fungal biomass determination in compost using ergosterol and PLFA 18:2ω6,9. *Soil Biology and Biochemistry*, 36(1), 57-65.

Kreuzer-Martin, H. W. (2007). Stable isotope probing: linking functional activity to specific members of microbial communities. *Soil Science Society of America Journal*, 71(2), 611-619.

Manzoni, S., Taylor, P., Richter, A., Porporato, A., & Ågren, G. I. (2012). Environmental and stoichiometric controls on microbial carbon-use efficiency in soils. *New Phytologist*, 196(1), 79-91.

Middelburg, J. J., Barranguet, C., Boschker, H. T., Herman, P. M., Moens, T., & Heip, C. H. (2000). The fate of intertidal microphytobenthos carbon: An in situ 13C-labeling study. *Limnology and Oceanography*, 45(6), 1224-1234.

Pold, G., Domeignoz-Horta, L. A., & DeAngelis, K. M. (2020). Heavy and wet: The consequences of violating assumptions of measuring soil microbial growth efficiency using the 18O water method. *Elementa: Science of the Anthropocene*, 8(1), 069.

Reinhold-Hurek, B., Bünger, W., Burbano, C. S., Sabale, M., & Hurek, T. (2015). Roots shaping their microbiome: global hotspots for microbial activity. *Annual Review of Phytopathology*, 53(1), 403-424.

Rousk, J., & Bååth, E. (2007). Fungal biomass production and turnover in soil estimated using the acetate-in-ergosterol technique. *Soil Biology and Biochemistry*, 39(8), 2173-2177.

Sakamoto, K., & Oba, Y. (1994). Effect of fungal to bacterial biomass ratio on the relationship between CO2 evolution and total soil microbial biomass. *Biology and Fertility of Soils*, 17, 39-44.

Sinsabaugh, R. L., Manzoni, S., Moorhead, D. L., & Richter, A. (2013). Carbon use efficiency of microbial communities: stoichiometry, methodology and modelling. *Ecology Letters*, 16(7), 930-939.

Spohn, M., Pötsch, E. M., Eichorst, S. A., Woebken, D., Wanek, W., & Richter, A. (2016). Soil microbial carbon use efficiency and biomass turnover in a long-term fertilization experiment in a temperate grassland. *Soil Biology and Biochemistry*, 97, 168-175.

Strickland, M. S., & Rousk, J. (2010). Considering fungal: bacterial dominance in soils–methods, controls, and ecosystem implications. *Soil Biology and Biochemistry*, 42(9), 1385-1395.

Tian, H., Lu, C., Yang, J., Banger, K., Huntzinger, D. N., Schwalm, C. R., ... & Zeng, N. (2015). Global patterns and controls of soil organic carbon dynamics as simulated by multiple terrestrial biosphere models: Current status and future directions. *Global Biogeochemical Cycles*, 29(6), 775-792.

Wörmer, L., Lipp, J. S., & Hinrichs, K. U. (2017). Comprehensive analysis of microbial lipids in environmental samples through HPLC-MS protocols. In *Hydrocarbon and lipid microbiology protocols: Petroleum, hydrocarbon and lipid analysis* (pp. 289-317).

Wu, W., Meador, T., & Hinrichs, K. U. (2018). Production and turnover of microbial organic matter in surface intertidal sediments. *Organic Geochemistry*, 121, 104-113.

Zelles, L. (1999). Fatty acid patterns of phospholipids and lipopolysaccharides in the characterisation of microbial communities in soil: a review. *Biology and Fertility of Soils*, 29, 111-129.

Zhang, Y., Naafs, B. D. A., Huang, X., Zhao, M., Zeng, L., Blewett, J., ... & Xie, S. (2024). The stable carbon and hydrogen isotopic composition of microbial fatty acids traces microbial metabolism in soils and peats. *Geochimica et Cosmochimica Acta*, 365, 85-100.

Additional information

Table S1: Estimated fatty acid concentrations and biomass production in 2-week incubations of Blanský les Roots, A and O Horizons in June and October 2021.

Parameter	Date	Horizon	All Biomass	All Bacteria	Fungi	Gram -	Gram +	Actino + SRB	Generic
FAMEs Concentration ($mg\ g^{-1}$)	June 2021	A Horizon	0.09±0.05	0.09±0.06	0.004±0.002	0.018±0.008	0.009±0.005	0.006±0.005	0.05±0.04
		O Horizon	0.58±0.1	0.5±0.2	0.06±0.02	0.09±0.02	0.07±0.04	0.02±0.01	0.3±0.07
		Roots	0.68±0.21	0.54±0.3	0.14±0.06	0.12±0.05	0.1±0.09	0.02±0.006	0.3±0.1
	October 2021	A Horizon	0.07±0.03	0.06±0.03	0.004±0.002	0.017±0.008	0.008±0.006	0.002±0.001	0.04±0.02
		O Horizon	0.29±0.12	0.3±0.2	0.03±0.02	0.07±0.04	0.02±0.02	0.01±0.01	0.17±0.7
		Roots	0.66±0.2	0.5±0.4	0.17±0.06	0.13±0.05	0.2±0.1	0.02±0.009	0.14±0.1
FAMEs production ($mg\ g^{-1}\ y^{-1}$)	June 2021	A Horizon	0.14±0.7	0.14±0.12	0.003±0.002	0.02±0.01	0.3±0.3	0.008±0.006	0.9±0.8
		O Horizon	0.3±0.06	0.3±0.1	0.007±0.005	0.04±0.02	0.08±0.03	0.02±0.01	0.14±0.04
		Roots	1.1±0.4	0.9±0.6	0.3±0.1	0.3±0.1	0.2±0.2	0.01±0.003	0.4±0.2
	October 2021	A Horizon	0.15±0.09	0.13±0.1	0.01±0.01	0.3±0.2	0.2±0.3	n.d.	0.8±0.5
		O Horizon	0.12±0.8	0.1±0.1	0.02±0.02	0.04±0.03	0.2±0.3	0.01±0.01	0.04±0.03
		Roots	1.5±0.6	0.8±1	0.7±0.3	0.2±0.1	0.4±0.5	0.04±0.03	0.2±0.1

Parameter	Date	Horizon	All Biomass	All Bacteria	Fungi	Gram -	Gram +	Actino + SRB	Generic
Biomass Concentration ($mg\ C\ g^{-1}$)	June 2021	A Horizon	2.7±1.5	1.5±1.1	1.2±0.5	0.3±0.2	0.2±0.1	0.1±0.1	0.9±0.7
		O Horizon	28±9	9.2±2.2	19±6	1.6±0.5	1.3±0.3	0.4±0.2	5.9±1.2
		Roots	52±21	10±3	42±17	2.2±0.9	1.8±0.6	0.4±0.1	5.3±1.7
	October 2021	A Horizon	2.3±1.1	1.2±0.5	1.1±0.6	0.3±0.1	0.1±0.1	n.d.	1.1±0.6
		O Horizon	12±7	4.7±2.2	7.5±4.2	1.3±0.7	0.3±0.1	0.2±0.1	3.0±1.3
		Roots	61±21	8.8±4.3	52±17	2.3±0.9	3.5±1.6	0.4±0.2	2.6±1.7
Biomass production ($mg\ C\ g^{-1}\ y^{-1}$)	June 2021	A Horizon	3.4±2.7	2.5±2.1	1.0±0.6	0.3±0.2	0.5±0.4	0.1±0.1	1.5±1.4
		O Horizon	7.0±3.0	4.9±1.6	2.1±1.4	0.7±0.3	1.4±0.5	0.3±0.1	2.5±0.6
		Roots	91±45	15±5	75±40	4.5±1.7	3.2±0.6	0.1±0.1	7.5±2.7
	October 2021	A Horizon	6.0±4.6	2.4±1.4	3.6±3.2	0.6±0.3	0.4±0.3	n.d.	1.4±0.9
		O Horizon	7.4±6.5	1.8±1.3	5.6±5.3	0.6±0.5	0.3±0.2	0.2±0.2	0.8±0.5
		Roots	235±81	14±9	221±72	3.5±1.5	6.8±4.8	0.7±0.6	3.3±2.3
Biomass turnover (weeks)	June 2021	A Horizon	33±24	32±34	64±46	48±20	18±8	62±34	59±41
		O Horizon	107±31	98±39	458±334	88±40	59±16	69±24	336±553
		Roots	32±16	33±16	29±20	31±14	29±9	28±13	145±177
	October 2021	A Horizon	24±18	25±19	16±17	50±43	18±4	n.d.	264±573
		O Horizon	125±101	136±115	70±76	84±30	33±28	71±15	566±566
		Roots	22±11	32±25	12±6	29±13	80±140	28±6	68±63

Manuscript IV

Production and dark carbon assimilation of aquatic macroplankton and microbial heterotrophs

Stanislav Jabinski, *Matthias Pilecky, Len I. Wassenaar, Martin J. Kainz, Travis B. Meador*

(2024)

Production and dark carbon assimilation of aquatic macroplankton and microbial heterotrophs

***Stanislav Jabinski*[1,2*], *Matthias Pilecky*[3,4], *Len I. Wassenaar*[3], *Martin J. Kainz*[3,4], *Travis B. Meador*[1,2]**

[1] University of South Bohemia, Faculty of Science, Department of Ecosystem Biology, Branišovská 1760, 370 05 České Budějovice, Czechia

[2] Institute of Soil Biology and Biochemistry, Biology Centre CAS, Na Sádkách 7, 370 05 České Budějovice, Czechia

[3] WasserCluster Lunz – Biologische Station, Inter-University Center for Aquatic Ecosystem Research, Dr. Carl-Kupelwieser Promenade 5, 3293 Lunz/See, Austria

[4] Donau-Universität Krems, Dr. Karl-Dorrek Straße 30, 3500 Krems, Austria

* Corresponding author: stanislav.jabinski@bc.cas.cz

Key words: Dual-SIP, microbial fatty acids, water column incubation, microbial production, oligotrophic lake

Abstract

Fungi and bacteria are the major organic matter decomposers on land but have major contributions in aquatic systems. Our knowledge and the particular role of fungi in aquatic food webs is still limited or the diversity and metabolic potentials are poorly characterized. To get a better understanding in the ecological function, in this study we investigated the microbial activity in an oligotrophic subalpine lake in Austria (Lunz am See) by applying a dual stable isotope assay with heavy water (^2H_2O) and inorganic carbon (^{13}C-DIC) for the epilimnion and hypolimnion in the spring and autumn season of 2022. Incubations were performed over a course of 10 days in the dark to remove phytoplankton contribution. Our results, based on the hydrogen incorporation into fatty acids, demonstrate that the production of C biomass was equal between the different depths in spring, but was around 80% lower in autumn. Although fungi contributed to less than 10% of biomass C in this system, there estimated turnover times varied between seasons, and were fast (~ 9 weeks) and similar to bacteria in the spring hypolimnion. This suggests that fungi play alternative roles in the food web throughout the year and likely thrive when primary production is high and injects sinking particles to depth. DIC assimilation was almost undetectable, except for the fungal 18:2 biomarker and some longer, polyunsaturated fatty acids, which may be indicative of lipid recycling.

1. Introduction

Inland waters are hotspots of activity, where nutrients and substrates from the terrestrial biosphere support autotrophic and heterotrophic communities alike. The metabolic balance of aquatic communities is controlled by the conversion of solar energy to reduced carbon (C) by primary producers, and the subsequent cascade of trophic transfers that nourish both higher trophic levels (Farjalla et al., 2006) and microbial decomposers (a.k.a., the microbial loop; Azam et al., 1983). Despite representing only, a very minor percentage of global aquatic surface

area in contact with the atmosphere, inland waters account for disproportionally large annual fluxes of CO_2 (e.g., Bauer et al., 2013), thereby connecting local ecosystems and food-webs to global geochemical cycles and climate. Apportioning the activity and interactions among aquatic heterotrophs, ranging from large, individual zooplankton to single-celled bacteria, can therefore improve our understanding of food web dynamics and controls on the metabolic balance of aquatic ecosystems. Similarly to bacterioplankton, aquatic fungi are thought to fulfil a saprotrophic role as decomposers in nearly all habitats on Earth (Romani et al., 2006); however, they are frequently unaccounted for in aquatic ecosystems (Grossart et al., 2019), where they may contribute to nutrient recycling and the degradation of energy rich particles and dissolved organic matter (DOM) (Sigee 2005; Duarte et al., 2016).

Stable isotopes analysis is a proven and valuable tool for determining the activity of organisms and their interactions in complex environmental systems (Whiteman et al., 2019). In particular, stable isotope probing (SIP) approaches have improved our understanding of ecosystem fluxes, as isotopically labeled substrates can be tracked through components of the food web (e.g., Middelburg, 2014), including microbial biomarkers (Boschker et al., 1998; Dumont and Murrell, 2005; Kreuzer-Martin, 2007), such as membrane lipid fatty acids (Willers et al., 2015). In recent years, hydrogen (H) isotopes have been used as a tracer of microbial activity and community production in a diverse range of environments (Caro et al., 2023; Huguet et al., 2017; Kellermann et al., 2012; Kellermann et al., 2016; Kopf et al., 2015; Wegener et al., 2016; Wu et al., 2018;), as water is required by all life and is the ultimate source of H in biosynthesis (Hoefs, 2018; Kopf et al., 2015). To fully exploit the potential of SIP experiments, a new lipid-based dual-SIP approach was developed to track total microbial production by adding heavy water (D_2O) together with labeled ^{13}C-dissolved inorganic carbon (DIC), to enable estimates of both total and autotrophic metabolism (Kellerman et al., 2016; Wegener et al., 2012; Wegener et al., 2016; Wu et al., 2020). Favorably, the addition of minor quantities of ^{13}C-bicarbonate and D_2O to environmental incubation experiments does not significantly alter biogeochemical conditions (Wegener et al., 2012). Also, even though microorganisms mainly feed on organic substrates, they were shown to also fix relatively small amounts of inorganic C to replenish intermediates of the tricarboxylic acid (TCA) cycle (Kornberg, 1965). The relevance and the metabolic controls on how much inorganic C is fixed by heterotrophic microorganisms remain poorly understood due to the lack of reliable estimates for most organisms and habitats (Braun et al., 2021). As such, the ratio of inorganic C assimilation to water-H incorporation into lipid biomarkers has the potential to distinguish between microbes operating primarily as autotrophs (ratio ~1) versus heterotrophs (ratio < 0.3) (Wegener et al., 2012).

In this study, we prepared dark, dual stable isotope probing incubation experiments to investigate seasonal heterotrophic production rates and inorganic C incorporation into lipids of planktonic bacteria, fungi and higher trophic levels in Lake Lunz (Lunz am See, Austria), a pristine, well monitored, sub-alpine lake. In addition to estimating heterotrophic community production by determining the incorporation of ^{2}H-H_2O into membrane fatty acids, we hypothesized that the incorporation of ^{13}C-bicarbonate into fatty acids would reflect the changes in predominance of metabolisms engaged to respire different C substrates available in the lake during spring (recent photosynthate) versus autumn (allochthonous inputs and recycled DOM).

2. Materials and Methods

2.1 Field sampling

Lake Lunz (47°51′10″N, 15°02′50″E) is an oligotrophic (mean phosphorous concentration of 4.63 ± 1.67 µg L^{-1}; Rasconi et al., 2018) subalpine lake (with very little human disturbance; McMeans et al., 2015) in the eastern Austrian Alps located 608 m.a.s.l; covers an area of 68 ha, its maximum depth reaches 34 m and is typically covered by ice during winter (Kainz et al., 2017). Sampling was performed during the end of Spring (June) and Autumn (November) 2023. Water column samples for the incubation were collected from the Epilimnion (EPI; 3 – 5 m) and Hypolimnion (HYP; 25 – 28 m).

2.2 Dual SIP incubations and harvest

Epilimnion (EPI) and hypolimnion (HYP) samples were filtered through a 40 µm mesh to remove seston. Lake water, 1 L in spring (June 2022) and 2 L in autumn (November 2022), was pre-incubated at 15 °C in the dark, and after 2 days, the dual-SIP experiments were initiated by adding ^{13}C-bicarbonate (^{13}C-DIC, $NaH^{13}CO_3$) and deuterated water (D_2O) according to Fig. 1. Four isotope treatments were conducted in triplicate, with Treatment I being natural abundance lake water in spring or autumn. In spring, lake waters were spiked with label in Treatments II, III, and IV to obtain δ^2H_{H2O} ≈ +1000‰, +3000‰, and +5000‰, and at% 13C-DIC = 2.5, 5, and 10%, respectively. To account for a lower production signal expected in November, the isotope enrichments of Treatments II, III, and IV were increased to δ^2H_{H2O} ≈ +2000‰, +4000‰, and +8000‰, and at% $^{13}C_{DIC}$ ≈ 2.5%, 5%, and 10%, respectively. Samples for lipid extraction were collected at the onset of the incubation and after an incubation period of 10 days. Upon harvest, all samples were filtered through a MN GF-5 0.4 µm filter to collect the biomass. Filters were lyophilized and stored at -20 °C until further analysis.

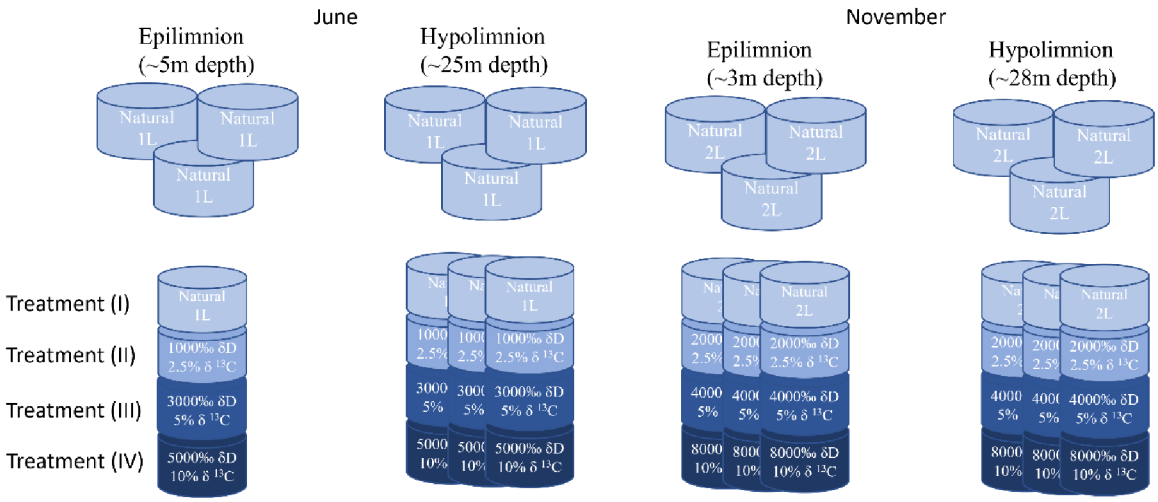

Figure 1: Dual-SIP incubation setup for June and November 2023 at Lake Lunz with different isotope level treatments.

2.3 Lipid extraction & FA methylation

Lyophilized samples were placed in a glass vial with 2 mL chloroform, then capped and left overnight at -80 °C. At the beginning of the extraction (Pilecky et al., 2023), samples were brought to room temperature and 1 mL of

MeOH + 1mL of MeOH:Chloroform (2:1; v:v) and 0.8 mL of NaCl (0.8% in MilliQ) were added. Samples were ultrasonicated for 10 min, shaken for 1 min and then centrifuged for 5 min at 3000 rpm at 4°C. The organic phase was collected, and the samples were re-extracted 2 more times, combined to the total lipid extract (TLE) and evaporated under a gentle N_2 stream and stored at -20 °C until further analysis.

Fatty Acids (FA) were methylated to Fatty Acid Methyl Ester (FAME) using the dried TLE with the addition of 1 mL of Toluol + 2 mL of 1% H_2SO_4 (in MeOH) and left in an incubator at 50 °C for 16 hours. Afterwards 2 mL of 2% $KHCO_3$ (in MilliQ) was added to stop the reaction. 5 mL of n-hexane was added, the sample was centrifuged at 1500 rpm for 3 min at 4 °C and the hexane phase was collected. The samples were extracted one more time with hexane, combined and dried under N_2 and stored at -20 °C until further analysis.

2.4 Measurements

2.4.1 Heavy water (D_2O) isotope analysis

Liquid samples for δ^2H analysis of water were collected from each incubation bottle at the start and the end of the incubation. Samples were transferred into 1.5 ml glass vials through a 0.2 µm syringe filter and were analyzed for $^{2/1}$H content by a 2130-i (Picarro Inc., Santa Clara, CA, US). Analytical error in of the δ^2H_{H2O} measurement was < 10‰.

2.4.2 Dissolved inorganic carbon (DIC) isotopes

Water aliquots (3 mL) were collected from the incubations and injected into a helium-flushed 12 mL exetainer vial (Exetainer, Labco Limited, UK), and then were acidified with 0.1 mL 85% H_3PO_4, and left to equilibrate for at least 24 hours before measurement using a GasBench device (Thermo Scientific, Bremen, Germany). Headspace CO_2 was purged using a double-holed needle with helium carrier gas into a 250 µL sample loop, injected onto a Carboxen PLOT 1010 column (0.53 mm ID; Supelco, Bellefonte, USA) held at 70 °C with a flow rate of ~ 2.5 mL min^{-1} (0.75 bar), and then introduced into the MAT253 Plus IRMS (Thermo Scientific, Bremen, Germany) via a Conflo IV interface. Each sample was injected three times during one analysis. The isotopic composition was determined using Isodat 3.0 software against the corresponding CO_2 working gas (-4.191‰ for δ^{13}C) and the values were corrected for linearity and normalized to the VPDB scale using international standards IAEA-603 and IAEA-303A (2.46‰ and 93.3‰ for δ^{13}C, respectively). The analytical error was < 1‰.

2.4.3 FAME analysis on GC-FID/IRMS

FAME were analyzed using a gas chromatograph (TRACE 1310 GC Thermo Scientific, Bremen, Germany) equipped with a split/splitless (SSL) injector using a single taper liner (4 × 6.3 × 78.5 mm, operated at 250 °C. Samples were injected in splitless mode onto a Supelco SP-2560 column (non-bonded; poly(biscyanopropyl siloxane) phase; 100 m, 25 mm ID, 0.2 µm df) with a temperature ramp starting at 140 °C hold for 5 min and then ramped at 4 °C min^{-1} to 240 °C and maintained for 20 min. Quantification was performed using a flame ionization detector (FID) detector with helium as the carrier gas at 1 mL min^{-1}, H_2 at 40 mL min^{-1}, N_2 45 mL min^{-}

^{1} and air at 450 mL min^{-1}. Identification of FAMEs was achieved based on the retention time of a 37-component FAME mix (47885-U, Supelco, Sigma-Aldrich, Darmstadt, Germany).

Stable carbon and hydrogen isotope compositions of FAMEs were determined by GC-IRMS via a GC-Isolink II equipped with a CO_2 combustion reactor, filled with Ni, Pt and Cu wires, at a temperature of 1000 °C, and a high thermal conversion (HTC) reactor (empty ceramic tube) for δ^2H analysis kept at 1420°C; coupled to a Delta V Advantage IRMS via a Conflo IV interface. Isotope composition values are expressed in standard delta notation ($\delta^{13}C$ and δ^2H). For FAME separation a VF-WAXms column (Polyethylen Glycol (PEG); 60 m, 0.25 mm ID, 0.25 µm df, Agilent Technologies, Santa Clara, CA, USA) was used. For $\delta^{13}C$, the helium flow rate of 1.2 ml min^{-1} was applied and the GC oven started at 80 °C, hold for 2 min, then raised by 30 °C min^{-1} to 175 °C, then by 5 °C min^{-1} to 200 °C and finally by 2.4 °C min^{-1} to 250 °C, which was maintained for 30 min. For δ^2H, the GC oven started at 80 °C, hold for 2 min, then raised by 30 °C min^{-1} to 175 °C, then by 5 °C min^{-1} to 240 °C, and maintained for 35 min. The isotopic composition was determined using Isodat 3.0 software normalized to VPDB or VSMOW/SLAP scales and isotope corrections were performed according to the response of USGS70 (-30.53‰ for $\delta^{13}C$, -183.9‰ for δ^2H), USGS71 (-10.5‰ for $\delta^{13}C$, -4.9‰ for δ^2H) and USGS72 (-1.54‰ for $\delta^{13}C$, 348.3‰ for δ^2H) reference standards. The analytical error was <1‰ and <10‰ for $\delta^{13}C$ and δ^2H, respectively.

2.5 Statistic and Calculations

Fatty acid production rates (ng L^{-1} yr^{-1}) were calculated based on the ^2H-water incorporation following equation 1 and inorganic C assimilation into fatty acids (ng L^{-1} yr^{-1}) were calculated based on equation 2. To calculate the turnover time (τ; yr) equation 3 was used. Errors refer to the standard errors of the mean (±SEM), which for epilimnion in spring was n = 3, and for the other 3 treatments (hypolimnion (spring), epilimnion and hypolimnion (autumn)) were n = 9 if not otherwise mentioned.

$$Production_{(Lipids)} = Concentration_{Lipids} * \frac{F^{2H}{}_{lipids\ labeling} - F^{2H}{}_{lipids\ control}}{\left(F^{2H}{}_{medium\ labeling} - F^{2H}{}_{medium\ control}\right) * time}$$

Equation 1: Lipid production (ng L^{-1} yr^{-1}) was calculated using the lipid concentration and multiplying it by the difference of the Fraction of the lipids from the labeling experiment compared to the natural (control), with F^{2H} of the medium subtracted from the F^{2H} of the medium natural (control) and multiplied by the incubation time (cf. Wegener et al., 2012).

$$IC_{(Lipids)} = Concentration_{Lipids} * \frac{F^{13C}{}_{lipids\ labeling} - F^{13C}{}_{lipids\ control}}{\left(F^{13C}{}_{medium\ labeling} - F^{13C}{}_{medium\ control}\right) * time}$$

Equation 2: Inorganic C incorporation (ng L^{-1} yr^{-1}) was calculated using the lipid concentration and multiplying it by the difference of the Fraction of the lipids from the labeling experiment compared to the natural (control), with F^{13C} of the medium subtracted from the F^{13C} of the medium natural (control) and multiplied by the incubation time.

The biomass was calculated after equation 3.

$$Turnover_{(years)} = \frac{Concentration\ (ng * L^{-1})}{Production\ or\ Inorganic\ C_{assim}\ (ng *\ L^{-1} *\ yr^{-1})}$$

Equation 3: The turnover rate (τ) represents the time FA or biomass need to fully renewal the corresponding pool and was calculated from the concentration divided by either the production rate based on equation 1 or by the inorganic C incorporation equation 2.

3. Results

3.1 Fatty acids methyl ester (FAME) distribution

The fatty acid (FA) profiles (Fig. 2) of EPI and HYP for the late spring season included bacterial FA (C_{14} – $C_{18:1}$) accounting for 51%, fungal FA ($C_{18:2}$) accounting for 0.8% and macroplankton FA [C_{20} and polyunsaturated FA (PUFA); $C_{18:3}$ – $C_{20:5}$] accounting for 48% of the total FA pool. The total concentrations of FA were higher in the EPI, with 66 ± 16 ng L^{-1} (N = 3; ±SEM), in comparison to HYP (47±4 ng L^{-1}; N = 9; ±SEM). The distributions of FA in November differed from spring, with 88% microbial, 2% fungal, and 10% macroplankton. The FA profiles in EPI and HYP incubations were generally consistent, but the overall FA concentration was 4 to 6-fold lower in Autumn (9 ± 0.6 ng L^{-1}; N = 9 and 10 ± 0.3 ng L^{-1}; N = 9; ±SEM, respectively). α-Linolenic acid (ALA; $C_{18:3\omega3}$) which accounted for 40% of total FA in Spring was almost completely missing in Autumn (< 1%).

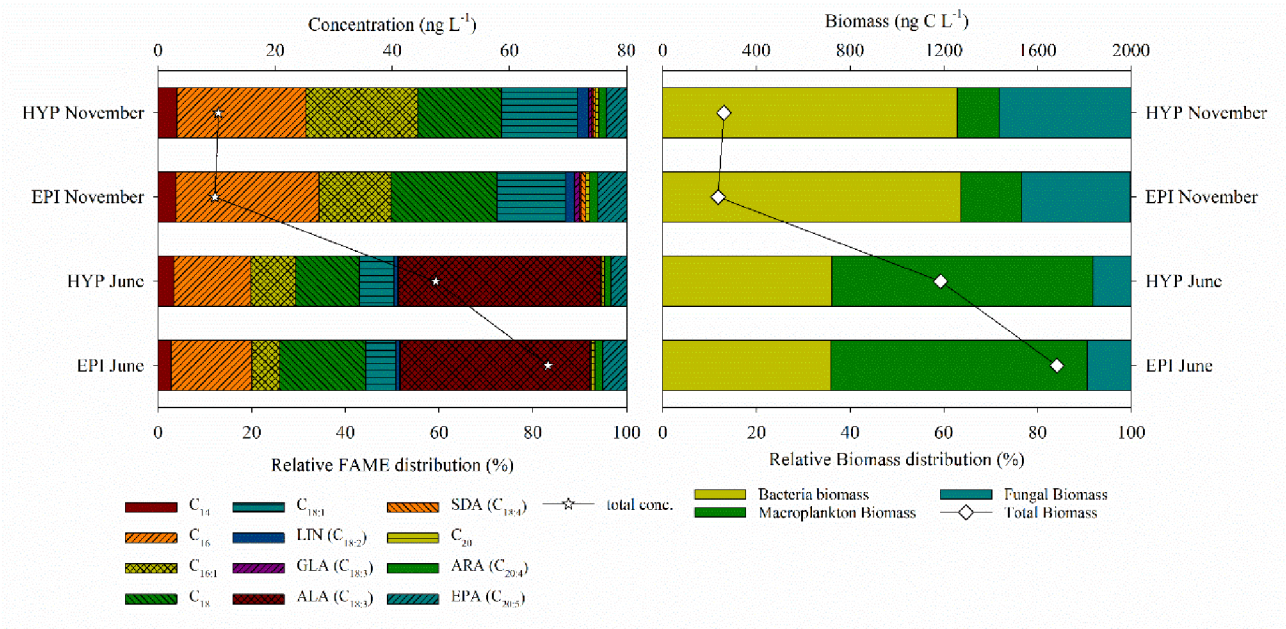

Figure 2: total concentration and the relative distribution of FAMEs (left panel) and estimated biomass (right panel) for the EPI and HYP of two different seasons during 2022. GLA = gamma-linolenic acid; ALA = alpha-linolenic acid; SDA = Stearidonic acid; ARA = Arachidonic acid, EPA = Eicosapentaenoic acid.

To estimate the total biomass carbon from FA concentrations, a conversion factor of 0.056 $g_{Lipids} * g_{biomass}^{-1}$ was assumed for bacterial FA (Middelburg et al., 2000; Wu et al., 2018), 0.0033 $g_{C18:2} * g_{biomass}^{-1}$ was assumed for fungal FA (Klamer and Baath 2004) and a conversion factor of 0.035 $g_{Lipids} * g_{biomass}^{-1}$ was assumed for macroplankton FA (Fouilland et al., 2013; Middelburg et al., 2000). Total biomass for EPI and HYP in spring was estimated at 1683±438 ng C L^{-1} (36±7% bacterial, 10±2% fungi and 53±6% macroplankton) and 1186±101 ng C L^{-1} (36±1% bacterial, 8±0.5% fungal and 56 ± 1% macroplankton), respectively. In autumn the estimated total biomass for EPI and HYP was 236 ± 16 ng C L^{-1} (63±0.7% bacterial, 23±0.7% fungal and 13±0.6% macroplankton) and 261±10 ng C L^{-1} (63±0.5% bacterial, 28±0.5% fungal and 9±0.4% macroplankton), respectively.

Table 1. Estimated fatty acid concentrations and biomass production in 10-day dark incubations of Lake Lunz epilimnion (EPI) and hypolimnion (HYP) waters

Parameter	Date	Depth	All Biomass	Bacteria	Fungal	Macro-plankton
Fatty acid ($ng\ C\ L^{-1}$)	June 2022	EPI	1680 ± 440	600 ± 150	160 ± 50	920 ± 300
		HYP	1190 ± 100	430 ± 40	100 ± 10	660 ± 60
	Nov. 2022	EPI	240 ± 20	150 ± 10	55 ± 4	31 ± 2
		HYP	260 ± 10	160 ± 6	73 ± 3	24 ± 1
Total production ($ng\ C\ L^{-1}\ y^{-1}$)	June 2022	EPI	4660 ± 890	2410 ± 600	370 ± 300	2000 ± 240
		HYP	10080 ± 1150	7270 ± 950	780 ± 80	2030 ± 310
	Nov. 2022	EPI	1580 ± 120	1260 ± 110	200 ± 30	110 ± 30
		HYP	2280 ± 130	1900 ± 90	140 ± 20	240 ± 60
DIC assimilation ($ng\ C\ L^{-1}\ y^{-1}$)	June 2022	EPI	330 ± 140	260 ± 100	70 ± 45	0
		HYP	270 ± 110	110 ± 20	110 ± 50	110 ± 80
	Nov. 2022	EPI	33 ± 5	28 ± 4	5.3 ± 1.9	1.1 ± 0.2
		HYP	30 ± 3	26 ± 2	3.8 ± 1.4	0
Turnover time (weeks)	June 2022	EPI	15 ± 3	12 ± 4	35 ± 24	16 ± 2
		HYP	6 ± 1	3 ± 1	7 ± 2	20 ± 4
	Nov. 2022	EPI	9 ± 1	8 ± 1	17 ± 2	14 ± 3
		HYP	4 ± 1	3 ± 1	23 ± 3	4 ± 1

3.2 ^{2}H lipid production and turnover time

Hydrogen incorporation into FA in spring for EPI and HYP was highest for $C_{16:1}$; $C_{18:1}$ and ARA ($C_{20:4}$) with δ^2H values reaching +2300‰, +1830‰, and +1630‰, respectively. C_{18} and C_{20} did not show any increase in δ^2H values. In autumn, ^{2}H incorporation was highest in $C_{16:1}$; GLA (γ-Linolenic acid; $C_{18:3\omega6}$) and ARA with δ^2H values ca. +3500‰, +9000‰, and +2580‰, respectively. EPA ($C_{20:5}$) did not show any increase in δ^2H values.

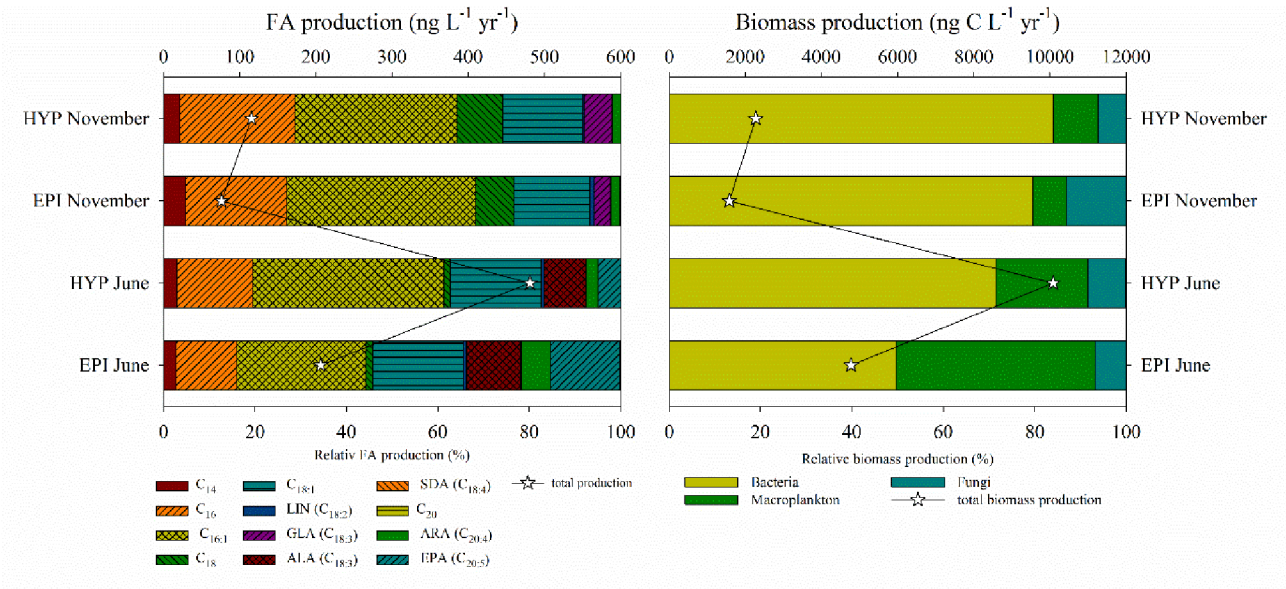

Figure 3: Fatty acid and biomass production calculated by the ^2H incorporation into microbial membrane lipids.

In spring, the total FA production was 206±36 ng L^{-1} yr^{-1} for EPI and 481±59 ng L^{-1} yr^{-1} for HYP. $C_{16:1}$ and $C_{18:1}$ were the major FA produced in both depths, with $C_{16:1}$ production in HYP roughly triple that of EPI (188±30 ng L^{-1} yr^{-1} vs. 59±10 ng L^{-1} yr^{-1}). Total biomass production estimates for EPI and HYP were 4.78±0.87 µg C L^{-1} yr^{-1} and 10.08±1.15 µg C L^{-1} yr^{-1}, respectively. Macroplankton biomass (i.e., protists and zooplankton) production was similar in EPI (2.00±0.24 µg C L^{-1} yr^{-1}; 44% of total production) and HYP (2.03±0.31 µg C L^{-1} yr^{-1}; 20% of total production), whereas bacterial biomass production was higher in HYP (7.27±0.95 µg C L^{-1} yr^{-1}; 72±3% of total production) relative to EPI 2.50 ± 0.60 µg C L^{-1} yr^{-1} (50±6% of total production). Fungal total biomass production was relatively low in both EPI and HYP (370±200 ng C L^{-1} yr^{-1}, 7±3% of total production; and 780±80 ng C L^{-1} yr^{-1}, 8±1% of total production), respectively.

In autumn, the total FA production was 76±6 ng L^{-1} yr^{-1} for EPI and 115±6 ng L^{-1} yr^{-1} for HYP. C_{16} and $C_{16:1}$ were the predominant FA produced in both layers. Upscaling from lipids, total biomass production for EPI and HYP was estimated at 1.58±0.12 µg C L^{-1} yr^{-1} and 2.28±0.13 µg C L^{-1} yr^{-1}, respectively. Bacterial biomass dominated production in EPI (1.26±0.11 µg C L^{-1} yr^{-1}; 79±2% of total production) and HYP (1.90±0.87 µg C L^{-1} yr^{-1}; 84±2% of total production). Macroplankton biomass production was higher in the HYP (240±64 ng C L^{-1} yr^{-1}; 10±2% of total production) vs EPI (114±31 ng C L^{-1} yr^{-1}; 8±2% of total production). Fungal total biomass production was higher in EPI (203±27 ng C L^{-1} yr^{-1}; 13±1% of total production) vs HYP (138±23 ng C L^{-1} yr^{-1}; 6±1% of total production).

Total biomass turnover was generally slower in EPI (15±3 and 9±1 weeks in spring and autumn, respectively) than in HYP incubations (6±1 and 4±1 weeks, respectively). Bacterial biomass turnover in EPI and HYP in spring (12±4 and 3±1 weeks) was similar to the turnover time in autumn (8±1 and 3±1 weeks). Macroplankton biomass turnover in EPI during spring and autumn were similar (~15 weeks) but was very different in HYP incubations (20±4 weeks in spring vs. 4±1 weeks in autumn). Fungal biomass turnover time in EPI were similar in spring (19±8 weeks) and autumn (17±2 weeks) whereas, but in HYP incubations, the turnover time was much faster in spring (7±2 weeks) than in autumn (23±3 weeks), opposite to the trend observed for macroplankton.

3.3 Heterotrophic Inorganic carbon assimilation

Rates of dark inorganic C incorporation in to all FA in spring were: 15±5.9 ng L^{-1} yr^{-1} (n = 3) for EPI and 9.8±3.9 ng L^{-1} yr^{-1} (n = 6) for HYP. C_{18} and $C_{18:1}$ exhibited the highest inorganic C assimilation in EPI, and ALA, C_{18}, and C_{16} were the highest in HYP incubations. Notably, no ^{13}C-DIC incorporation was detected for macroplankton FA in spring EPI incubations. In autumn, corresponding rates were much lower: 1.6±0.2 ng L^{-1} yr^{-1} (n = 9) for EPI and 1.5±0.1 ng L^{-1} yr^{-1} (n = 9) for HYP incubations. $C_{16:1}$ and $C_{18:1}$ exhibited the highest inorganic C assimilation in both EPI and HYP.

In spring, total biomass production supported by dark C fixation in EPI incubations was on average 465±72 ng C L^{-1} yr^{-1} (77±16% bacterial, fungal 15±10%, macroplankton 0%), and for HYP was 270±110 ng C L^{-1} yr^{-1} (40 ± 18% bacterial, 41±30% fungal, macroplankton 40±35%). Bacterial biomass dark C fixation was higher in EPI (360±50 ng C L^{-1} yr^{-1}) than in HYP (110±20 ng C L^{-1} yr^{-1}), fungal assimilation of inorganic C was variable and slightly higher in HYP than in EPI (110±50 vs 70±45 ng C L^{-1} yr^{-1}) and macroplankton dark C assimilation was absent in EPI but anomalously high and variable between HYP incubations (110 ± 80 ng C L^{-1} yr^{-1}). In autumn, biomass dark C fixation was much lower in both EPI (33±5 ng C L^{-1} yr^{-1}; 82±3% bacterial, 15±3% fungal, 4±1% macroalgal) and HYP incubations (30±3 ng C L^{-1} yr^{-1}; 88±3% bacterial, 12±3% fungal, macroalgal < 0.1%).

4. Discussion

We have generated a dataset of microbial, fungal, and macroplankton biomass production rates and turnover times based on incorporation of water-H into membrane lipids. Water column samples of two different depths (epilimnion (EPI) and hypolimnion (HYP)) were taken in two different seasons, (spring and autumn) from an oligotrophic lake and incubated for 10 days under dark conditions.

4.1 Spring and Autumn activity/production

As previously reported, water-H incorporation into lipid biomarkers is suggested to be a function of the isotope effects of hydrogen transporters and electron acceptors (NADPH and NADH), as they are the main portals for hydrogen incorporation in biosynthesis pathways (Valentine, 2009; Wijkers et al., 2019; Wegener et al., 2012; Kopf et al., 2015). However, when calculating production rates based on water-H incorporation, a water-H assimilation factor may be included to account for alternative sources of H and isotope fractionation during H assimilation (Kopf et al., 2015; Caro et al., 2023). In this study, a water-H assimilation factor of 0.7 (Caro et al., 2023) was applied to better approximate heterotrophic production rates.

Collectively, based on all FA abundances, heterotrophic biomass-C was slightly higher in Lake Lunz epilimnion than hypolimnion in spring, and biomass-C decreased > 4-fold at both depths in autumn to roughly equal concentrations (Table 1). Production rate estimates based on the incorporation of water-H into membrane fatty acids over 10 days were typically higher in HYP relative to EPI (Table 1). Presumably, higher heterotrophic production in EPI would be expected, given higher chlorophyll *a* concentration in the first 5 m (Roman and Sabata, 1999). However, the incubations were performed in the dark and isotope label was added after two days of pre-incubation, which may have favored the hypolimnion heterotrophic community already acclimated to these conditions. Macroplankton production rates in spring were an exception to this trend, exhibiting similar

production rates in both EPI and HYP (~ 2 µg C L^{-1} y^{-1}), where their production rates were 2- and 5-fold lower than bacteria (Table 1). The corresponding turnover times are faster for bacteria (15±3 and 6±1 weeks; EPI and HYP) than for macroplankton (16±2 and 20±4 weeks; EPI and HYP). Changes in macroplankton production in spring were observable from the biomarkers EPA ($C_{20:5}$) and ARA ($C_{20:4}$), which together accounted for 21% of total production in EPI but only 7% in HYP. In contrast, the macroplankton biomarker ALA ($C_{18:3\omega3}$) contributed alone 12% of total production in EPI and remained relatively high in HYP (9%). The difference in macroplankton FA content and production might represent a shift in the surface and subsurface community phylogeny or nutritional strategy. Macroplankton production was much higher than fungi at both depths, yet their turnover times were similar in EPI, and fungal (LIN; $C_{18:2}$) turnover time was much faster in HYP (7±2 vs. 20±4 weeks; Table 1). This finding suggests that fungi and/or other LIN producers were relatively more active than other PUFA producers in the deeper part of the lake in spring, and promotes the conclusion by Taube et al., 2018 that fungi are important in low-nutrient freshwater systems, despite their low biomass.

Total heterotrophic biomass-C production of dark incubations in autumn was reduced to 17% (EPI) and 23% (HYP) of that observed in spring, with production in HYP again higher than in EPI (Table 1). Ratios of bacterial versus macroplankton biomass-C increased in autumn by up to 7-fold. Bacteria biomass-C production rates were 1 to 4-fold higher than macroplankton in spring, and 8 to 11-fold higher in autumn. The increase in autumn likely owes to the general lack of an algal bloom (i.e. prey), when the chlorophyll *a* concentration (2.5 µg * L^{-1}) was less than half that measured in spring (Fig. S1). As algal photosynthate likely represents a substantial portion of labile DOM substrates that feeds the microbial loop (Farjalla et al., 2006; Azam et al., 1983), the generally lower bacterial biomass-C observed in autumn can be expected. The seasonal change likely exerted a greater impact on grazers than heterotrophs who can access the stockpile of DOM, which is also contributed by allochthonous sources (Ejarque et al., 2018). This notion may explain the consistent turnover times of bacteria dwelling in EPI or HYP during spring and autumn (Table 1). The smaller macroplankton biomass-C abundance observed in autumn was coincident with the predominance of GLA ($C_{18:3}$; Fig. 3) and a faster turnover time in HYP (4±1 weeks), which was similar to bacteria and may reflect a modulation of macroplankton community structure.

4.2 Dark carbon fixation

Inorganic C assimilation is known to contribute to a small portion of heterotrophic biomass (2 - 8%; Roslev et al., 2004; Braun et al., 2021), via anaplerotic pathways that replenish intermediates in the TCA cycle (Kronberg, 1965), for example. This flux has been suggested to play an important but underappreciated role in environmental systems (Braun et al., 2021) and especially for lakes (Santoro et al., 2013). Our data suggest that heterotrophic inorganic C assimilation was relatively variable and low in Lake Lunz (Table 1; Fig. 4), and approached detection limits for macroplankton fatty acid biomarkers identified in this study in both seasons and depths. The exception was the HYP incubation in spring, when measurable inorganic C was incorporated into ALA ($C_{18:3\omega3}$), SDA ($C_{18:4}$), and C_{20}. This could be a signal of anaplerotic reactions that supported the recycling of phytoplankton-derived fatty acids at depth. The consistently small fluxes of inorganic C into C_{14}, C_{16}, $C_{16:1}$, $C_{18:1}$, and LIN ($C_{18:2}$), suggest that the mechanisms of bacterial and fungal production were more uniform in both seasons and depths.

4.3 Ra/p

The ratio (Ra/p), which represents inorganic C assimilation normalized by total production (water-H incorporation), can distinguish the preferred metabolic mode of autotrophs vs. heterotrophs (Wegener et al., 2012; Wegener et al., 2016; Huguet et al., 2017; Wu et al., 2018). As defined by Wegener et al. (2012), a Ra/p value of < 0.3 is expected for heterotopic metabolism, whereas values between 0.3 and 0.7 represent mixotrophy, and Ra/p > 0.7 denotes autotrophy. Independent of the season or depth, the total community Ra/p values in our incubations were mostly far below the 0.3 threshold for heterotrophs, and closer to a value of 0.05. The highest Ra/p values for individual fatty acid were observed in spring, particularly for the fungal/LIN ($C_{18:2}$) biomarker (0.2 - 0.4 vs bacteria and macroplankton < 0.1; Fig. 4). Alternate substrates available to fungi (or LIN producers) in spring could induce such an increase. Anomalously high Ra/p values observed for C_{18} and $C_{18:1}$ in EPI, and for ALA ($C_{18:3w3}$) in HYP (Fig. 4) may be indicative of anaplerotic reactions required for lipid recycling, as noted in the previous section. Most bacteria Ra/p values did not change with season or depth, suggesting that a similar substrate pool and niche accommodated their metabolic demands in spring and autumn.

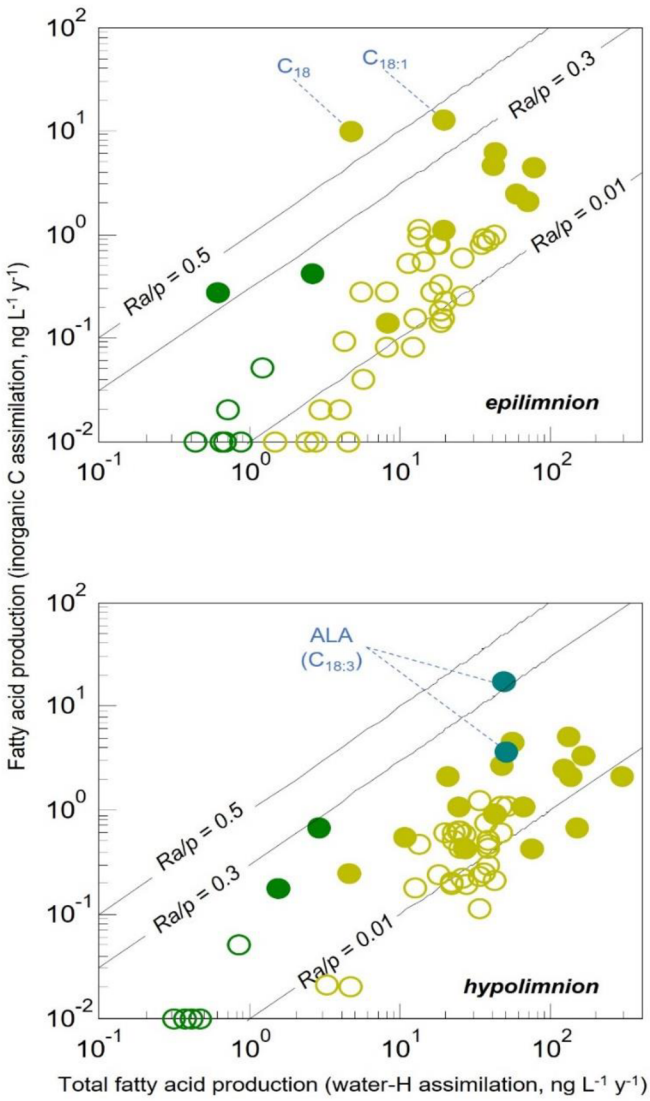

Figure 4. Ra/p values for individual fatty acids assigned to bacteria (yellow), fungi (green), or macroplankton (cyan) harvested from replicate incubations of the respective depth layers in June (filled symbols) or November (open symbols). The axes are plotted as a log scale to better illustrate trends in fatty acid production that spanned orders of magnitude. The solid black lines represent projections for Ra/p = 1, 0.3 or 0.01. The dashed blue lines and blue text indicate individual fatty acids exhibiting anomalously high Ra/p values.

5. Conclusion

The purpose of this work was (I) to quantify the microbial activity in the sub alpine oligotrophic Lake Lunz am See in two different seasons and depths. Our results demonstrate that in the spring season the activity/production of C biomass of the microbial community under dark conditions was equal between the two depths in spring and around 80% higher than during the autumn season. Also, the community was primarily heterotrophic as indicated by the Ra/p values and that inorganic C assimilation was playing a very minor role in this system. For the purpose (II) to quantify the contribution of fungi in this system, our results demonstrate that although production was less than 10% of the entire C biomass during both seasons and depths indicating a minor contribution but turnover times indicated a very active role. Interestingly the Ra/p values indicated different C sources used between spring and autumn with slightly higher inorganic C assimilation in spring. Nevertheless, further investigation to fully understand fungal role in this Lake ecosystems are needed.

Acknowledgements

This Project was funded by the Czech Science Foundation GACR nr. 20-223805 (FUNSIF) and supported by MEYS CZ grant LM2015075 Projects of Large Infrastructure for Research, Development and Innovations as well as the European Regional Development Fund-Project: research of key soil-water ecosystem interactions at the SoWa Research Infrastructure (No. CZ.02.1.01/0.0/0.0/16_013/0001782). Erasmus+ Student mobility for traineeship of the University of South Bohemia (Erasmus ID code: CZ CESKE01) supported travel expenses for this international collaboration. We thank the Samuel-Karl Kaemmer and Christina Beke for their contributions to this study.

References

Azam, F., Fenchel, T., Field, J. G., Gray, J. S., Meyer-Reil, L. A., & Thingstad, F. J. M. E. P. S. (1983). The ecological role of water-column microbes in the sea. *Marine Ecology Progress Series*, 10(3), 257-263.

Bauer, J. E., Cai, W. J., Raymond, P. A., Bianchi, T. S., Hopkinson, C. S., & Regnier, P. A. (2013). The changing carbon cycle of the coastal ocean. *Nature*, 504(7478), 61-70.

Boschker, H. T. S., Nold, S. C., Wellsbury, P., Bos, D., De Graaf, W., Pel, R., ... & Cappenberg, T. E. (1998). Direct linking of microbial populations to specific biogeochemical processes by 13C-labelling of biomarkers. *Nature*, 392(6678), 801-805.

Braun, A., Spona-Friedl, M., Avramov, M., Elsner, M., Baltar, F., Reinthaler, T., ... & Griebler, C. (2021). Reviews and syntheses: Heterotrophic fixation of inorganic carbon–significant but invisible flux in environmental carbon cycling. *Biogeosciences*, 18(12), 3689-3700.

Caro, T. A., McFarlin, J., Jech, S., Fierer, N., & Kopf, S. (2023). Hydrogen stable isotope probing of lipids demonstrates slow rates of microbial growth in soil. *Proceedings of the National Academy of Sciences*, 120(16), e2211625120.

Duarte, S., Bärlocher, F., Pascoal, C., & Cássio, F. (2016). Biogeography of aquatic hyphomycetes: current knowledge and future perspectives. *Fungal Ecology*, 19, 169-181.

Dumont, M. G., & Murrell, J. C. (2005). Stable isotope probing - linking microbial identity to function. *Nature Reviews Microbiology*, 3(6), 499-504.

Ejarque, E., Khan, S., Steniczka, G., Schelker, J., Kainz, M. J., & Battin, T. J. (2018). Climate-induced hydrological variation controls the transformation of dissolved organic matter in a subalpine lake. *Limnology and Oceanography*, 63(3), 1355-1371.

Farjalla, V. F., Azevedo, D. A., Esteves, F. A., Bozelli, R. L., Roland, F., & Enrich-Prast, A. (2006). Influence of hydrological pulse on bacterial growth and DOC uptake in a clear-water Amazonian lake. *Microbial Ecology*, 52, 334-344.

Fouilland, E., Tolosa, I., Bonnet, D., Bouvier, C., Bouvier, T., Bouvy, M., ... & Vidussi, F. (2014). Bacterial carbon dependence on freshly produced phytoplankton exudates under different nutrient availability and grazing pressure conditions in coastal marine waters. *FEMS Microbiology Ecology*, 87(3), 757-769.

Grossart, H. P., Van den Wyngaert, S., Kagami, M., Wurzbacher, C., Cunliffe, M., & Rojas-Jimenez, K. (2019). Fungi in aquatic ecosystems. *Nature Reviews Microbiology*, 17(6), 339-354.

Hoefs, J. (2018). *Stable isotope geochemistry: Theoretical and experimental principles* (3rd edition; pp 1-318) Berlin, Springer.

Huguet, A., Meador, T. B., Laggoun-Défarge, F., Könneke, M., Wu, W., Derenne, S., & Hinrichs, K. U. (2017). Production rates of bacterial tetraether lipids and fatty acids in peatland under varying oxygen concentrations. *Geochimica et Cosmochimica Acta*, 203, 103-116.

Kainz, M. J., Ptacnik, R., Rasconi, S., & Hager, H. H. (2017). Irregular changes in lake surface water temperature and ice cover in subalpine Lake Lunz, Austria. *Inland Waters*, 7(1), 27-33.

Kellermann, M. Y., Wegener, G., Elvert, M., Yoshinaga, M. Y., Lin, Y. S., Holler, T., ... & Hinrichs, K. U. (2012). Autotrophy as a predominant mode of carbon fixation in anaerobic methane-oxidizing microbial communities. *Proceedings of the National Academy of Sciences*, 109(47), 19321-19326.

Kellermann, M. Y., Yoshinaga, M. Y., Wegener, G., Krukenberg, V., & Hinrichs, K. U. (2016). Tracing the production and fate of individual archaeal intact polar lipids using stable isotope probing. *Organic Geochemistry*, 95, 13-20.

Klamer, M., & Bååth, E. (2004). Estimation of conversion factors for fungal biomass determination in compost using ergosterol and PLFA 18:2ω6,9. *Soil Biology and Biochemistry*, 36(1), 57-65.

Kopf, S. H., McGlynn, S. E., Green-Saxena, A., Guan, Y., Newman, D. K., & Orphan, V. J. (2015). Heavy water and 15N labelling with Nano SIMS analysis reveals growth rate-dependent metabolic heterogeneity in chemostats. *Environmental Microbiology*, 17(7), 2542-2556.

Kornberg, H. L. (1965). Anaplerotic sequences in microbial metabolism. *Angewandte Chemie International Edition in English*, 4(7), 558-565.

Kreuzer-Martin, H. W. (2007). Stable isotope probing: linking functional activity to specific members of microbial communities. *Soil Science Society of America Journal*, 71(2), 611-619.

McMeans, B. C., Koussoroplis, A. M., & Kainz, M. J. (2015). Effects of seasonal seston and temperature changes on lake zooplankton fatty acids. *Limnology and Oceanography*, 60(2), 573-583.

Middelburg, J. J. (2014). Stable isotopes dissect aquatic food webs from the top to the bottom. *Biogeosciences*, 11(8), 2357-2371.

Middelburg, J. J., Barranguet, C., Boschker, H. T., Herman, P. M., Moens, T., & Heip, C. H. (2000). The fate of intertidal microphytobenthos carbon: An in situ 13C-labeling study. *Limnology and Oceanography*, 45(6), 1224-1234.

Pilecky, M., Wassenaar, L. I., Taipale, S., & Kainz, M. J. (2023). Protocols for sample preparation and compound-specific stable-isotope analyses (δ2H, δ13C) of fatty acids in biological and environmental samples. *MethodsX*, 11, 102283.

Rasconi, S., Ptacnik, R., & Kainz, M. J. (2018). Seston fatty acid responses to physicochemical changes in subalpine Lake Lunz, Austria. *Water Resources Research*, 54(10), 8442-8455.

Roman, A. M., & Sabater, S. (1999). Effect of primary producers on the heterotrophic metabolism of a stream biofilm. *Freshwater Biology*, 41(4), 729-736.

Romaní, A. M., Fischer, H., Mille-Lindblom, C., & Tranvik, L. J. (2006). Interactions of bacteria and fungi on decomposing litter: differential extracellular enzyme activities. *Ecology*, 87(10), 2559-2569.

Roslev, P., Larsen, M. B., Jørgensen, D., & Hesselsoe, M. (2004). Use of heterotrophic CO2 assimilation as a measure of metabolic activity in planktonic and sessile bacteria. *Journal of Microbiological Methods*, 59(3), 381-393.

Santoro, A. L., Bastviken, D., Gudasz, C., Tranvik, L., & Enrich-Prast, A. (2013). Dark carbon fixation: an important process in lake sediments. *PLoS One*, 8(6), e65813.

Sigee, D. C. (2005). *Freshwater Microbiology: Biodiversity and Dynamic Interactions of Microorganisms in the Aquatic Environment*. John Wiley & Sons.

Taube, R., Ganzert, L., Grossart, H. P., Gleixner, G., & Premke, K. (2018). Organic matter quality structures benthic fatty acid patterns and the abundance of fungi and bacteria in temperate lakes. *Science of the Total Environment*, 610, 469-481.

Valentine, D. L. (2009). Isotopic remembrance of metabolism past. *Proceedings of the National Academy of Sciences*, 106(31), 12565-12566.

Wegener, G., Bausch, M., Holler, T., Thang, N. M., Prieto Mollar, X., Kellermann, M. Y., ... & Boetius, A. (2012). Assessing sub-seafloor microbial activity by combined stable isotope probing with deuterated water and 13C-bicarbonate. *Environmental Microbiology*, 14(6), 1517-1527.

Wegener, G., Kellermann, M. Y., & Elvert, M. (2016). Tracking activity and function of microorganisms by stable isotope probing of membrane lipids. *Current Opinion in Biotechnology*, 41, 43-52.

Whiteman, J. P., Elliott Smith, E. A., Besser, A. C., & Newsome, S. D. (2019). A guide to using compound-specific stable isotope analysis to study the fates of molecules in organisms and ecosystems. *Diversity*, 11(1), 8.

Wijker, R. S., Sessions, A. L., Fuhrer, T., & Phan, M. (2019). 2H/1H variation in microbial lipids is controlled by NADPH metabolism. *Proceedings of the National Academy of Sciences*, 116(25), 12173-12182.

Willers, C., Jansen van Rensburg, P. J., & Claassens, S. (2015). Phospholipid fatty acid profiling of microbial communities–a review of interpretations and recent applications. *Journal of Applied Microbiology*, 119(5), 1207-1218.

Wu, W., Meador, T., & Hinrichs, K. U. (2018). Production and turnover of microbial organic matter in surface intertidal sediments. *Organic Geochemistry*, 121, 104-113.

Wu, W., Meador, T. B., Könneke, M., Elvert, M., Wegener, G., & Hinrichs, K. U. (2020). Substrate-dependent incorporation of carbon and hydrogen for lipid biosynthesis by Methanosarcina barkeri. *Environmental Microbiology Reports*, 12(5), 555-567.

Additional information

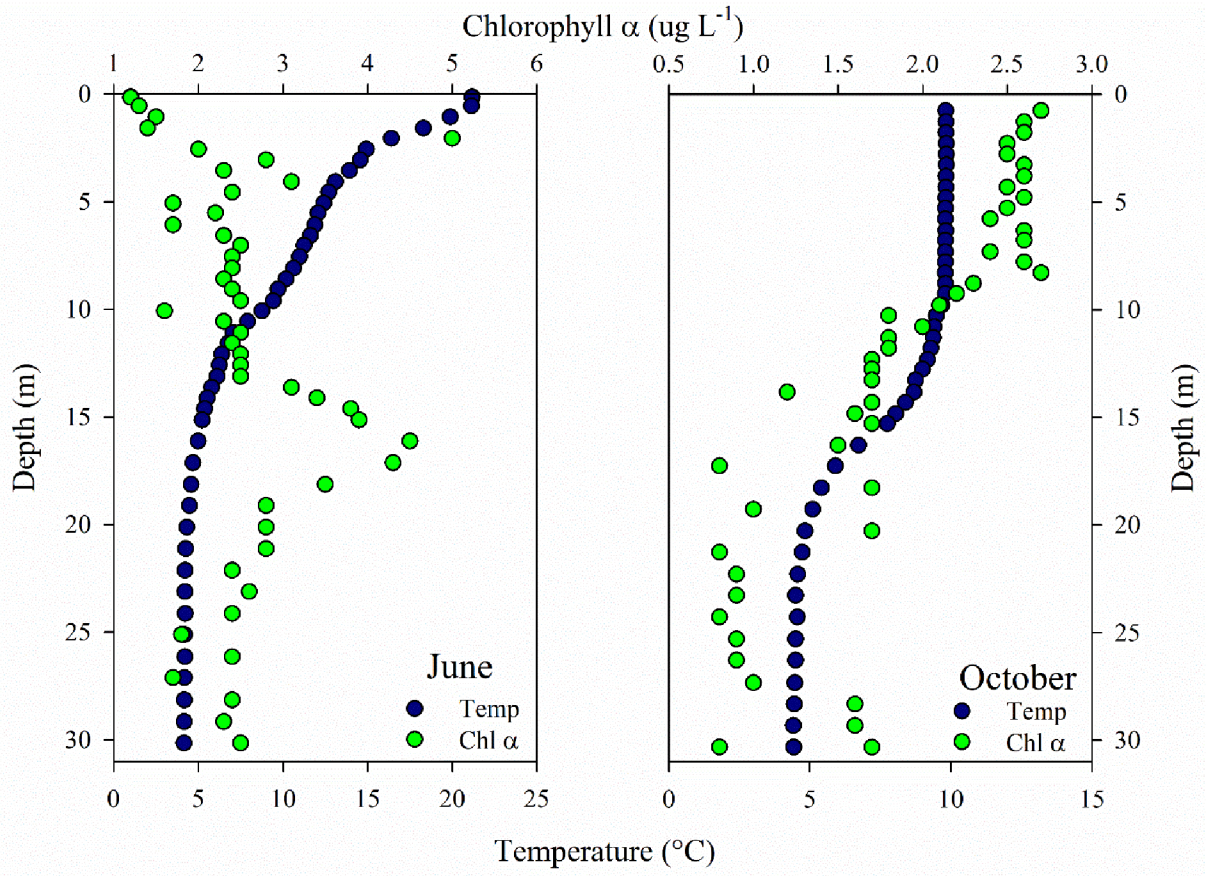

Figure S1: Lake Lunz chlorophyll a (µg L^{-1}) and temperature (°C) in spring and autumn around the sampling time

Table S2: Detailed summary estimation of fatty acid concentrations and biomass production in 10-day dark incubations of Lake Lunz epilimnion (EPI) and hypolimnion (HYP) waters

Parameter	Date	Depth	C14	C16	C16:1	C18	C18:1	LIN	GLA	ALA	SDA	C20	ARA	EPA
Fatty acid (ng C L^{-1})	June 2022	EPI	1.8±0.5	11±3	4.0±1.2	12±5	4.3±1.2	0.5±0.2	0.1±0.04	27±9	0.2±0.07	0.5±0.1	1.1±0.3	3.5±1.1
		HYP	1.6±0.2	7.8±0.7	4.5±0.5	6.4±0.6	3.6±0.3	0.3±0.01	0.1±0.01	21±2	0.1±0.02	0.3±0.02	0.6±0.2	1.6±0.2
	Nov. 2022	EPI	0.4±0.03	2.9±0.2	1.5±0.1	2.2±0.2	1.4±0.1	0.2±0.01	0.1±0.01	n.d.	0.1±0.01	0.1±0.01	0.2±0.01	0.6±0.04
		HYP	0.4±0.02	2.8±0.1	2.5±0.2	1.8±0.1	1.7±0.1	0.2±0.01	0.1	n.d.	n.d.	0.1	0.2±0.01	0.5±0.02
Fatty acid production (ng C L^{-1} y^{-1})	June 2022	EPI	5.9±1.5	27±7	58±10	4.7±0	41±14	1.2±0.7	n.d.	24±0.2	0.5±0.3	n.d.	13±2	31±8
		HYP	13±4	75±13	188±31	7.1±1.2	90±13	2.6±0.2	n.d.	43±4	n.d.	n.d.	12±2	24±5
	Nov. 2022	EPI	3.6±0.4	17±2	31±3	6.4±1.2	13±1	0.7±0.1	3.0±1.3	n.d.	0.1±0.01	0.1±0.07	1.5±0.2	n.d.
		HYP	4.1±0.4	29±2	41±2	11±2	20±2	0.5±0.07	7±2.5	n.d.	n.d.	0.1 ±0.01	2±0.3	0.2±0.09
Fatty acid production (DIC) (ng C L^{-1} y^{-1})	June 2022	EPI	0.14	3.7±2.6	3.8±0.7	9.9	7.4±5.3	0.4±0.1	n.d.	n.d.	n.d.	n.d.	n.d.	n.d.
		HYP	0.4±0.1	3.0±0.5	2.8±0.7	2.8	1.1±0.3	0.4±0.2	n.d.	10±7	0.1±0.03	0.1±0.03	n.d.	n.d.
	Nov. 2022	EPI	0.03±0.01	0.2±0.02	0.7±0.1	n.d.	0.7±0.1	0.02±0.01	n.d.	n.d.	n.d.	n.d.	n.d.	0.04±0.01
		HYP	0.02	0.2±0.03	0.7±0.1	n.d.	0.5±0.1	0.01	n.d.	n.d.	n.d.	n.d.	n.d.	n.d.
Turnover time (weeks)	June 2022	EPI	16	22	4	136	5	22	n.d.	56	21	n.d.	4	6
		HYP	6	5	1	47	2	6	n.d.	24	n.d.	n.d.	3	3
	Nov. 2022	EPI	5	9	3	18	6	14	2	74	56	48	6	n.d.
		HYP	5	5	3	8	4	28	n.d.	n.d.	99	52	4	148

3. Conclusion and future prospects

The studies performed in this PhD project have investigated the potential of fungal metabolic activity to assimilate inorganic carbon and hydrogen water incorporation into their membrane lipids, in order to quantify the contribution of fungi to ecosystem processes. Overall, the research presented in this thesis provides the first investigation of hydrogen water assimilation factors by fungal species, estimates of heterotrophic CO_2 fixation into fungal biomarkers, and an application of this knowledge to assess ecosystem fluxes of primarily heterotrophic microbial communities in environmental systems.

Laboratory incubations

Our goal was to establish the fundamental relationship between the organic C source and the isotopic signals in fungal membrane lipids resulting from heavy water assimilation and heterotrophic CO_2 fixation. This was accomplished by pure culture incubations of Ascomycota (Paper I) from the fungal collection, and a verity of Ascomycota, Basidiomycota and Zygomycota (manuscript II) from a collaboration with the Institute of Microbiology in Prague. Here we reported the water assimilation factor (α_W) for fungal biomarker (α_W = 0.69) for the first time, which as mentioned above, is a key parameter to estimate activity, production and turnover fluxes and until now, only existed for bacteria. We found that this factor for fungi is similar to that reported for bacteria (α_W = 0.71; Caro et al., 2023), indicating similar mechanisms in water assimilation and fractionation between these two groups. As for the heterotrophic CO_2 assimilation, our reports were more variable with Ascomycota (Paper I) indicating a broad range of inorganic C fixation by fungi (2 – 12%), but with a broader range of phyla (manuscript II), the inorganic C assimilation was estimated to account for only less than 3% of C incorporated into fungal lipids. The observed variability could have resulted from the general difficulty to establish controlled growth conditions for fungi, which required both oxic conditions and closed batch incubations to ensure the ^{13}C label was not lost to the atmosphere. Due to the sheer number of co-occurring incubations (n = 288), some fungal incubations could not be harvested quickly upon reaching a target level of CO_2 accumulation in the headspace, and some incubations yielded very low biomass and were atypical of typical microbial growth curves. These growth experiments required a re-evaluation of assumptions related to isotope incorporation and stand in contrast to the incubations in paper I, where all incubations were stopped when a certain CO_2 concentration in the headspace was reached. As a consequence, the calculated inorganic C fixation into fungal lipids in manuscript II incorporated an isotope mixing model, which likely improved accuracy, relative to the higher values reported in paper I. Future studies employing continuous cultivation and isotope pulse-chase techniques, for example, could build on these findings in order to further constrain lipid isotopic fractionation signals among pure fungal cultures and growth substrates, particularly for the slow-growing Basidiomycota.

Environmental incubations

By applying the SIP assay developed in papers I and manuscript II to environmental incubations, we could provide an insight and quantify microbial activity in the soils of the Blanský Les natural reservoir/Czech Republic (manuscript III), from which samples were collected in different seasons (spring and autumn) and different soil horizons (A horizon, O horizon and roots which were removed from the O horizon). Fungi are expected to

dominate soil environments but grow more slowly than bacteria (Rousk and Baath, 2007). In our study, we could demonstrate that fungal biomass indeed dominated the different soil horizons, based on FAME abundances, but also exhibited higher production rates and shorter turnover times in comparison to bacteria. This was especially visible in the incubations of the roots for both seasons. For the other horizons, bacteria showed higher production rates in spring but fungal production dominated in autumn, which we suggested be due to the possible change in available substrates, from freshly produced photosynthates in spring verses relatively less labile C that had accumulated in soils in autumn. Assimilation of ^{13}C into lipids was below detection limits, and no conclusions could be made about the metabolic mode that supported lipid biosynthesis, which should have been based on the rates of inorganic C and water-H assimilation. Future applications of this assay in environmental soils could be improved by employing continuous flow reactors that better control the provision of ^{13}C-labeled bicarbonate.
The dual-SIP assay was successfully applied to investigate the seasonal and spatial dynamics of heterotrophic activity in Lake Lunz (Lunz am See, Austria; manuscript IV). Isotope incorporation signals provided estimates of production and turnover rates of bacteria, fungi and microalgae in spring and autumn. Although fungi accounted for only minor relative abundances and fluxes, the assay could demonstrate major changes in fungal and macroalgal turnover times with depth and season, whereas bacteria remained relatively constant. These findings inform the ecosystem fluxes and contributions of the heterotrophic communities to the food web structures that modulate throughout the year. Also, assimilation of small amounts of inorganic C into the fungal biomarker, particularly in spring, suggested that heterotrophic CO_2 fixation may be indicative of recycling of plankton-derived lipids, and should be further studied.

The highlights of this PhD thesis include:

- The first report of a water isotope assimilation factor for fungi, a key parameter for estimating production, growth and turnover rates by the heavy water lipid-SIP approach (fungal mean $a_W = 0.69$)

- Inorganic C assimilation into fungal biomarkers was variable for aquatic populations, but pure culture studies could not identify taxonomy or C substrate as robust explanatory factors

- Fungal production rates in roots and soil O and A horizons were always significantly higher in autumn than in spring

- Fungal production in forest roots exhibited relatively high carbon use efficiency and ranged up to 235 mg C g^{-1} y^{-1}, representing a yearly turnover of roughly ½ of root C.

- Bacterial biomass turnover times were unexpectedly faster in the forest soil A horizon compared to the overlying, substrate-rich O horizon

- Variable turnover times of fungal and macroplankton biomass with water depth and season suggest alternative food sources and lake ecosystem roles, in contrast to bacteria, who likely rely on a consistent source of dissolved substrates.

- The relative rates of inorganic C and water-H assimilation into the fungal biomarker 18:2 indicate the highest Ra/p values for the aquatic heterotrophic community

In the last few decades, the field of microbial ecology has gained a massive number of insights due to the development of new analytical methods and techniques in microbiology and geochemistry and their combination. This thesis primarily targeted the $C_{18:2}$ fatty acid, which serves as an accepted biomarker for fungi in soil ecosystems. Ergosterol is an alternative lipid biomarker of fungi, but our findings indicated that its isotopic composition was less responsive to the different metabolic modes employed by fungi. Nevertheless, incorporation of water-H into ergosterol was quantifiable ($\alpha_w = 0.66$). Ergosterol may therefore serve as a useful biomarker of fungal production for future SIP investigations, particularly for aquatic ecosystems, where $C_{18:2}$ may also be contributed by zooplankton and cannot be attributed to fungal production alone.

The information provided by the lipid biomarker Dual-SIP assay developed and employed in this thesis represents another puzzle piece of a vast picture, which is needed to delineate energy flow, production rates, growth rates and turnover times for microbial communities and fungi in environmental ecosystems. But as in all environmental investigations, it should be combined with other, independent measurements of ecosystem functions, such as CO_2 release, nutrient fluxes, and omics approaches, to achieve the more complete understanding key processes, microbial interactions, and their involvement in biogeochemical cycles. This will enable us to model biogeochemical fluxes, which are needed to predict future climate developments and countermeasures as climate change and its various effects are challenging life on Earth as we know it.

4. References

Amann, R. I. (1995). Fluorescently labelled rRNA-targeted oligonucleotide probes in the study of microbial ecology. *Molecular Ecology*, 4(5), 543-554.

Anderson, I. C., & Cairney, J. W. (2004). Diversity and ecology of soil fungal communities: Increased understanding through the application of molecular techniques. *Environmental Microbiology, 6*(8), 769-779.

Bakker, B. M., Overkamp, K. M., Van Maris, A. J., Kötter, P., Luttik, M. A., Van Dijken, J. P., & Pronk, J. T. (2001). Stoichiometry and compartmentation of NADH metabolism in *Saccharomyces cerevisiae*. *FEMS Microbiology Reviews, 25*(1), 15-37.

Baldrian, P., Voříšková, J., Dobiášová, P., Merhautová, V., Lisá, L., & Valášková, V. (2011). Production of extracellular enzymes and degradation of biopolymers by saprotrophic microfungi from the upper layers of forest soil. *Plant and Soil, 338*, 111-125.

Beillouin, D., Cardinael, R., Berre, D., Boyer, A., Corbeels, M., Fallot, A., ... & Demenois, J. (2022). A global overview of studies about land management, land-use change, and climate change effects on soil organic carbon. *Global Change Biology, 28*(4), 1690-1702.

Beney, L., & Gervais, P. (2001). Influence of the fluidity of the membrane on the response of microorganisms to environmental stresses. *Applied Microbiology and Biotechnology, 57*, 34-42.

Bird, M. I., Chivas, A. R., & Head, J. (1996). A latitudinal gradient in carbon turnover times in forest soils. *Nature, 381*(6578), 143-146.

Blackwell, M. (2011). The fungi: 1, 2, 3… 5.1 million species? *American Journal of Botany, 98*(3), 426-438.

Blattner, F. R., Plunkett III, G., Bloch, C. A., Perna, N. T., Burland, V., Riley, M., ... & Shao, Y. (1997). The complete genome sequence of *Escherichia coli* K-12. *Science, 277*(5331), 1453-1462. https://doi.org/10.1126/science.277.5331.1453

Boer, W. D., Folman, L. B., Summerbell, R. C., & Boddy, L. (2005). Living in a fungal world: Impact of fungi on soil bacterial niche development. *FEMS Microbiology Reviews, 29*(4), 795-811.

Bossche, H. V., & Marichal, P. (1993). Is there a role for sterols and steroids in fungal growth and transition from yeast to hyphal-form and vice versa? An overview. In *Dimorphic Fungi in Biology and Medicine* (p. 177).

Bradford, M. A., Berg, B., Maynard, D. S., Wieder, W. R., & Wood, S. A. (2016). Future directions: Understanding the dominant controls on litter decomposition. *Journal of Ecology, 229*-238.

Brassell, S. C., Eglinton, G., Marlowe, I. T., Pflaumann, U., & Sarnthein, M. (1986). Molecular stratigraphy: A new tool for climatic assessment. *Nature, 320*(6058), 129-133.

Braun, A., Spona-Friedl, M., Avramov, M., Elsner, M., Baltar, F., Reinthaler, T., ... & Griebler, C. (2021). Reviews and syntheses: Heterotrophic fixation of inorganic carbon–significant but invisible flux in environmental carbon cycling. *Biogeosciences, 18*(12), 3689-3700.

Butler, J. L., Williams, M. A., Bottomley, P. J., & Myrold, D. D. (2003). Microbial community dynamics associated with rhizosphere carbon flow. *Applied and Environmental Microbiology, 69*(11), 6793-6800.

Cantrell, S. A., Dianese, J. C., Fell, J., Gunde-Cimerman, N., & Zalar, P. (2011). Unusual fungal niches. *Mycologia, 103*(6), 1161-1174.

Carvalhais, N., Forkel, M., Khomik, M., Bellarby, J., Jung, M., Migliavacca, M., ... & Reichstein, M. (2014). Global covariation of carbon turnover times with climate in terrestrial ecosystems. *Nature, 514*(7521), 213-217.

Castellano, M. J., Mueller, K. E., Olk, D. C., Sawyer, J. E., & Six, J. (2015). Integrating plant litter quality, soil organic matter stabilization, and the carbon saturation concept. *Global Change Biology, 21*(9), 3200-3209.

Chen, S., Huang, Y., Zou, J., & Shi, Y. (2013). Mean residence time of global topsoil organic carbon depends on temperature, precipitation and soil nitrogen. *Global and Planetary Change, 100*, 99-108.

Coleman, D. C., Reid, C. P. P., & Cole, C. V. (1983). Biological strategies of nutrient cycling in soil systems. In *Advances in Ecological Research* (Vol. 13, pp. 1-55). Academic Press.

Craig, H. (1957). Isotopic standards for carbon and oxygen and correction factors for mass-spectrometric analysis of carbon dioxide. *Geochimica et Cosmochimica Acta, 12*(1-2), 133-149.

Curiel Yuste, J., Baldocchi, D. D., Gershenson, A., Goldstein, A., Misson, L., & Wong, S. (2007). Microbial soil respiration and its dependency on carbon inputs, soil temperature and moisture. *Global Change Biology, 13*(9), 2018-2035.

Darling, G. W., Bath, A. H., Gibson, J. J., & Rozanski, K. (2006). Isotopes in water (pp. 1-66). Springer Netherlands.

Davidson, E. A., & Janssens, I. A. (2006). Temperature sensitivity of soil carbon decomposition and feedbacks to climate change. *Nature, 440*(7081), 165-173.

Dijkstra, P., Thomas, S. C., Heinrich, P. L., Koch, G. W., Schwartz, E., & Hungate, B. A. (2011). Effect of temperature on metabolic activity of intact microbial communities: evidence for altered metabolic pathway activity but not for increased maintenance respiration and reduced carbon use efficiency. *Soil Biology and Biochemistry, 43*(10), 2023-2031.

Dungait, J. A., Hopkins, D. W., Gregory, A. S., & Whitmore, A. P. (2012). Soil organic matter turnover is governed by accessibility not recalcitrance. *Global Change Biology, 18*(6), 1781-1796.

Elvert, M., Suess, E., & Whiticar, M. J. (1999). Anaerobic methane oxidation associated with marine gas hydrates: superlight C-isotopes from saturated and unsaturated C20 and C25 irregular isoprenoids. *Naturwissenschaften, 86*(6), 295-300.

Erb, T. J. (2011). Carboxylases in natural and synthetic microbial pathways. *Applied and Environmental Microbiology, 77*(24), 8466-8477.

Evershed, R. P., Crossman, Z. M., Bull, I. D., Mottram, H., Dungait, J. A., Maxfield, P. J., & Brennand, E. L. (2006). 13C-Labelling of lipids to investigate microbial communities in the environment. *Current Opinion in Biotechnology, 17*(1), 72-82.

Fahy, E., Subramaniam, S., Murphy, R. C., Nishijima, M., Raetz, C. R., Shimizu, T., ... & Dennis, E. A. (2009). Update of the LIPID MAPS comprehensive classification system for lipids. *Journal of Lipid Research, 50*, S9-S14.

Falkowski, P., Scholes, R. J., Boyle, E. E. A., Canadell, J., Canfield, D., Elser, J., ... & Steffen, W. (2000). The global carbon cycle: a test of our knowledge of earth as a system. *Science, 290*(5490), 291-296.

Fierer, N., Strickland, M. S., Liptzin, D., Bradford, M. A., & Cleveland, C. C. (2009). Global patterns in belowground communities. *Ecology Letters, 12*(11), 1238-1249.

Fioretto, A., Di Nardo, C., Papa, S., & Fuggi, A. (2005). Lignin and cellulose degradation and nitrogen dynamics during decomposition of three leaf litter species in a Mediterranean ecosystem. *Soil Biology and Biochemistry, 37*(6), 1083-1091.

Floudas, D., Binder, M., Riley, R., Barry, K., Blanchette, R. A., Henrissat, B., ... & Hibbett, D. S. (2012). The Paleozoic origin of enzymatic lignin decomposition reconstructed from 31 fungal genomes. *Science, 336*(6089), 1715-1719.

Francey, R. J., Trudinger, C. M., Van Der Schoot, M., Law, R. M., Krummel, P. B., Langenfelds, R. L., ... & Rödenbeck, C. (2013). Atmospheric verification of anthropogenic CO2 emission trends. *Nature Climate Change, 3*(5), 520-524.

Friedrich, M. W. (2006). Stable-isotope probing of DNA: insights into the function of uncultivated microorganisms from isotopically labeled metagenomes. *Current Opinion in Biotechnology, 17*(1), 59-66.

Frostegård, A., & Bååth, E. (1996). The use of phospholipid fatty acid analysis to estimate bacterial and fungal biomass in soil. *Biology and Fertility of Soils, 22*, 59-65.

Fuhrer, T., & Sauer, U. (2009). Different biochemical mechanisms ensure network-wide balancing of reducing equivalents in microbial metabolism. *Journal of Bacteriology, 191*(7), 2112-2121. https://doi.org/10.1128/JB.01335-08

Fuhrman, J. A. (2009). Microbial community structure and its functional implications. *Nature, 459*(7244), 193-199.

Giardina, C. P., & Ryan, M. G. (2000). Evidence that decomposition rates of organic carbon in mineral soil do not vary with temperature. *Nature, 404*(6780), 858-861.

Gill, R. A., & Jackson, R. B. (2000). Global patterns of root turnover for terrestrial ecosystems. *The New Phytologist, 147*(1), 13-31.

Gulis, V., & Bärlocher, F. (2017). Fungi: biomass, production, and community structure. In *Methods in Stream Ecology, Volume 1* (pp. 177-192). Academic Press.

Gulis, V., Suberkropp, K., & Rosemond, A. D. (2008). Comparison of fungal activities on wood and leaf litter in unaltered and nutrient-enriched headwater streams. *Applied and Environmental Microbiology, 74*(4), 1094-1101.

Hamada, S., & Fujita, S. (1983). DAPI staining improved for quantitative cytofluorometry. *Histochemistry, 79*(2), 219-226.

Harvey, H. R., Fallon, R. D., & Patton, J. S. (1986). The effect of organic matter and oxygen on the degradation of bacterial membrane lipids in marine sediments. *Geochimica et Cosmochimica Acta, 50*(5), 795-804.

Hayes, J. M. (2001). Fractionation of carbon and hydrogen isotopes in biosynthetic processes. *Reviews in Mineralogy and Geochemistry, 43*, 225-278.

Hayes, J. M. (2004). Isotopic order, biogeochemical processes, and earth history: Goldschmidt lecture, Davos, Switzerland, August 2002. *Geochimica et Cosmochimica Acta, 68*(8), 1691-1700.

Heckman, D. S., Geiser, D. M., Eidell, B. R., Stauffer, R. L., Kardos, N. L., & Hedges, S. B. (2001). Molecular evidence for the early colonization of land by fungi and plants. *Science, 293*(5532), 1129-1133.

Hinrichs, K. U., Hayes, J. M., Sylva, S. P., Brewer, P. G., & DeLong, E. F. (1999). Methane-consuming archaebacteria in marine sediments. *Nature, 398*(6730), 802-805.

Hoefs, J. (2018). *Stable isotope geochemistry: Theoretical and experimental principles* (3rd edition; pp 1-318) Springer, Berlin.

Hofmockel, K. S., Fierer, N., Colman, B. P., & Jackson, R. B. (2010). Amino acid abundance and proteolytic potential in North American soils. *Oecologia, 163*, 1069-1078.

Högberg, P., Nordgren, A., Buchmann, N., Taylor, A. F., Ekblad, A., Högberg, M. N., ... & Read, D. J. (2001). Large-scale forest girdling shows that current photosynthesis drives soil respiration. *Nature, 411*(6839), 789-792.

Huguet, A., Meador, T. B., Laggoun-Défarge, F., Könneke, M., Wu, W., Derenne, S., & Hinrichs, K. U. (2017). Production rates of bacterial tetraether lipids and fatty acids in peatland under varying oxygen concentrations. *Geochimica et Cosmochimica Acta, 203*, 103-116.

IPCC (2007). Climate change 2007 - the physical science basis: Working group I contribution to the fourth assessment report of the IPCC (Vol. 4). Cambridge University Press.

Jansa, J., Gryndler, M., & Matucha, M. (1999). Comparison of the lipid profiles of arbuscular mycorrhizal (AM) fungi and soil saprophytic fungi. *Symbiosis*.

Janzen, H. H. (2006). The soil carbon dilemma: shall we hoard it or use it? *Soil Biology and Biochemistry, 38*(3), 419-424.

Joergensen, R. G., & Wichern, F. (2008). Quantitative assessment of the fungal contribution to microbial tissue in soil. *Soil Biology and Biochemistry, 40*(12), 2977-2991.

Johnston, D. T., & Fischer, W. W. (2012). Stable isotope geobiology. In *Fundamentals of Geobiology* (pp. 250-268).

Joint, I., Mühling, M., & Querellou, J. (2010). Culturing marine bacteria - an essential prerequisite for biodiscovery. *Microbial Biotechnology, 3*(5), 564-575.

Jonas, J. L., Wilson, G. W., White, P. M., & Joern, A. (2007). Consumption of mycorrhizal and saprophytic fungi by Collembola in grassland soils. *Soil Biology and Biochemistry, 39*(10), 2594-2602.

Jørgensen, B. (2006). Bacteria and Marine Biogeochemistry. In *Marine Geochemistry* (pp. 169-206).

Kallmeyer, J., Pockalny, R., Adhikari, R. R., Smith, D. C., & D'Hondt, S. (2012). Global distribution of microbial abundance and biomass in subseafloor sediment. *Proceedings of the National Academy of Sciences, 109*(40), 16213-16216.

Keiser, A. D., & Bradford, M. A. (2017). Climate masks decomposer influence in a cross-site litter decomposition study. *Soil Biology and Biochemistry, 107*, 180-187.

Kellermann, M. Y., Wegener, G., Elvert, M., Yoshinaga, M. Y., Lin, Y. S., Holler, T., ... & Hinrichs, K. U. (2012). Autotrophy as a predominant mode of carbon fixation in anaerobic methane-oxidizing microbial communities. *Proceedings of the National Academy of Sciences, 109*(47), 19321-19326.

Kellermann, M. Y., Yoshinaga, M. Y., Wegener, G., Krukenberg, V., & Hinrichs, K. U. (2016). Tracing the production and fate of individual archaeal intact polar lipids using stable isotope probing. *Organic Geochemistry, 95*, 13-20.

Kendall, C., & Caldwell, E. A. (1998). Fundamentals of isotope geochemistry. In *Isotope Tracers in Catchment Hydrology* (pp. 51-86). Elsevier.

Killham, K., & Prosser, J. I. (2015). *The Bacteria and Archaea*. Cambridge, MA: Academic Press. 41-76.

Kirk, P. M. C. P., Cannon, P., Minter, D., & Stalpers, J. (2008). *Ainsworth and Bisby's dictionary of the fungi* (No. Ed. 10, pp 1-771).

Kirk, T. K., & Farrell, R. L. (1987). Enzymatic "combustion": the microbial degradation of lignin. *Annual Review of Microbiology, 41*, 465-505.

Klamer, M., & Bååth, E. (2004). Estimation of conversion factors for fungal biomass determination in compost using ergosterol and PLFA 18:2ω6,9. *Soil Biology and Biochemistry, 36*(1), 57-65.

Kopf, S. H., McGlynn, S. E., Green-Saxena, A., Guan, Y., Newman, D. K., & Orphan, V. J. (2015). Heavy water and 15N labelling with Nano SIMS analysis reveals growth rate-dependent metabolic heterogeneity in chemostats. *Environmental Microbiology, 17*(7), 2542-2556.

Kornberg, H. L. (1965). Anaplerotic sequences in microbial metabolism. *Angewandte Chemie International Edition in English, 4*(7), 558-565.

Kreuzer-Martin, H. W. (2007). Stable isotope probing: linking functional activity to specific members of microbial communities. *Soil Science Society of America Journal, 71*(2), 611-619.

Kselíková, V., Vítová, M., & Bišová, K. (2019). Deuterium and its impact on living organisms. *Folia Microbiologica, 64*, 673-681.

Kuypers, M. M., Blokker, P., Erbacher, J., Kinkel, H., Pancost, R. D., Schouten, S., & Sinninghe Damsté, J. S. (2001). Massive expansion of marine archaea during a mid-Cretaceous oceanic anoxic event. *Science*, 293(5527), 92-95.

Lal, R. (2004). Soil carbon sequestration impacts on global climate change and food security. *Science*, 304(5677), 1623-1627.

Lau, A. P., Lee, A. K., Chan, C. K., & Fang, M. (2006). Ergosterol as a biomarker for the quantification of the fungal biomass in atmospheric aerosols. *Atmospheric Environment*, 40(2), 249-259.

Lehmann, J., & Kleber, M. (2015). The contentious nature of soil organic matter. *Nature*, 528(7580), 60-68.

Lin, Y. S. (2009). In vitro study of microbial carbon cycling in subseafloor sediments (Doctoral dissertation, Universität Bremen).

Locey, K. J., & Lennon, J. T. (2016). Scaling laws predict global microbial diversity. *Proceedings of the National Academy of Sciences*, 113(21), 5970-5975.

Madsen, E. L. (2011). Microorganisms and their roles in fundamental biogeochemical cycles. *Current Opinion in Biotechnology*, 22(3), 456-464.

Malone, J. G., Mittova, V., Ratcliffe, R. G., & Kruger, N. J. (2006). The response of carbohydrate metabolism in potato tubers to low temperature. *Plant and Cell Physiology*, 47(9), 1309-1322.

Manefield, M., Whiteley, A. S., Griffiths, R. I., & Bailey, M. J. (2002). RNA stable isotope probing, a novel means of linking microbial community function to phylogeny. *Applied and Environmental Microbiology*, 68(11), 5367-5373.

Nelson, D. L., & Cox, M. M. (2008). *Lehninger Principles of Biochemistry* (5th ed., pp 1-1200). New York: W.H. Freeman and Company.

Nes, W. R. (1974). Role of sterols in membranes. *Lipids*, 9(8), 596-612.

Neubauer, C., Sessions, A. L., Booth, I. R., Bowen, B. P., Kopf, S. H., Newman, D. K., & Dalleska, N. F. (2018). Towards measuring growth rates of pathogens during infections by D2O-labeling lipidomics. *Rapid Communications in Mass Spectrometry*, 32(24), 2129-2140.

Oliveira, L. G., Cavalcanti, M. A. Q., Fernandes, M. J. S., & Lima, D. M. M. (2013). Diversity of filamentous fungi isolated from the soil in the semiarid area, Pernambuco, Brazil. *Journal of Arid Environments*, 95, 49-54.

Olsson, P. A., & Wallander, H. (1998). Interactions between ectomycorrhizal fungi and the bacterial community in soils amended with various primary minerals. *FEMS Microbiology Ecology*, 27(2), 195-205.

Olsson, P. A., Bååth, E., Jakobsen, I., & Söderström, B. (1995). The use of phospholipid and neutral lipid fatty acids to estimate biomass of arbuscular mycorrhizal fungi in soil. *Mycological Research*, 99(5), 623-629.

Owen, O. E., Kalhan, S. C., & Hanson, R. W. (2002). The key role of anaplerosis and cataplerosis for citric acid cycle function. *Journal of Biological Chemistry*, 277(34), 30409-30412.

Pace, N. R. (1997). A molecular view of microbial diversity and the biosphere. *Science*, 276(5313), 734-740.

Parkes, R. J., Cragg, B., Roussel, E., Webster, G., Weightman, A., & Sass, H. (2014). A review of prokaryotic populations and processes in sub-seafloor sediments, including biosphere: geosphere interactions. *Marine Geology*, 352, 409-425.

Paul, E. A. (2014). Soil microbiology, ecology, and biochemistry: An exciting present and great future built on basic knowledge and unifying concepts. *Soil Microbiology, Ecology, and Biochemistry*, 1-13.

Pedrós-Alió, C., & Manrubia, S. (2016). The vast unknown microbial biosphere. *Proceedings of the National Academy of Sciences*, 113(24), 6585-6587.

Pepper, I. L., & Gentry, T. J. (2015). Earth environments. In *Environmental Microbiology* (pp. 59-88). Academic Press.

Ragauskas, A. J., Beckham, G. T., Biddy, M. J., Chandra, R., Chen, F., Davis, M. F., ... & Wyman, C. E. (2014). Lignin valorization: Improving lignin processing in the biorefinery. *Science*, 344(6185), 1246843.

Ralser, M., Wamelink, M. M., Kowald, A., Gerisch, B., Heeren, G., Struys, E. A., ... & Krobitsch, S. (2007). Dynamic rerouting of the carbohydrate flux is key to counteracting oxidative stress. *Journal of Biology*, 6, 1-18.

Rappé, M. S., & Giovannoni, S. J. (2003). The uncultured microbial majority. *Annual Reviews in Microbiology*, 57(1), 369-394.

Rodriguez, R. J., Low, C., Bottema, C. D., & Parks, L. W. (1985). Multiple functions for sterols in *Saccharomyces cerevisiae*. *Biochimica et Biophysica Acta (BBA)-Lipids and Lipid Metabolism*, 837(3), 336-343.

Romanenko, V. I. (1964). Heterotrophic assimilation of CO2 by bacterial flora of water. *Microbiology (Mikrobiologiya)*, 33(4), 610-614.

Roslev, P., Larsen, M. B., Jørgensen, D., & Hesselsoe, M. (2004). Use of heterotrophic CO2 assimilation as a measure of metabolic activity in planktonic and sessile bacteria. *Journal of Microbiological Methods*, 59(3), 381-393.

Rounick, J. S., & Winterbourn, M. J. (1986). Stable carbon isotopes and carbon flow in ecosystems. *BioScience*, 36(3), 171-177.

Rousk, J., & Bååth, E. (2007). Fungal biomass production and turnover in soil estimated using the acetate-in-ergosterol technique. *Soil Biology and Biochemistry*, 39(8), 2173-2177.

Rousk, J., & Bååth, E. (2011). Growth of saprotrophic fungi and bacteria in soil. *FEMS Microbiology Ecology*, 78(1), 17-30.

Rousk, J., & Frey, S. D. (2015). Revisiting the hypothesis that fungal-to-bacterial dominance characterizes turnover of soil organic matter and nutrients. *Ecological Monographs*, 85(3), 457-472.

Rousk, J., Brookes, P. C., & Bååth, E. (2009). Contrasting soil pH effects on fungal and bacterial growth suggest functional redundancy in carbon mineralization. *Applied and Environmental Microbiology*, 75(6), 1589-1596.

Rowland, I., Gibson, G., Heinken, A., Scott, K., Swann, J., Thiele, I., & Tuohy, K. (2018). Gut microbiota functions: Metabolism of nutrients and other food components. *European Journal of Nutrition*, 57, 1-24.

Ruiz-Dueñas, F. J., & Martínez, Á. T. (2009). Microbial degradation of lignin: How a bulky recalcitrant polymer is efficiently recycled in nature and how we can take advantage of this. *Microbial Biotechnology*, 2(2), 164-177.

Sachse, D., Billault, I., Bowen, G. J., Chikaraishi, Y., Dawson, T. E., Feakins, S. J., ... & Kahmen, A. (2012). Molecular evidence for the reliance of terrestrial ecosystems on the marine biosphere. *Nature Communications*, 3, 1-7.

Schubert, D. J., Amon, R. M. W., & Goodwin, D. J. (2008). The use of stable carbon isotopes to measure microbial carbon flow and productivity in different marine ecosystems. *Marine Ecology Progress Series*, 371, 41-50.

Seitzinger, S. P., & Garber, J. (2003). The role of sediment transport in the export of organic carbon from coastal ecosystems. *Estuaries*, 26(4), 1133-1143.

Simkiss, K. (1974). Metal ions and the cellular chemistry of organisms. *Biochemical Society Transactions*, 2(1), 19-21.

Smith, S. E., & Read, D. J. (2008). *Mycorrhizal Symbiosis* (3rd ed., pp 1-787). Academic Press.

Soares, M. I. M., & de Freitas, M. R. (2020). Investigating the metabolic potential of filamentous fungi from tropical forests. *Fungal Biology*, 124(5), 399-408.

Sousa, D. S., & Laville, E. (2016). Genomic diversity of bacteria associated with the roots of tropical plants. *FEMS Microbiology Ecology*, 92(7), fiw081.

Sphar, C., & Bull, A. T. (2009). Organic carbon turnover in deep-sea sediments. *Environmental Microbiology*, 11(5), 1020-

Sperling, S. (2010). The role of microorganisms in the biogeochemical cycling of phosphorus. *FEMS Microbiology Reviews*, 34(4), 531-548.

Staley, J. T., & Konopka, A. (1985). Measurement of in situ activities of nonphotosynthetic microorganisms in aquatic and terrestrial environments. *Applied and Environmental Microbiology*, 49(4), 697-705.

Tebo, B. M., & Obraztsova, A. (2017). Geomicrobiology: How microorganisms affect the Earth's crust. *Environmental Microbiology*, 19(1), 205-218.

Van der Heijden, M. G. A., Bardgett, R. D., & Van Straalen, N. M. (2008). The unseen majority: Soil microbes as drivers of plant diversity and productivity in terrestrial ecosystems. *Ecology Letters*, 11(3), 296-310.

Van Veen, J. A., & Kuikman, P. J. (1990). Soil structural aspects of decomposition of organic matter. *Soil Biology and Biochemistry*, 22(5), 687-696.

Vázquez, M., & Ochoa, M. (2016). Biochemical diversity in microorganisms. In *Microbial Diversity and Bioprospecting* (pp. 165-180).

Wilkins, D., & Wilkins, P. (2021). Soil microbial communities: Linkages to ecosystem functions and climate change. *Environmental Microbiology Reports*, 13(4), 438-457.

Zelles, L. (1999). Fatty acid patterns of phospholipids and lipopolysaccharides in the characterization of soil microbial communities: A review. *Biology and Fertility of Soils*, 29(3), 258-272.

5. *Curriculum vitae*

Stanislav Jabinski

born on 29.01.1992 in Republic of Moldova
moved to Germany in 1995
Nationality: German
stanislav.jabinski@bc.cas.cz

Education

09/2019 – 2024 PhD Student at the department of Ecosystem Biology and Ecology, University of South Bohemia in České Budějovice, Czech Republic

Thesis title: Enzymatic combustion and pyrolysis products to reveal cycling of recalcitrant organic matter in soils and sediments

Supervisor: Dr. Travis B. Meador

10/2016 – 03/2019 Master of Science (MSc)

International Marine Geosciences, University of Bremen

MSc thesis: Development of a method to track microbial activity by ultra-high resolution mass spectrometry isotope pattern matching (Dez. 2018)

Supervisors: Prof. Dr. Kai-Uwe Hinrichs, Dr. Gunter Wegener

Co supervisor: Dr. Julius Lipp

10/2012 - 09/2016 Bachelor of Science (BSc)

Geosciences Department, University Bremen

BSc Thesis: First insights of high-resolution imaging of biomarker and elemental analysis of the sediments of the Gotland Basin (2016).

Supervisors: Prof. Dr. Kai-Uwe Hinrichs, Prof. Dr. Gesine Mollenhauer

Co supervisor: Dr. Lars-Peter Wörmer

Job Experience

Since 06/2019 Research Assistant and technician

Meador-Lab, Isotope facility, ISBB – Biology Center CAS, Czechia

02/2015 – 03/2019 Research Assistant

Hinrichs-Lab, Organic Geochemistry, MARUM-University of Bremen, Germany

Training

11/2007 - 12/2007 Network support and administration IALB University Bremen

08/2015 - 09/2015 Freiluftmuseum Dinosaurier Park Münchehagen

Technical Skills

Cell & Lipid extraction, IPL & Biomarker analysis on QTOF, QQQ, GC, Isolink, GC-FID/irMS, LC-MS,

FTICR-MS analysis, Isotope analysis, DPA extraction, culturing of microorganisms

Software: office package, DataAnalysis, Xcalibur, Inkscape, Isodat, SigmaPlot

Language

Russian (mother tongue), German (fluent), English (C1)

Other contributions

09.2014 – 10.2018 September academy workshop assistant for new beginners

2014 – 2019 Committee member as student representative of several PhD defenses

2019 – 2021 Co-supervision of Bachelor Thesis (4 people)

Scientific Contribution

Peer-reviewed publications

Jabinski, S., d. M. Rangel, W., Kopáček, M., Jílková, V., Jansa, J., & Meador, T. B.* (2024). Constraining activity and growth substrate of fungal decomposers via assimilation patterns of inorganic carbon and water into lipid biomarkers. *Applied and Environmental Microbiology, 90(4), e02065-23*.

Angst, G*., Angst, Š., Frouz, J., **Jabinski, S**., Jílková, V., Kukla, J., ... & Angel, R. (2024). Stabilized microbial necromass in soil is more strongly coupled with microbial diversity than the bioavailability of plant inputs. *Soil Biology and Biochemistry, 190, 109323*.

Nezhad, M. T. K*., Šamonil, P., Daněk, P., Jaroš, J., Hájek, M., Hájková, P., **Jabinski, S**., Meador, T.B., & Roleček, J. (2024). Lipid biomarkers and stable isotopes uncover paleovegetation changes in extremely species-rich forest-steppe ecosystems, Central Europe. *Environmental Research, 259, 119564*.

Jílková, V*., Al Haj Ishak Al Ali, R., Devetter, M., **Jabinski, S**., & Jandová, K. (2024). Organic matter stability in temperate forest soils is affected by tree species identity but not by litter quality. *Plant and Soil, 1-12*.

International scientific conferences

S. Jabinski*, W.Rangel, V.Jilkova, T.B. Meador (2022). Stable isotope Signatures from substrate utilization by different fungal ecotypes via a dual-SIP approach (GRC organic geochemistry, poster).

S. Jabinski*, W.Rangel, V.Jilkova, T.B. Meador (2022). Stable isotope Signatures from substrate utilization by different fungal ecotypes via a dual-SIP approach (IsoEcol, talk).

S. Jabinski*, W.Rangel, F. Lorence, T.B. Meador (2021). Stable isotope Signatures from substrate utilization by different fungal ecotypes via a dual-SIP approach (IMOG, virtuel flash talk).

S. Jabinski*, W.Rangel, F. Lorence, T.B. Meador (2021). Rapid analysis of fungal membrane lipids and their isotopic composition by TMSH Pyrolysis GC-MS/IRMS analysis (Goldschmidt, virtuel poster presentation).

J.S. Lipp*, **S. Jabinski**, N. Gajendra, M. Könneke, K.-U. Hinrichs (2018). Advancing the scope of lipid-based

stable isotope probing by mass spectrometric separation of lipid isotopologues (3 Cluster Conferenz, Berlin, poster presentation).

S. Jabinski*, J.S. Lipp N. Gajendra, M. Könneke, K.-U. Hinrichs (2018). Tracking of microbial activity by Ultra-high-MS Isotope Pattern Matching (Youmares, Oldenburg, poster,).

J.S. Lipp*, N. Gajendra, **S. Jabinski**, M. Könneke, F. Schubotz, K.-U. Hinrichs (2017). Stable Isotope Probing of Complex Lipids through Isotope Pattern Matching of Mass Spectra (IMOG, Florence, poster).

R.R. Adhikari*, V. B. Heuer, L. Wörmer, **S. Jabinski**, T. Hoshino, F. Inagaki, A. Kitte, J. Kallmeyer, K.-U. Hinrichs (2017). Subseafloor life and carbon cycling in the Bengal Fan (IODP Exp. 354) (IODP/ICDP Colloquium, Braunschweig, abstract)

*** Corresponding author**